Master's Thesis

TRANSFECTION ACTIVITY ENHANCEMENT OF A GENE ENCODING DNA ORIGAMI-LIKE NANOSTRUCTURE

Aug 2023

Nanobiotechnology,
Department of Materials and Production, Aalborg University

AALBORG UNIVERSITET

STUDENTERRAPPORT

w/

Department of Materials and Production

Nanobiotechnology

Skjernvej 4A

9220 Aalborg Øst

Title:

Transfection Activity Enhancement of a Gene Encoding DNA Origami-Like Nanostructure

Project:

Master's Thesis

Project period:

Nov 2022 to Aug 2023

Supervisors:

Leonid Gurevich

Evamaria Petersen

Number of pages:

77

Number of appendices:

3

Finish date:

Aug 2023

Abstract:

DNA origami has gained a wide array of applications due to accurately programmable structure at nano scale. A gene-encoding DNA origami can be used as an extremely versatile platform for gene delivery studies, while overcoming some barriers of gene therapy simply by compaction of the DNA to a well-defined structure. To this end, a DNA origami-like structure has previously been designed. The general goal of this

study was to investigate different methods to enhance gene transfection activity of this structure, mainly by decoration with positively-charged peptides and polymers. To this end, low molecular weight Poly-ethyleneimine (PEI), poly-L-lysine, and TAT sequence (a cell-penetrating peptide), were used to enhance transfection activity. The peptide was synthesized using automated f-moc chemistry. Poly-ethyleneimine (PEI) was also derivatized with hydrophobic fatty acids to enhance transfection. The results

showed modest transfection activity with the selected carriers when using plasmid DNA and double-stranded scaffold sequence, while no significant activity was observed using the single-stranded scaffold or the folded nanostructure. These results warrant further investigation into the design of promoter sequences optimal for single-stranded DNA transcription and subsequent translation.

Preface

This report summarizes the extended thesis project, performed throughout the academic year 2022-2023, to obtain a Masters of Science degree in Nano-biotechnology at the Department of Materials and Production, Aalborg University.

In this project, the transfection activity of a DNA origami-like structure was studied by means of conjugation with non-viral chemical carriers, including poly-cations and a cell-penetrating peptide. Lab-scale synthesis and isolation methods for the origami scaffold were explored and optimized. Various potential DNA carriers were prepared and screened for their DNA transfection activity and toxicity. Finally, the transfection activity of the DNA origami-like structure was assessed *in vitro*.

Vancouver citation style is used throughout the document, in which every citation is presented as [number], where the number refers to a specific reference in the bibliography. These references list the authors' last name, the title, journal, year of publication, and page numbers. When a reference has three or more authors, the first author's last name is written followed by et al.

The contents of this thesis, including figures and tables, are either composed originally by the author, or referenced properly. Artificial intelligence (AI) tools were used in accordance with the guidelines presented by the Study Board of Materials and Production. These tools were used merely to provide codes and frameworks to facilitate the analysis and presentation of data. No part of this report is "generated" or majorly edited by AI tools by any means.

Seyed Meghdad Tabatabai
stabat21@student.aau.dk

Aalborg University, Aug 2023

List of Abbreviations

Table 0.1. *List of abbreviations*

Abbreviation	Extended Form
AAV	Adeno-associated virus
AFM	Atomic force microscopy
AGE	Agarose gel electrophoresis
AI	Artificial intelligence
aPCR	Asymmetric PCR
bp	Base pair
CAD	Computer-assisted design
CME	Clathrin mediated endocytosis
CMVIE	Cytomegalovirus immediate early
CPP	Cell-penetrating peptide
CVME	Caveolae-mediated endocytosis
DMEM	Dulbecco's Modified Eagle's Medium
DNA	Deoxyribonucleic acid
dNTP	Deoxynucleoside triphosphate
DON	DNA origami-like nanostructure
dsDNA	Double-stranded DNA
DSN	double-specific nuclease
EDC	1-ethyl-3-(3-dimethylaminopropyl)-carbodiimide
ESI	Electro-spray ionization
EtBr	Ethidium bromide
h	hours
HPLC	High performance liquid chromatography
ITR	Inverted terminal repeat
kb	Kilobase pair
LATE	Linear after exponential
LB	Lysogeny Broth
min	minutes
Mw	Molecular weight
MWCO	Molecular weight cutoff
NHS	N-hydroxy succinimide
nt	Nucleotide
PCR	Polymerase chain reaction
pDNA	plasmid DNA
PEG	Poly-ethyleneglycol
PEI	Poly-ethyleneimine
PLL	Poly-L-lysine
PTD	Protein transduction domain

Table 0.1 continued from previous page

rcf	Relative centrigugal force
RFP	Red fluorescent protein
RNA	Ribonucleic acid
rpm	Revolutions per minute
sec	seconds
SOC	Super Optimal Broth with Catabolite repression
SPPS	Solid phase peptide synthesis
ssDNA	Single-stranded DNA
TAE	Tris acetate EDTA buffer
Taq	Thermus aquaticus
TAR	Trans-activator of transcription
TAT	Trans-activator of transcription
TB	Tris buffer
Tm	Melting temperature

Contents

Introduction 1

1.1 State of the Art

DNA origami is and relatively novel technique in nanotechnology, which entails compaction of a long single-stranded scaffold DNA into any arbitrary shape using staples, i.e. short oligonucleotides that are complementary to different regions on the scaffold. This technology has enabled unprecedented accuracy in design at nanoscale which is self-assembled and fully addressable.

DNA nanostructures have been used in a variety of setups including structural scaffolds for nanolithograpjhy, sensors, molecular electronics, nano machines and dynamic objects, drug delivery, and computing. The technology however has not gained widespread commercial use due to problems such as cost of production and stability. Nevertheless, this technology is fast developing with new methods of synthesis that have much higher yield and are not as costly.

Gene delivery is a methodology used in a variety of life sciences and medical applications. Genetic modification is a prominent tool in several biological studies and it has been long surveyed as a powerful means for *in vivo* therapeutics. The recent COVID outbreak led to a revolution in nucleic acid medicine where for the first time a nucleic acid medicine was used on a large population of humans worldwide.

The central question in gene delivery is how to design a system that protects the genetic material throughout its path within the human body to the designated cells or tissues. These systems should also be able to trespass barriers set against them by the cell itself, particularly owing to the fact that nucleic acids yield a net negative charge that is repelled by the cell surface. Also, nucleic acids are prone to degradation by extra- and intracellular nucleases and other processes such as lysosomal degradation which inhibit their function.

The idea of using DNA nanostructures as drug delivery vehicles has been explored for a long time. One prominent example is a 2009 study at Aarhus university, where a DNA origami nano-cage was developed that could successfully encapsulate an organic molecule and deliver it to designated cells [1]. However, the structural aspects of DNA origami has been far more studied and paid attention to than the possible functional role of DNA origami, most notably it's coding function.

The DNA origami technology allows for virtually any sequence of DNA to be folded to any possible two or three-dimensional shape. The resulting structures are self assembled, extremely monodisperse, and fully addressable. Both shape and aspect ratio are properties that have been implicated in the success and efficiency of gene delivery systems [2]. This means that using this technology, the cargo may take up many roles of the carrier which makes

the use of such carriers redundant or less necessary. For example, the particulate structure can improve the enhanced penetration and retention (the EPR effect)[3] without a need for chemical carriers. The structure can also be easily functionalized by targeting molecules and other components needed for a multi functional delivery system. Another possible benefit of packaging DNA into an origami is that less catatonic molecules are needed for efficient delivery. It has been shown that higher molecular weight polycations are generally more effective than their lower molecular weight counterparts while exerting higher cytotoxicity [4]. It is therefore hypothesized that the decoration of these structures with smaller cationic molecules can yield more or less the same transfection efficiency while lowering toxicity.

Very few studies have explored DNA origami as a transfection agent. In one of the most recent of these studies, DNA origami structures were delivered via electroporation, a physical gene delivery method that internalizes the genetic material by transient disruption of the membrane potential [5].

In the current study, a more or less different approach is going to be explored, namely non viral chemical gene delivery. It should also be borne in mind that selection of a proper promoter sequence is essential in designing such a DNA origami, as the molecular machinery and dynamics of transcription of single stranded DNA is not the same as the more conventional double stranded DNA. In this study an array of chemical carriers will be screened for their transfection activity and toxicity and the selected ones will be complexed with the DNA origami structure and studied *in vitro*. A comparison will also be made between double stranded versus single stranded coding sequence that acts as the origami scaffold.

If successful, this gene encoding DNA origami will provide a relatively simple but extremely versatile platform for studies regarding the shape and aspect ratio of nanoparticles in drug and gene delivery. It will also introduce a new method for delivery of larger RNA and DNA sequences needed for some genetic disease. Since DNA origami also provides logical gates and computing possibilities[6], this technology can develop into a stimuli responsive multi functional (multi gene expressing) gene delivery system that would intelligently release one or more of the genetic material based on the given logic signal.

1.2 Problem Analysis

This paper builds on previous work by Konstantinos Grarentis [7]. In that study, a DNA origami-like nanostructure was designed using a 1.9 nt scaffold, 10 large (100 nt to 120 nt) fragments, and 18 staple sequences. The initial idea was to reduce the number of staples required to make the structure easier to produce, while retaining the particulate nature of the structure. Asymmetric PCR was the method used for production of the ssDNA scaffold and the fragments, while the staples were synthesized and provided by an external company.

The study managed to show formation of the structure by AFM studies. However, transfection results were not satisfactory. Another confining factor of the study was that due to low yield of the ssDNA scaffold, some purification steps were circumvented and crude aPCR products were used in origami folding, thus introducing dsDNA impurities that would interfere with the transfection assays. The cell viability after treatment with DON was also not investigated. Moreover, the transfection studies were not controlled, so the overall reliability of the assays

may not be confirmed.

1.3   Problem Statement

DNA origami yields a negative surface charge due to the presence of multiple phosphate groups in the backbone. As a result, it is expected to be repelled by the negatively charged cell membrane, thus showing negligible transfection activity, as is the case with naked DNA. Other studies regarding DNA origami transfection also use means to facilitate the entry of the DNA into the cells, for example via physical transfection (gene guns) [5].

This project aims to use chemical gene delivery methods to overcome possible barriers to transfection activity of the DON. The idea stems from a study by Ahmadi *et. al.*[8], where the complexation of DNA origami with polycationic polymers such a PEI and chitosan was shown to render these structures more stable against nuclease activity and salt depletion. These polycations, which are commonly used in non-viral delivery systems, attached reversibly and did not disrupt the origami structure [8]. Therefore, the use of cationic transfection enhancers seems to be a plausible approach to enhance the DON transfection activity.

In this study, low Mw branched PEI, PLL, and TAT (a cell-penetrating peptide) are investigated as possible means to enhance the transfection activity. Modification of PEI by hydrophobic chains will also be explored. Also, methods to increase the yield of the ssDNA scaffold will be experimented with. Transfection activity as well as cell viability after treatment with the transfection agents will be also be screened. Finally transfection activity of the DON alone or complexed with the selected carriers will be tested.

Theory 2

2.1 Gene Delivery Systems

There are two main approaches to gene delivery, which consist of viral and non viral systems. Non viral systems include chemical and physical delivery systems. A summary of these systems is illustrated in figure 2.1.
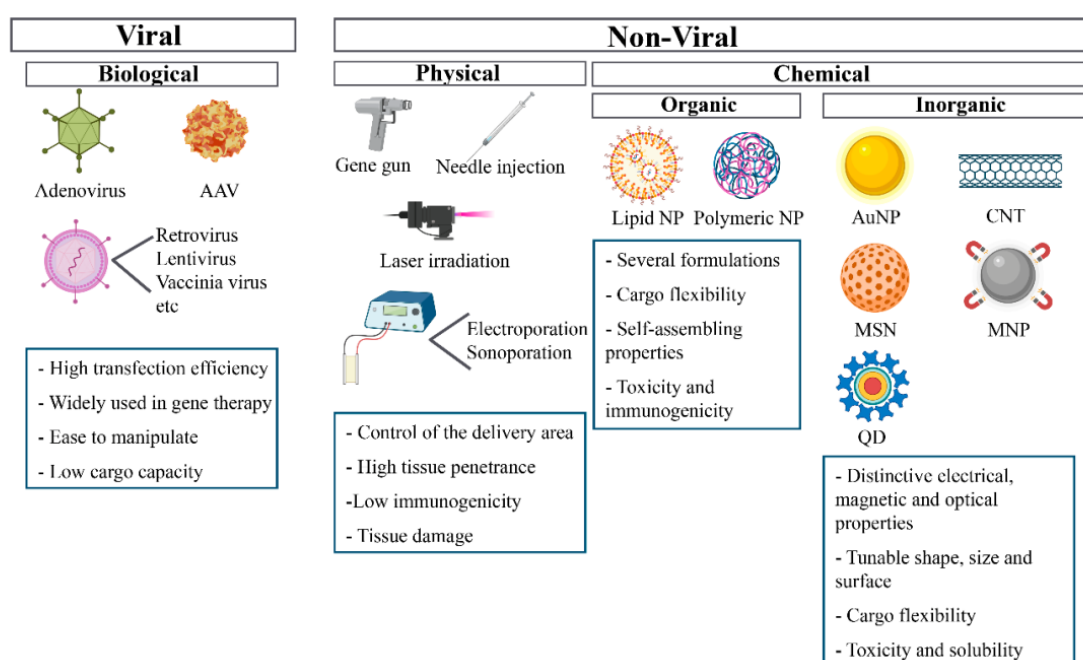
Figure 2.1. *A summary of common viral, physical, and chemical gene delivery systems. Picture source: [9].*

2.1.1 Physical Gene Delivery Systems

Physical gene transfer are methods that transfer genetic material (most commonly plasmids) by physical forces, rather than chemical carriers, such as lipids or polymers. There are a variety of methods for physical gene transfer.

Electroporation

In this method, also known as electropermeabilization, the integrity of cellular membrane is transiently disrupted by application of short pulses of high voltage electric field. This method provides efficient gene transfer, which does not require addition of potentially toxic chemicals. This method has been studied for local gene delivery to tumors and cell-based therapies. It is generally believed that application of high voltage pulses (in the order of 200 V/cm) leads to formation of hydrophilic pores that allow for DNA molecules to enter the cytoplasm through

diffusion and electrophoretic forces. The downside of this method is the fact that is affects expression of other genes in the host cells [10].

Gene guns and other physical methods

Ballastic gene delivery entails bombardment of cell with DNA-coated particles. This method has been used in DNA vaccine delivery to skin tissue, and in plant biotechnology. This method is limited to superficial tissue delivery. Other methods such as laser-induced gene tansfer and application of magnetic fields have also been investigated [11].

2.1.2 Viral Gene Delivery Systems

Viral vectors are inspired by the life-cycle of viruses that infect specific target cells. They are made by replacing some of a virus's genetic elements with a coding gene of interest. In many cases, this replacement results in the loss of replication competence of the viral particles. Different genetic material such as ssDNA, dsDNA, ssRNA, and dsRNA, can be integrated in a viral vector, based on the type of the vector. Viral vectors can be integrative or non-integrative, which exert stable and transient gene expression, respectively. The advantages of viral systems include high potency, tissue specificity, and stable and transient expression potential. On the other hand, immunogenicity, non-specific integration risk, and limited size of genetic cargo, limit their use [12]. The most common viral vectors include adenoviruses (dsDNA), retroviruses (ssRNA), poxviruses, adeno-associated viruses (AAV, ssDNA), and herpes simplex viruses (dsDNA) [13].

2.1.3 Non-Viral Gene Delivery

Non-viral gene delivery takes advantage of a series materials to pack genetic material into particles that are capable of entering cells. These materials include polymers, lipids, peptides, inorganic compounds, and hybrid systems.

In comparison with viral vectors, non-viral system offer some advantages such as lower cytotoxicity, immunogenicity, and mutagenesis, and less limitations in nucleic acid loading capacity. However, non-viral vectors generally have lower gene transfer efficiency, specificity, gene expression duration compared to viral vectors, while still having safety concerns in their own right [14].

2.1.4 Polythyleneimine (PEI)

Polyethylenimine (PEI) is one of the earliest and most extensively studied polycationic polymers. It has been synthesized in various architectures and molecular weights. The presence of multiple amines in the backbone, allows for partial protonation in the physiological pH range. However, as the endosome becomes acidified by the activity of a proton pump, additional amine groups are protonated, generating an osmotic effect, also known as, proton sponge effect, which leads to more pump activity and eventual endosome burst, which is believed to enhance the transfection efficiency by lowering gene degradation. PEI is available in a variety of linear and branched arrangements and different molecular weights figure 2.2. Today, 25 kDa PEI is used as a gold standard for measuring the transfection efficiency of non-viral vectors.
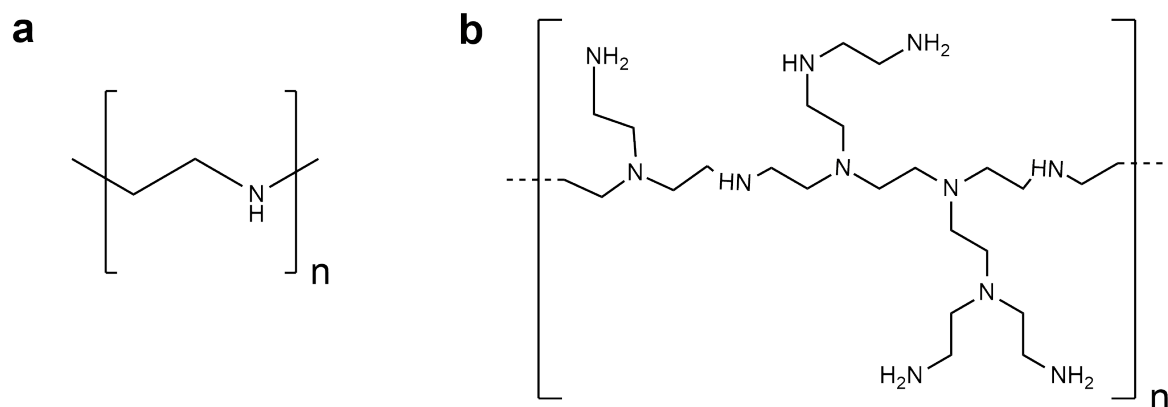
Figure 2.2. *PEI structure a) Linear, b) Branched*

Although considered a promising non-viral vector, PEI in its native form has problems such as low transfection (compared to viral vectors), toxicity, and lack of specificity. It is also not biodegradable, which means accumulation in the cell may cause untoward effects [14].

PEI and other polycations have been modified with a variety of moieties to enhance transfection efficiency and curb cytotoxicity, which are the two main shortcomings of the polymer. PEI toxicity is attributed to factors such as accumulation due to non-degradable amide bonds, as well as the positive charge, that causes hemolysis or immune response in blood circulation . Therefore, one strategy to reduce toxicity is by masking the readily protonated primary amines with other less reactive amines. Modification of polycations with heterocyclic amines such as histidine and pyridine, has been shown to significantly increase the transfection activity [15]. Moreover, partial modification of primary amines with hydrophobic substituents such as alkylhalides [16], has shown improved transfection (possibly by better intraction with the membrane, while lowering toxicity [17].

Higher molecular weight PEIs also tend to show higher toxicity. Therefore, one strategy is to decorate less toxic particles with low molecular weight PEIs. For instance, self-assembled nanoparticles from cyclodextrin-grafted low molecular weight PEI (800 Da) presented low cytotoxicity and a high transfection efficiency [18].

Several other modifications have been made to increase the effectiveness and reduce toxicity. Some other examples include, bio-reducible crosslinking [19] , PLGA conjugation [20], and PEGylation[21].

2.1.5 Poly-L-Lysine (PLL)

Poly-l-lysine (PLL) is a term used to describe homopolymers of the amino acid L-lysine. This aminoacid has two amine groups, one at the α and the other at the ϵ carbon. Both of these sites can be used to polymerize L-lysine. ϵ-PLL has antimicrobial properties and is used as a food preservative [22]. Linear α-PLL, as well as hyper-branched and dendritic PLL figure 2.3, have applications in drug delivery and tissue culture. PLL can be used to attach cells and other negatively charged molecules to other surfaces such as microscopy substrates[23]. PLL offers some advantages over PEI, including biodegradability and thus higher biocompatibility. However, due to lower buffering capacity, which results in lower

endosomal escape and decreased transfection efficacy. conjugation with other polymers such as PEI, as well as modification with hydrophobic moities have been shown to improve the transfection activity of PLL [24]
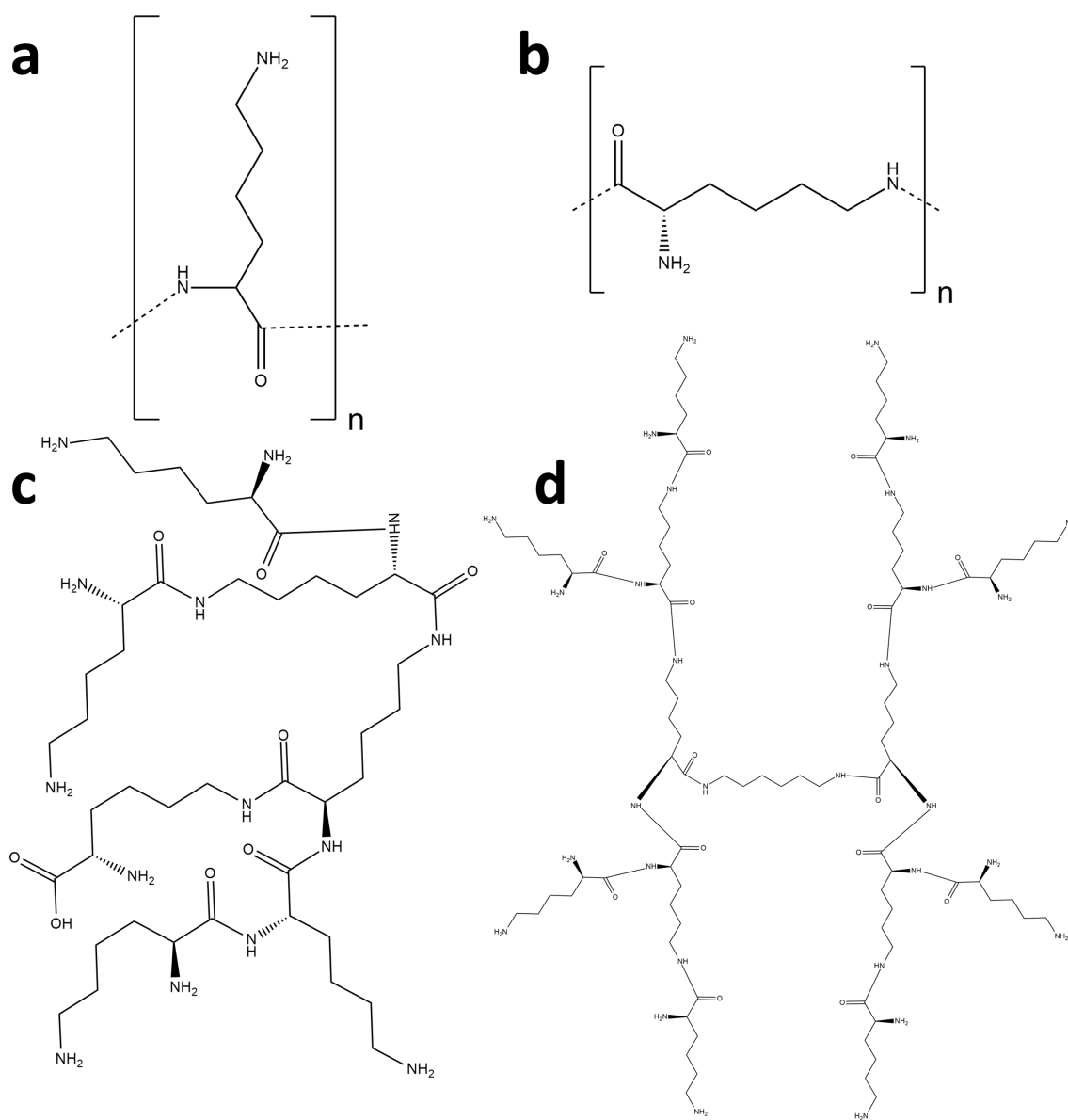
Figure 2.3. *Different arrangements of PLL: a) Linear α-PLL, b) Linear ϵ-PLL, c) Branched PLL, d) Dendritic PLL. The structures were sketched using ChemDraw Ultra 12.0 software, with inspirations from [23].*

2.2   Cellular Internalization Pathways of Nanoparticles

Nanostructures can enter the cells via a variety of mechanisms. Very small molecules and ions can diffuse through the membrane in and out of the cells. However, most macromolecules enter cells via a mechanism called endocytosis. Different enegrgy-dependent uptake pathways are illustrated in figure 2.4.
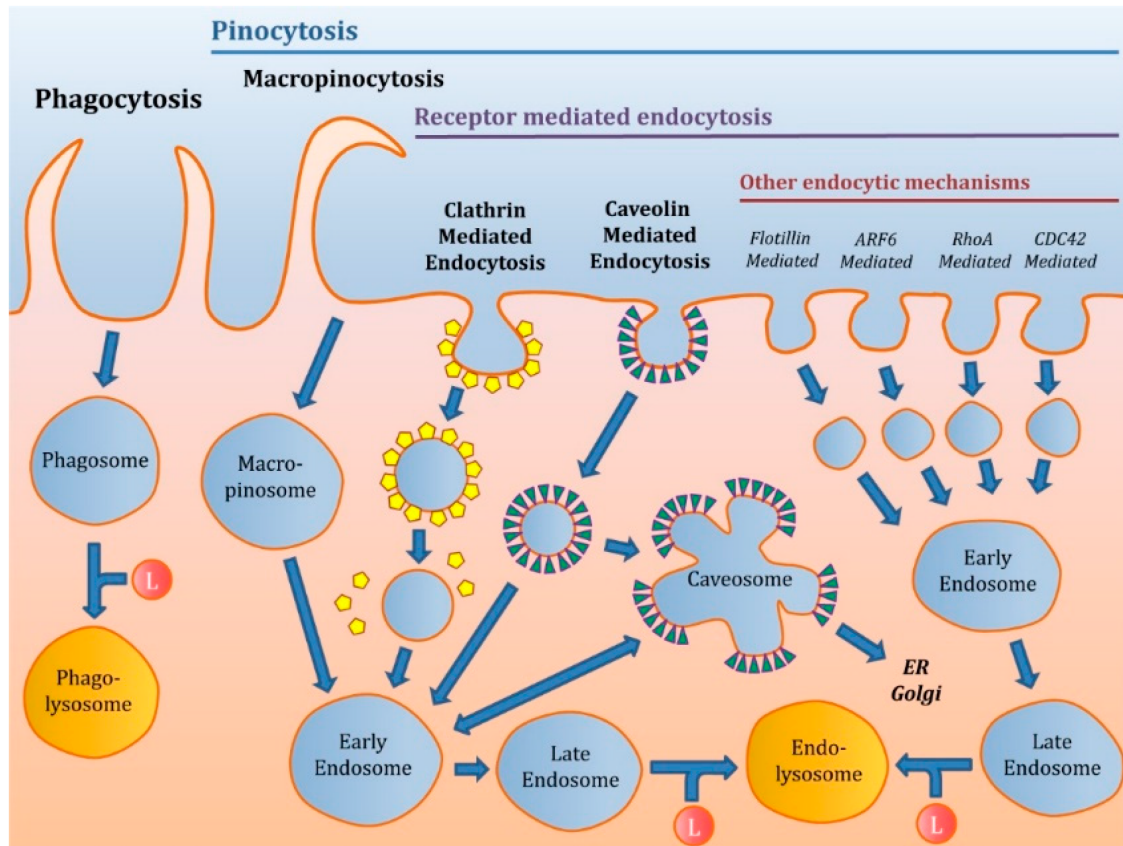
Figure 2.4. *Main uptake pathways of the cells. Reprinted from [25]*

2.2.1 Clathrine-Mediated Endocytosis

Clathrine-mediated endocytosis (CME) is a well-chatacterized internalization pathway, where a change in the composition of the membrane triggers the recruitment of clatherine to the cytosolic leaflet of the membrane. A group of "adaptor" proteins are responsible for formation of a pit in the cell membrane and formation of a clathrin coated vesicle. The lumen of the vesicle is acidified by and H^+-ATPase in the vesicle membrane. Clathrine and adaptor proteins then detach from the vesicle in the cell, and the uncoated vesicle fuses with an early endosome. The acidification continues in the early endosome, reaching pHs of 6.8-6.5 [26].

2.2.2 Caveolae-Mediated Endocytosis

Caveolae-Mediated Endocytosis (CVME) is a process wherein invaginations of the plasma membrane are formed to uptake extracellular fluid contents. Unlike in Clathrin-Mediated Endocytosis, proteins involved in CVME, such as caveolin-1, bind to cholesterol in lipid rafts and remain associated with the vesicles even after uptake. These caveolin-coated vesicles can then fuse with each another to form structures known as caveosomes, which subsequently fuse with early endosomes. These vesicles can further travel to the smooth endoplasmic reticulum or the Golgi apparatusfigure 2.4 [25]. It is generally believed that particles larger than 200 nm are preferentially uptaken by the CVME, whereas smaller particles are more likely to be taken up by the CME. Also, the CVME pathway seems to be lessaffected by endosomal acidification. [26]

2.2.3 Endosomal Escape

The internalized particle could enter a degenerative path by further acidification and enzyme degradation in the late endosome (pH 5.2-6.2) or lysosome (pH 4.5-5.2). The lysosome contains a several acid hydrolases that can degrade the internalized cargo. Many strategies for drug delivery encompass a conformational change as a result of endosome acidification which would cause endosomolysis or "endosomal escape"figure 2.5. This could be achieved for example by using polycations that act as a "proton sponge", scavanging the H^+ groups, leading to increased activity of H^+-ATPase and and a osmotic burst of the endosome. Clathrine mediated endocytosis can lead to other pathways, such as recycling pathway for receptors, or transcytotic pathway, usually in case of polarized cells.[24]
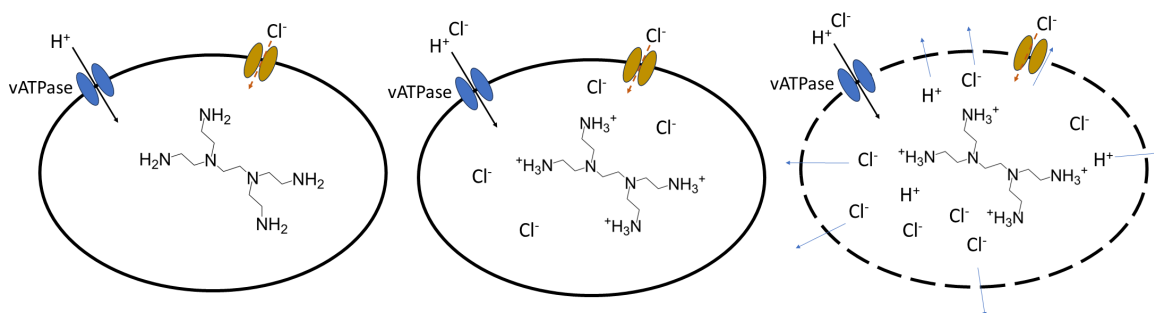
Figure 2.5. *The proton sponge effect. Presence of protable amines inside a late endosome results in over-activity of the proton pump, leading to increased osmotic pressure inside the vesicle and eventual rupture of the endosome.*

2.3 Cell-Penetrating Peptides

Several biologically active molecules such as peptides, nucleic acids, and even small-molecule agents are not able to traverse the cell membrane efficiently. Cell penetrating peptides (CPPs) are a group of peptides that facilitate the internalizaiton of such intracellular cargo.There is great potential in CPPs as they can realize the potential of many bioactive molecules, including drug candidates [27].

2.3.1 CPP Types

CPPs can be classified into three classes of cationic, amphiphilic and hydrophobic. The cationic class are positively-charged at physiological pH and usually contain short strands of arginine and lysine. It hase been suggested that the central role of arginine may stem from the formation of bidentate H-bonds with various negative functional groups on the cell membrane [28].

Amphiphilic CPPs contain polar and nonpolar regions. Other than arginine and lysine, these peptides are also rich in hydrophobic residues.

The CPPs can also be classified based on their origin. Natural CPPs are present in the nature and aid in transport of eg viral particles into the cells. Chimeric CPPs contain a combination of natural and synthetic sequence. Chimeric amphiphilic CPPs have been obtained by addition of a hydrophobic domain to a nuclear localization signal (NLS)[29].

Other primary amphiphilic CPPs are from natural origins. Secondary amphiphilic CPPs assume an α-helical or β-sheet conformation with hydrophobic and hydrophilic residues grouped on opposing sides. Proline-rich CPPs are also another subclass. Hydrophobic CPPs generally contain hydrophobic residues. Although this class of CPPs have not been studied extensively, it is possible that these peptides interact with the hydrophobic tails of membrane phospholipids. The role of hydrophobic interaction in cellular internalization has been proposed before[27].

2.3.2 Mechanism of Action of CPPs

CPPs act via a variety of proposed mechanisms. Cationic CPPs interact with the negatively charged head groups in the lipid bilayer. Membrane destabilization and pore formation may follow these interactions, resulting in the passive internalization of the particle. Other than pore formation, formation of inverted micelles and carpet-like destabilization of the membrane is proposed as mechanisms for internalization. Although early reports proposed that direct penetration was the main mechanism of CPP action, more recent studies suggest that many CPP-containing particles enter the cell via the endocytotic pathways [30].

CPPs have been modified to enhance their endosome disrupting effects thus enhancing "endosomal escape", for example, by insertion of histidine moieties with a possible proton sponge effect, or other pH-sensitive moieties that alter the protonation state of the peptides in low pH of the late endosome [28].

Several CPP-conjugated peptide drug candidates are under different stages of clinical trials. These formulations target a variety of diseases, including cancer, cardiovascular disease, Duchenne's muscular dystrophy, and aesthetic medicine [28]

2.3.3 TAT Peptide

HIV-1 TAT (Trans-Activator of Transcription) protein is an essential protein in replication and virulence of the HIV. It is a 14 kDA protein that binds to the transactivator response element (TAR) of viral genome and enhances transcription initiation and elongation. It also increases membrane permeability via a variety of mechanisms, including through the cationic protein transduction domain (PTD) [31].

The 11-amino acid domain with the sequence YGRKKRRQRRR, is an arginine-rich sequence that can enhance cellular uptake through various mechanisms. The guanidinium groups of the arginine are thought to interact with the anionic moieties on the cell membrane such as glycosaminoglycans [32]. Destabilization of the membrane and formation of a transmembrane pore has been proposed as the mechanism of TAT-induced internalization[33]. However, other studies have shown micropinocytosis as the main mechanism of action [34].

The GRKKR in the peptide also acts as nuclear transduction signal, that promotes translocation of the particles to the cell nucleus [35].

The TAT peptide has been used for enhanced delivery of a variety of small molecules and biomolecules including antibodies, proteins, liposomes, and nucleic acids [31]. It has also been shown to potentiate PEI-induced DNA transfection [36].

2.4 DNA Origami

2.4.1 Background

Ned Seeman is credited with developing the field of DNA nanotechnology in the early 1980s. His pioneering work focused on using DNA molecules as a building block for creating nanostructures. Seeman proposed the rational design of immobile Holliday junctions, which allowed DNA to extend in two dimensions, instead of the naturally ocurring one dimention double helix [37]. Holliday junctions are four-strand cross-shaped DNA structures that form during genetic recombination. In the nature, these junctions are mobile, due to the symmetry of the forming strands. However, formation of stable and immobile Holliday junctions leads to creation of DNA-based "tiles" that could be programmed to self-assemble into larger structures: Seeman's tiles were designed with specific binding sites that allowed them to connect to other tiles in a predetermined pattern figure 2.6. This work laid the foundation for DNA origami, which was introduced by Paul Rothemund in 2006 [38].
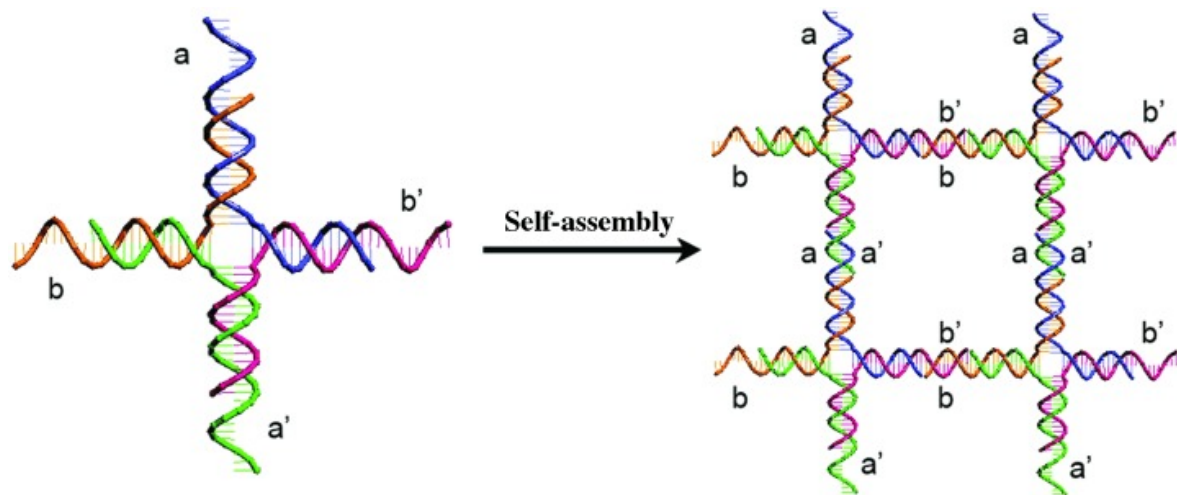
Figure 2.6. *The basic concept of DNA tile self-assembly. Immobile Holliday junctions with overhanging sequences can self-assemble to higher order constructs. Reprinted from [39]*

Origami is an ancient Japanese art that entails formation of complex shapes using a single paper sheet just by folding it. By analogy, DNA origami relies on folding a long ssDNA called the scaffold (typically viral DNA 7000 nucleotides long), with hundreds of designed short (20-60 nt) ssDNA strands called staples. Each staple has multiple binding domains that bind and bring together otherwise distant regions of the scaffold via crossover base pairing. The shape of the resulting structures can be precisely programmed with the staple sequences. Being programmable, DNA origami structures can be designed by computer-aided design (CAD) and universal synthesis protocols, which also enables automated fabrication. Compared to tile-based DNA assembly strategies, DNA origami synthesis usually has higher yield and robustness, and can be used to build any arbitrary shape, including 3D and non-periodic shapes. [40][38]

2.4.2 Applications of DNA Origami

Nanofabrication

DNA origami structures are highly customizable, enabling the assembly of various materials with nanoscale precision. These structures allow controlled arrangement of nanostructures through specific interactions, leading to programmable patterns, nanoparticle assemblies, and even dynamically rearrangeable nanoassemblies. Additionally, DNA origami serves as a platform for nanolithography, enabling the creation of complex and precise patterns onto different surfaces[41].

Enzymatic Catalysis

DNA origami has been used to enhance the activity of enzymes particularly bye spatially arranging different enzymes that perform a chain of biochemical reactions. Encapsulating single enzymes or enzyme pairs within DNA origami structures may lead to enhanced reaction rates and enzyme stability[42].

DNA Computation

DNA origami structures enhance computation by providing spatial organization, co-localization, and compartmentalization of circuit components. This framework accelerates reactions, modulates pathways, decreases errors, and enables potential *in vivo* computation. DNA origami robots can perform random walk-based sorting and DNA-based parallel algorithms for maze-solving. This spatial organization also allows using structural reconfiguration and assembly as computational architectures and coupling combinatorial selection results to specific input signals for enhanced functionality [43].

Molecular machines

DNA origami structures is formed by reversible non-covalent interactions, enabling dynamic devices with multiple stable states. Dynamic DNA origami devices transition between these states, often using external triggers. These devices incorporate both rigid dsDNA and flexible single-stranded domains. Mechanically interlocked domains can also guide motion. Recent studies have demonstrated autonomous motor movement, fueled by RNA-based reactions, resulting in microscale movement of DNA origami structures without external gradients [44].

Drug Delivery

DNA origami structures hold potential for drug delivery due to their biodegradability, addressablity, low toxicity, and the ability to load various therapeutic molecules. These structures can carry drugs via interactions like intercalation, base pairing, covalent binding, or encapsulation. DNA origami can cross biological barriers and even enter mammalian cells through endocytic pathways, accumulating in tumors or specific organs. specific targeting molecules can also be incorporated. To respond to diverse environments, DNA origami nanorobots have been designed with logic-gated mechanisms, opening upon specific receptor binding. Challenges include high cost, stability in biological environments, immunogenicity, and intracellular trafficking. DNA origami structures also have a variety of other applications in bioimaging, molecular probes, and biosensing [45].

2.4.3   DNA Origami Design and Modeling

In order to design DNA origami structure, one needs to translate the desired final morphology into the folding I of a scaffold using well-defined staple sequences. This can only be done using design software. The first generation DNA origami design tools such as caDNAno [46] and Tiamat [47] require manual or semi-automated scaffold and staple crossover creation and require extensive technical knowledge.

Second generation software have the ability to generate stable sequences automatically from user provided 3 dimensional designs. A prominant example of the second generation sofware is vHelix, an Autodesk Maya plugin, can simulate the folding and stability of origami structure in standard folding buffer[48].

Third generation design software integrate many of the features of first and second generationsoftware capabilities. Adenita is a third generation tool that can design lattice-based wireframes, multilayered structures, and DNA tiles. It also includes a simulation platform to predict the stability of the designed structure [49].

Conventional molecular dynamic simulations are too computationally expensive due to the large size of DNA and long (microsecond) time scales required to model long-range interactions. OxDNA is a simulation code originally developed to implement a coarse-grained (CG) DNA model. The basic CG unit is a rigid nucleotide with a set of interaction sites and a peripendicular vector that captures the planarity of the base through the orientational dependence of interactions, enabling the representation of co-planar base stacking and the linearity of base pairing. The pentose and phosphate groups are incorporated into a single "backbone" site figure 2.7.
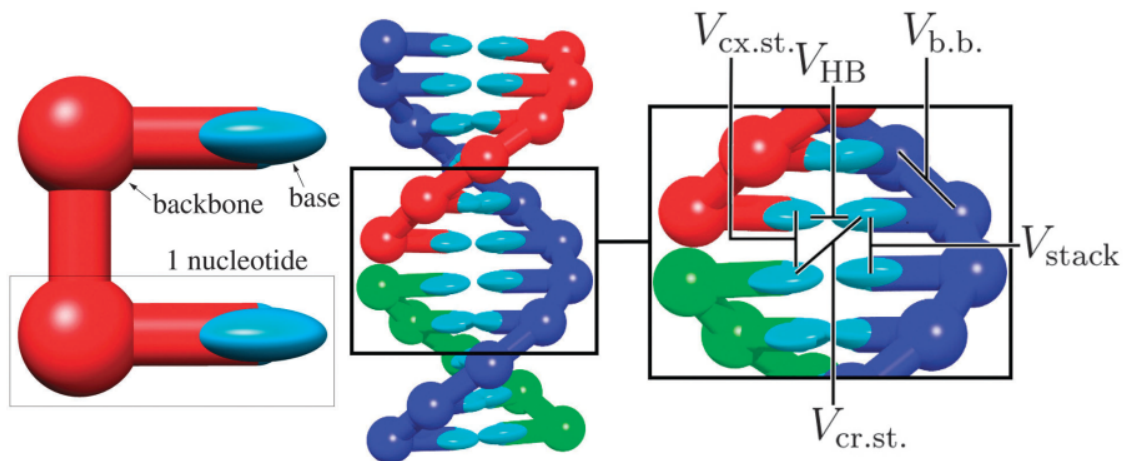
Figure 2.7.   *The coarse-grained units of oxDNA and different potentials. Reprinted from [50]*

In the newer version of the model, oxDNA2, some limitations are eliminated and new features are added to make the model more realistic. In this version, different widths for the major and minor grooves are introduced by defining an angle between the backbone site and the stacking site in a duplex without changing the duplex radius. Also, to allow for modelling

DNA structures in physiological conditions, salt concentration can be adjusted from 0.1 M or greater monovalent salt in a Debye-Hückel model. OxDNA2 also accounts for differences in DNA pitch in nicks and junctions of DNA, and sequnece-dependent AA and TT stacking.

The oxDNA2 potential can be summarized as:

$$V_{oxDNA2} = \sum_{\langle ij \rangle} (V*_{b.b.} + V*_{stack} + V'_{exc}) + \sum_{ij \notin \langle ij \rangle} (V*_{HB} + V_{cr.st.} + V_{exc} + V*_{cx.st.} + V*_{DH}) \quad (2.1)$$

The first term is sum over all adjacent nucleotides along the backbone of a strand, and the second term is sum over all other nucleotide pairs. $V_{b.b.}$ represent backbone connectivity, V_{exc} and V'_{exc} describe excluded volume, V_{HB} represent base pair H-bonding. Stacking of adjacent bases on a strand, cross-stacking, and co-axial stacking are represented by V_{stack}, $V_{cr.st.}$ and $V_{cx.st.}$, respectively. The * denotes modification in the terms from the earlier version, and V_{DH} is the Debye-Hückel potential.[51]

2.4.4 DNA Origami Production

the most common scaffold sequence for dinner agami is the M13 NP 18 viral genome a 7.2 kilobase long viral genome DNA I selected from the M13 bacteriophage there are other typical scaffolds they arrived from M13 that provide alternative length and sequences [42].

Another method which is particularly useful when the sequence of the scaffold is important for example in the case of gene encoding DNA origami is to make the sequence using asymmetric PCR which is a method to amplify one strand of the DNA preferentially. For a detailed discussion, see subsection 2.5.3.

Biotechnological production of DNA origami is another method which can significantly reduce the cost of production of DNA origami, especially at larger scales. This method entails designing a plasmid sequences containing alls the staple sequences, as well as the scaffold with self-excising DNAzyme sequences in between. In this method, bacteriophages are used to generate single stranded precursor DNA or phagemids from the said plasmid. The DNAzymes will then be activated by the presence of zinc ion, resulting in separation and release of the sequences (figure 2.8). The mixture is subsequently annealed to form the final origami structure. This method allows for all the sequences to be mass-produced in *E. coli*, significantly reducing the cost and facilitating large scale production of DNA origami[52].
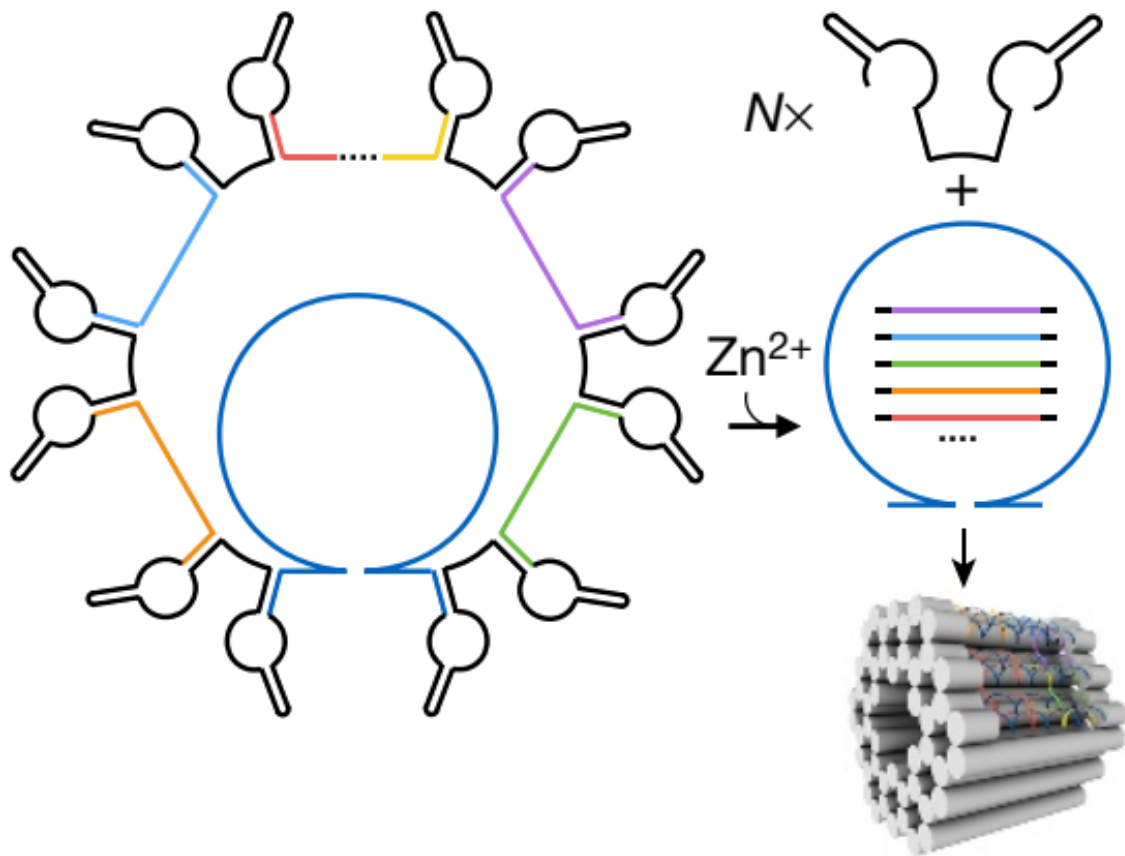
Figure 2.8. *Biotechnological production of DNA origami using self-cleaving DNAzymes. Reprinted from [52]*

2.4.5 DNA Origami Purification and Separation

Several methods have been tested to isolate, purify, and up-concentrate DNA origami.

Gel Extraction

Gel Extraction is a method used traditionally to separate DNA by first running it through gel electrophoresis, followed by excision of the desired band, and extraction of the liquid phase of the gel, which contains DNA. The liquid phase can be separated using the traditional "freeze and squeeze" method. Alternatively, the excised gel can be placed in a semi-permeable chamber and the DNA extracted by electrophoresis[53].

PEG Precipitation

In this method, poly-ethylene glycol (PEG) is used as a crowding agent for the depletion of mega-dalton scale DNA nanoparticles, while keeping oligonucleotides and incomplete assemblies in solution. This method is simple with high yields (>90%) and can be applied to a variety of DNA nanostructures. Moreover, it bypasses the filtration process (which may cause adsorption of the DNA to the filter) and gel contamination, while allowing for achieving higher concentration of DNA origami. However, PEG contamination may be introduced in

this method. Another limitation is that it includes larger off-target assemblies as well as the desired nanostructure in the precipitate. [54]

Ultra-Filtration

This method offers fast separation based on molecular weight cutoff of the ultra-filtration membrane. However, high ionic strength (eg 20 mM Mg^{2+}) decreases the yield. Another problem is that DNA nanostructures come in a variety of aspect ratios, which may result in decreased yields, for example in the case of long wire-frame origamis. Membrane adsorption is another problem associated with this method [40].

Size Exclusion Chromatography

Size exclusion chromatography (SEC) is mainly used in protein chemistry. The basis for SEC is separation of molecules/particles based on size, when passed through columns filled with porous particles. This method offers the advantage of excluding larger, multi-mer assemblies. DNA origami structures have been successfully separated using HPLC columns [40].

Microfluidic Separation and Concentration

Another less common but promising method for isolation of DNA origami structures is by using microfluidic separation systems. DNA origami structures alone or conjugated to gold nanoparticles have been successfully separated using dielectrophoretic forces [55]. Dielectrophoresis involves controlled movement of polarizable particles induced by alternating current non-uniform electric fields. Direct current-induced electrophoresis has also been used to separate colloidal particles [56] and DNA [57], and the technique can also be applied to DNA nanoparticles.

2.5 Polymerase Chain Reaction (PCR)

Polymerase chain reaction (PCR) was first introduced by Kary Mullis in 1983, and won him the Nobel Prize in chemistry. PCR remains as the method of choice for amplification of specific nucleic acid sequences via a cycle of denaturation, annealing, and extension, which happen at three different temperatures. The reaction involves Taq polymerase, a thermostable DNA polymerase as well as other ingredients. Numerous variations of this method are used for several biological and biomedical applications such as DNA sequenencing, cloning, site-directed mutagenesis, random mutagenesis, archeology, forensic sciences, and medicine. PCR the most accurate means of detecting specific pathogens.

2.5.1 PCR Components

The template DNA, as the names suggests, is the DNA sequence that contains the specific sequence that needs to be amplified. This specific sequence is designated by a pair of small oligonucleotides, known as primers, That bind to the two ends of the specific sequence, priming a polymerization reaction by Taq polymerase. Taq polymerase uses nucleoside triphosphates (dNTPs) to make a new strand of DNA. The reaction medium is buffered by Tris HCl, which is the buffer of choice for DNA applications as it protects DNA from degradation due to pH fluctuations. Other ingredients including magnesium, potassium, and ammonium are used in the reaction.

$MgCl_2$ is used in PCR mixtures at a final concentration of 0.5 to 5 mM. It acts as a co-factor for Taq polymerase. Mg^{2+} also interacts with the phosphate backbone of the DNA, resulting in higher T_m of the primers, thus improving the primer-template annealing and increasing yield. Mg^{2+} also bind the dNTPs and therefore should be present in excess. Too high an $MgCl_2$ concentration results in non-specific products.

KCl neutralizes the DNA backbone's charge, facilitating proper primer-template annealing during the elongation step, and enhancing stability by reducing repulsion between negatively charged DNA strands. This aids in initiating nucleotide addition by the polymerase from the bound primer. Lower KCl concentrations enhance long DNA segment amplification efficiency, while higher concentrations improve small product yield.[58]

Ammonium sulfate, $(NH_4)_2SO_4$, can replace KCl or be used alongside it to increases the specificity of PCR when used at 15-30 mM concentration. $(NH_4)_2SO_4$ destabilizes the hydrogen bonds between nucleotides, lowering Tm, and thus increasing the specificity of annealing. Other enhancers such as DMSO, formaldehyde, glycerol, and detergents are used are also used as PCR engancers.

2.5.2 PCR Procedure

The PCR reaction has three amin steps in a cycle: In the first step, called denaturation. the temperature is increased to 93°C, causing the template DNA to unfold and the two strands of the DNA to be separated. In the second step, known as annealing, the temperature is rapidly lowered to a few degrees below the melting temperature of the primer sequences, allowing complementary binding of the primers to the each of the DNA strands. In the third step, which is called elongation or extension, the temperature is raised to the optimal temperature for Taq polymerase activity, allowing the new strands to be polymerized. Repetition of this cycle results in exponential amplification of the part of the DNA designated by the primer pair.

2.5.3 Asymmetric PCR

Asymmetric PCR (aPCR) is variety of PCR whereby only one strand of the template DNA is preferentially amplified. It is a method to produce produce single-stranded DNA (ssDNA) from a double-stranded (dsDNA) template. ssDNA has applications such as in DNA aptamers, DNA probes, and DNA origami. ssDNA is amplified by adding unequal amount of forward and reverse primers in the PCR mixture. Once the limiting primer is depleted, the following cycles will involve only the excess primer. Unlike normal PCR reactions, the in aPCR amplification proceeds arithmetically rather than exponentially, leading to very low yield of the ssDNA product. Besides slow progression of amplification, other factors such as internal hybridization, and non-specific amplification contribute to the low efficiency of this method [59]. These problems can be ameliorated by a number of measures, including increasing the concentration of template, the asymmetric primer, and the Taq polymerase.

One aPCR modification, termed Linear-after-the-exponential PCR (LATE-PCR) increases the efficiency of aPCR by adjusting the melting temperature T_m of the primers using the nearest-neighbor equation, which takes into account the primer concentration, as well as GC content[60]. In another method, called primer-blocked PCR (PB-PCR), the same amount of

forward and reverese primers are present. However, most of the reverse primer is structurally modified to inhibit polymerase activity, thus eliminating non-specific products[61]. A copmparison between the conventional aPCR and the PB-PCR can be seen in figure 2.9 Ultimately, the aPCR reaction can be done in two steps. The first step entails a normal PCR that amplifies the desired region of the template DNA in dsDNA form. The dsDNA product is used as a template in the next step, where only one asymmetric primer is added to the mixture.
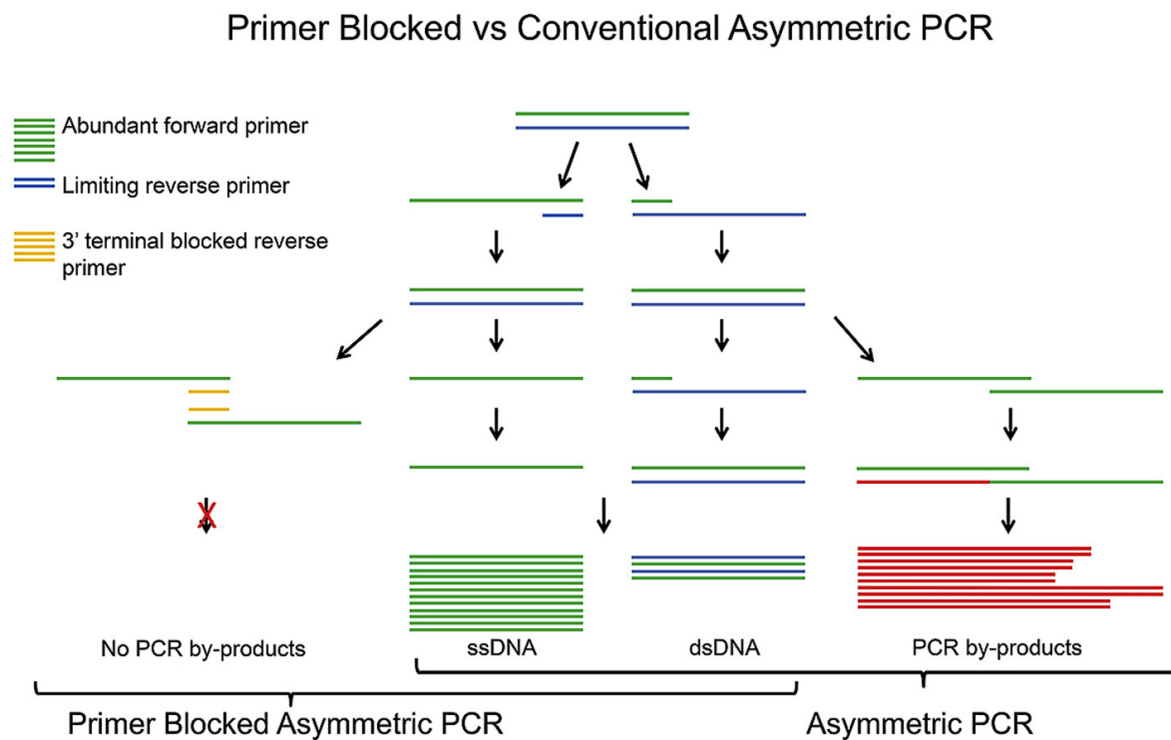
Figure 2.9. *Assymetric PCR and primer-blocked asymmetric PCR. figure source: [61]*

2.6   Solid Phase Peptide Synthesis

In the 1960s, a functionalized solid support that aminoacids could be attached to was introduced by Merrifield, conceiving the field of solid phase peptide synthesis (SPPS). The technique, still expanding and developing, has revolutionized synthetic peptide chemistry by allowing accurate, fast and high throughput synthesis of peptides with the desired sequence [62].

The first step in SPSS comprises fixation of a side chain- and amine-protected amino acid on a solid surface, often referred to as the resin, typically through covalent binding of the carboxyl group. Subsequent amino acids are then added one-by-one in cycles of deprotection and coupling.

In each step, first the N-terminal protection group is removed, without deprotection of the side chain. Then, the free N-terminus of the growing peptide is coupled to the activated carboxyl end of the next amino acid (also amine- and side chain-protected). The reaction continues in cycles until the last amino acid is attached. The peptide is then cleaved from the resin, and finally, the side chain protection groups are removed. The final deprotection

can be delayed if the peptide is required to undergo further chemical reactions, for instance specific attachment to a polymer. [63]

tert-butoxycarbonyl (Boc) and fluoren-9-ylmethyloxycarbonyl (Fmoc) are the most commonly used protection groups in SPSS. Fmoc chemistry is usually preferred as removal of Boc requires stronger acidic environment and the use of toxic HF. Fmoc, on the other hand, can be removed under mild conditions, typically 25% solution of piperidine in DMF [64].

Side chain protecting groups prevent nonspecific reactions of the functional groups on the side chains. In the case of cysteine, the acetamidomethyl (acm) protecting goup can be selectively removed with heavy metal salts, thus aallowing for controllable disulfide bond formation and cycliztion. Commonly used side chain protection groups in f-moc chemistry can be seen in figure 2.10 [63].
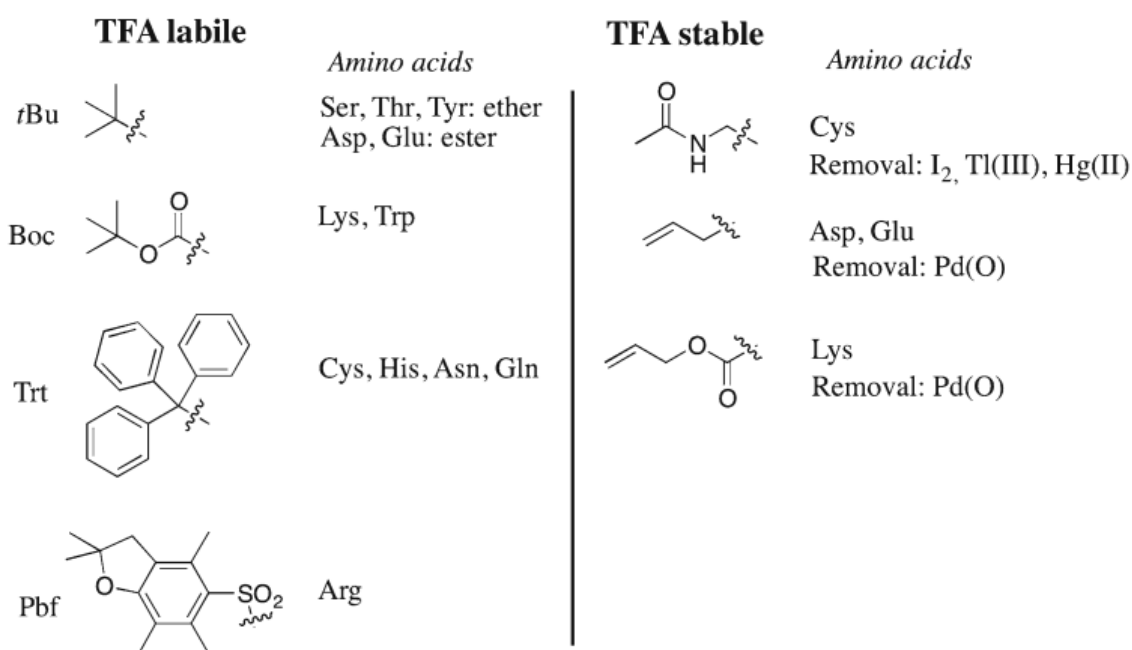
Figure 2.10. *Common side chain protecting groups for amino acids. figure source: [63]*

N-[(1H-benzotriazol-1-yl)(dimethy lamino)methylene]-N-methylmethanaminium hexafluorophosphate N-oxide (HBTU) is an *in situ* coupling reagent that provides fast coupling and low epimerization, as opposed to older coupling reagents that require an auxiliary nucleophile to prevent epimerization. *In situ* reagents have both electrophilic parts that interact with the carboxyl end, and nucleophilic parts that then activate the carboxyl end of the amino acid. This coupling agent is sometimes used in conjugation with a free amine such as N,N-Diisopropylethylamine (DEIA), which deprotonates the carboxyl group of the upcoming amino acid, this facilitating the electrophilic reaction of HBTU with COO^- (figure 2.11) [65]
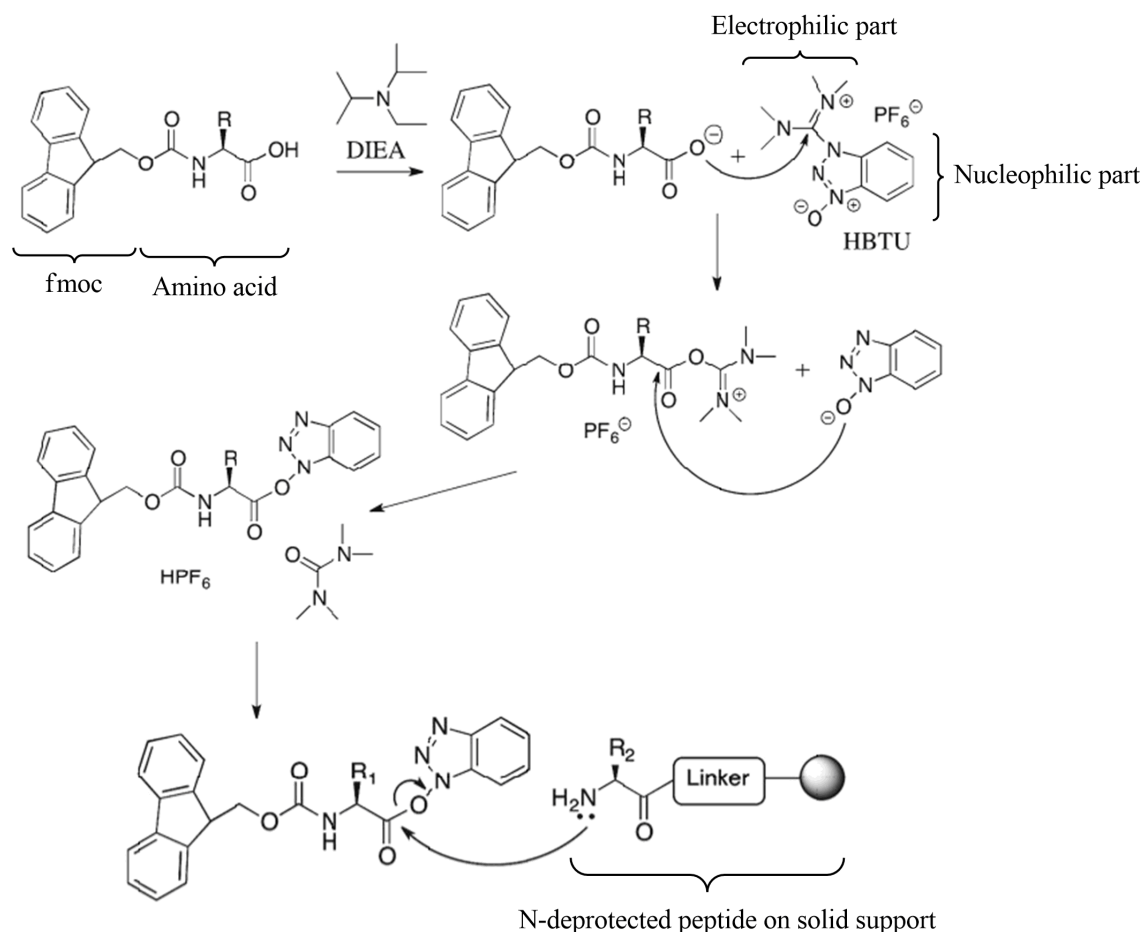
Figure 2.11. *Solid phase peptide chemistry using HBTU and DIEA. Piture from [63], with modifications.*

2.6.1 Cleavage and Deprotection

After the peptide sequence is completed, the peptide should be cleaved from the solid support, and the side chain protection groups should be removed. This can be done either in two steps (first the peptide is cleaved from the resin, then the side chain protection is removed), or in one step that combines cleavage and deprotection. The 4-alkoxybenzyl alcohol (Wang linker), which is most commonly used in Fmoc SPSS, can be cleaved with 50-100% trifluoroacetic acid (TFA) in DCM. [63]

The acidolytic cleavage and side chain deprotection reactions release reactive carbocations that may result in unwanted side reactions, some of which are irreversible. Scavengers are therefore used to prevent these side reactions. Some of these scavengers include water, triethylsilane (TES), ethanedithiol (EDT), and thiophenol. Some of these reagents such as EDT are extremely malodorous. An example of an unwanted side reaction is incomplete cleavage of Pbf from arginine, resulting in Pbf electrophile can alkylate nearby amino acids figure 2.12. The percentage of TFA, scavengers, and reaction time depends on the amino acid composition. In peptides with multiple Arg(Pbf) residues, stronger scavengers such as EDT, and longer reaction times should be used [66].

Once cleaved, the peptide is typically precipitated in ice-cold diethylether, which dissolves

most of the reagents and released protection groups, and resuspended in an acidic solution to remove TFA salts.
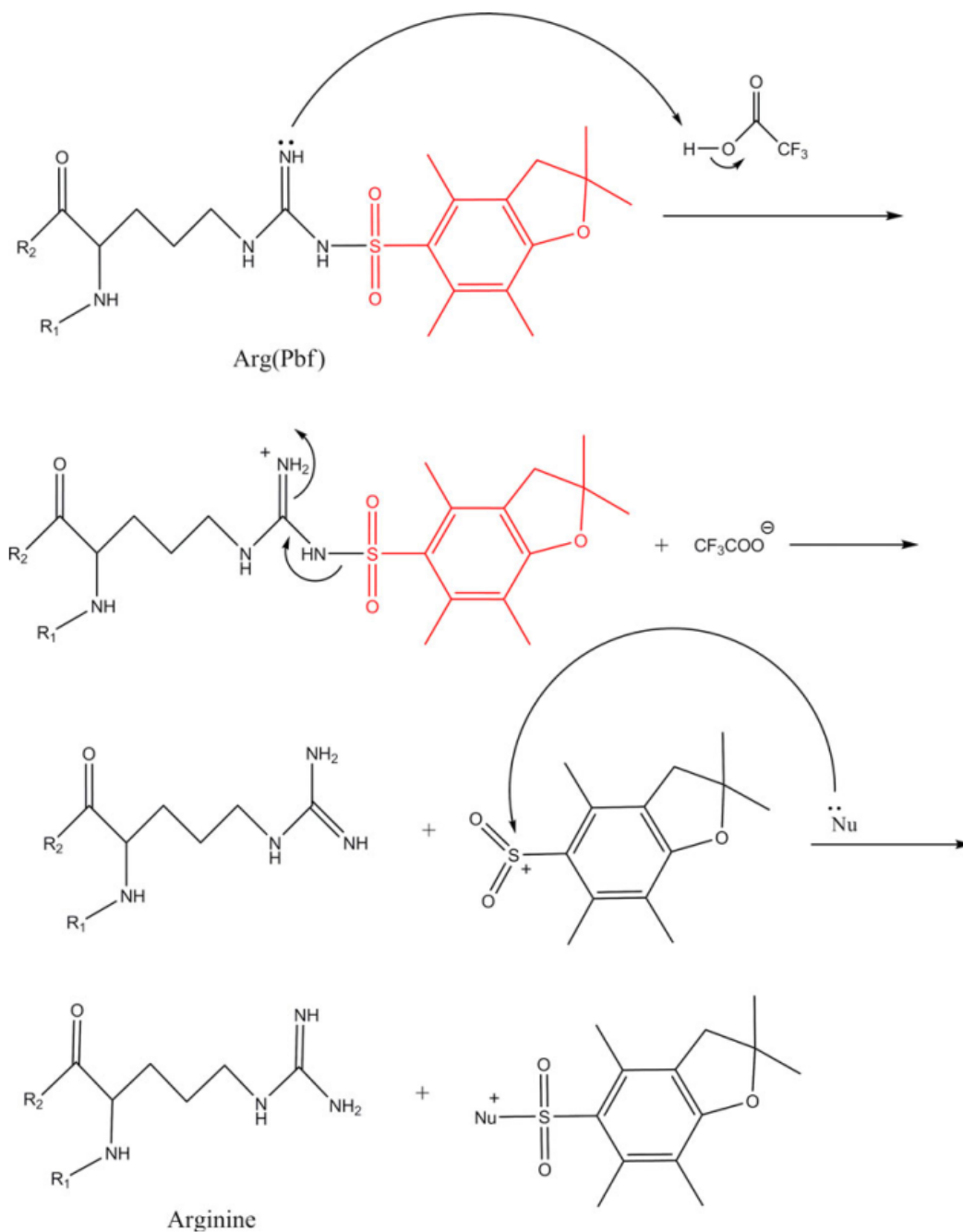
Figure 2.12. *Pbf cleavage from arginine. Picture source: [66]*

2.7 DNA Transcription

DNA transcription is a process whereby a DNA sequence is used as a template to generate a complementary RNA sequence. Many elements are involved in DNA transcription, including RNA polymerases and transcription elements. The resulting RNA sequences either code for a peptide/protein sequence, also known as messenger RNA (mRNA), or are involved in other structural, regulatory, and enzymatic activities of the cells (eg rRNA, tRNA, micro RNA,

long noncoding (lncRNA), etc.) [67].

Transcription starts by formation of the RNA polymerase complex as well as other initiation transcription factors to the promoter site on the template DNA. The RNA polymerase complex forms a transcription bubble by separating the two DNA strands. The RNA polymerase then adds ribonucleotides which are complementary to the anti-sense DNA strand. Once a short ribonucleic acid strand is formed (intiation step), the RNA polymerase moves along the DNA strand, adding more nucleotides to the emerging RNA strand with the help of other transcription elements (elongation). in eukaryotic systems, The RNA polymerase activity is terminated by template-independent addition of multiple adenines to the transcript, also known as poly-adenylation [67].

2.7.1 The CMV promoter

Promoter sequences are DNA sequences located upstream of the coding sequence that allow for attachment of RNA polymerase and other transcription factors. Other regulatory regions of the DNA, such as enhancers and silencers, may be present far away form the transcriptional start site. The promoter region may also contain CpG islands (hypermethylation of the CpG sites results in stable gene silencing), a TATA box (recognized by the general transcription factor TATA-binding protein (TBP)), and Transcription factor II B (TFIIB) recognition sites.

The human cytomegalovirus (CMV) has a dsDNA genome, which enters a lysogenic cycle and uses the host cell's transcription system [68]. The transctiption of the immediate early gene of the human CMV is dependent on a very strong enhancer/promoter. The CMV promoter is the most commonly used promoter in mammalian expression plasmids as it is active in a variety of mammalian cells and produces strong expression results [69].

2.7.2 Transcription of single-Stranded DNA

In the nature, ssDNA is transcribed from genomes or ssDNA viruses. Parvoviridae is a family of viruses that contain a linear ssDNA genome. Adeno-associated virus (AAV) is a member of this family. AAV infects humans and other primates. AAv is widely used as a viral vector for gene therapy. It is a replication-dfective evirus, meaning it cannot replicate unless co-infected with a helper virus, typically the adenovirus (hence the name Adeno-associated). wild-type AAV undergoes a lysogenic life cycle by intrgration in a specific site on chromosome 19. The lytic cycle can be activated by the helper virus[70].

The coding regions of AAV are flanked by inverted terminal repeats (ITRs). ITRs are 145 bases long and have a complex T-shaped structure. These repeats are the origins for DNA replication and serve as the primary packaging signal. ITRs are the only cis-active sequences required for making rAAV vectors. A recombinant AAV (rAAV) system can therefore be produced by taking out the viral ORFs and replacing them with the DNA sequence of choice[70].
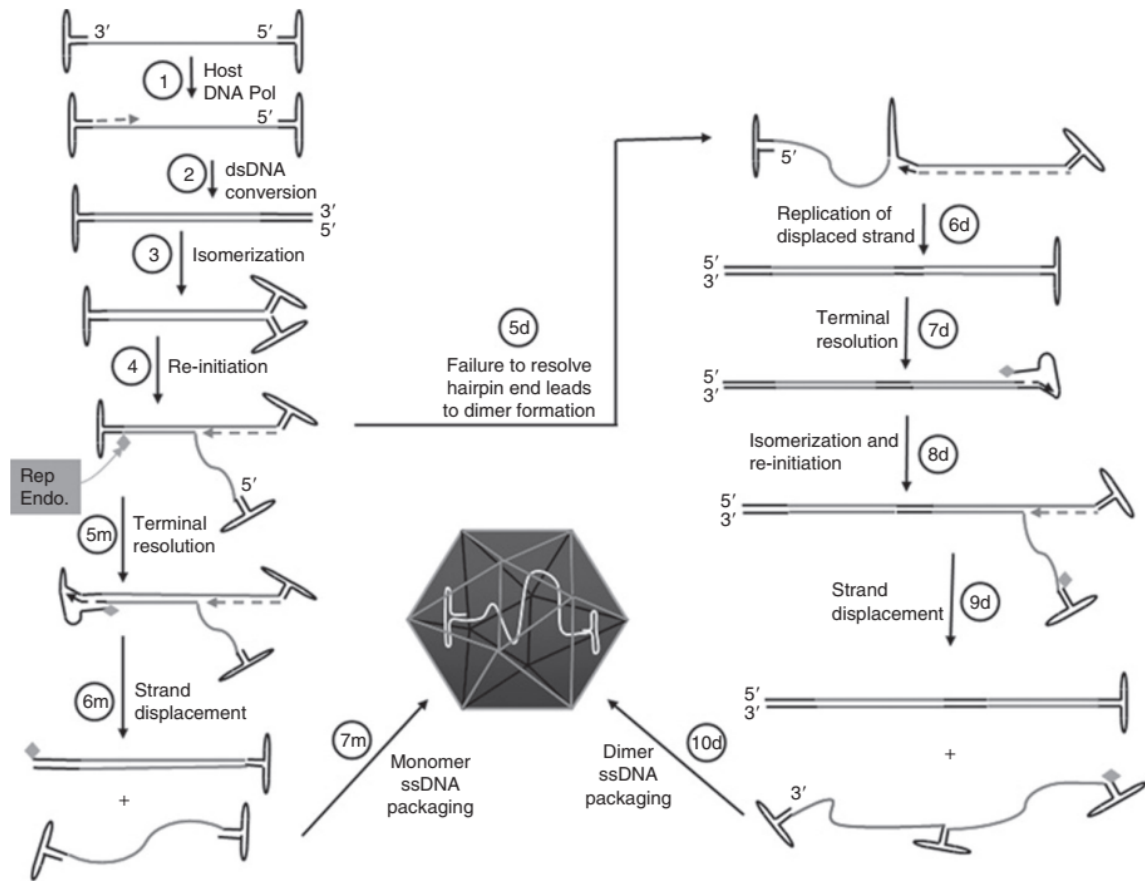
Figure 2.13. *The replication cycle of the AAV genome. left: with, and right: without a nick in by the REP viral protein. Taken from [71]*

Upon entry of AAV into the cells, a host DNA polymerase will extend the 3' end toward the 5' end, forming a dsDNA containing sequences for 2 ITRs. The ITRs will fold to form new initiation sites for DNA polymerase. The DNA sequence is nicked then by a REP, a specific viral protein, forming another 3' end OH that triggers synthesis of another strand, which finally leads to release of newly made ssDNA with to ITRs at each end. The ssDNA is then packaged into viral prticles. If REP does not recognize the restriction site on the DNA, the result would be a single-stranded self-complementary (sc) DNA. scAAV is therefore a highly common architecture for AAV gene delivery vectors. Although scAAV vectors provide a lower gene capacity compared to ssAAVs, ssAAV DNA should undergo a further replication step, while scAAV DNA can provide a transcription initiation site immediately. Therefore, scAAV has more efficient and more stable gene expression compared to ssAAV. ssAAV needs to go through a replication step to form the complementary strand, which is required for subsequent activation of the host cell transcription machinery. The additional replication (turning ssDNA to ds DNA) by host polymerases may result in eventual degradation of the foreign DNA sequence (figure 2.14) [71].
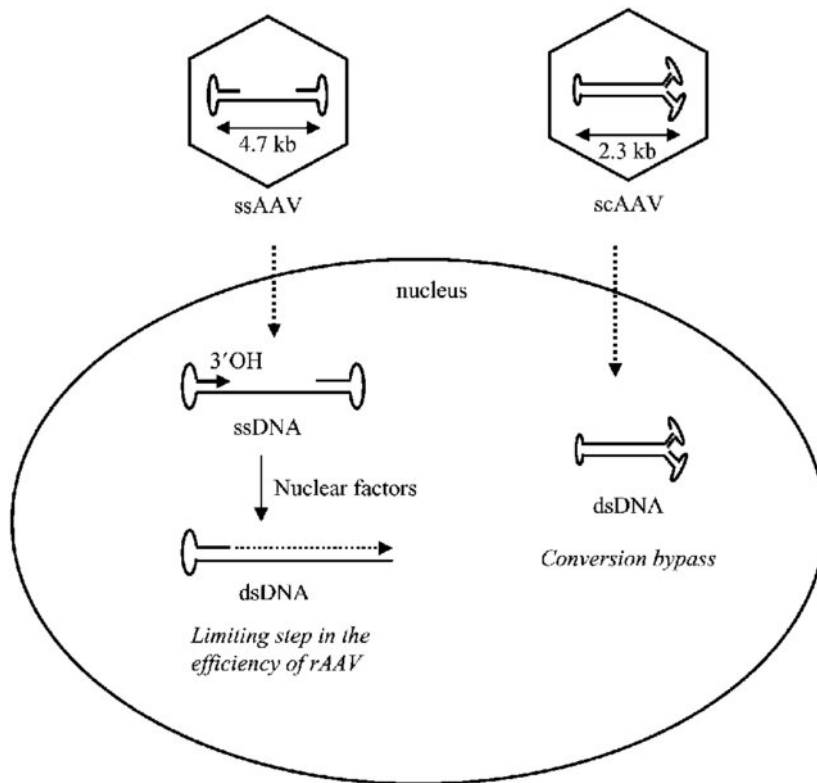
Figure 2.14. *A comparison of ssAAV and scAAV. Figure source [72]*

2.8   The pTagRFP-C Vector

The pTagRFP-C is a 4725 bp mammalian expression vector that encodes TagRFP, a red (orange) fluorescent protein figure 2.15.The codon usage of TagRFP is optimized for efficient expression in mammalian cells. Kozak consensus translation initiation site is positioned upstream of the TagRFP coding sequence. The Multiple Cloning Site (MCS) is positioned between the TagRFP coding sequence and the polyadenylation signal to facilitate fusion protein design[73]. The underlying structure of the vector includes the immediate early promoter of cytomegalovirus (PCMV IE) for protein expression., the SV40 origin for replication in mammalian cells, and the pUC origin of replication for propagation in *E. coli*, and the f1 origin of replication for producing single-stranded DNA. Kanamycin and Neomycin resitance genes are used as selection markers for bacterial and eukaryotic cells, respectively. [74]
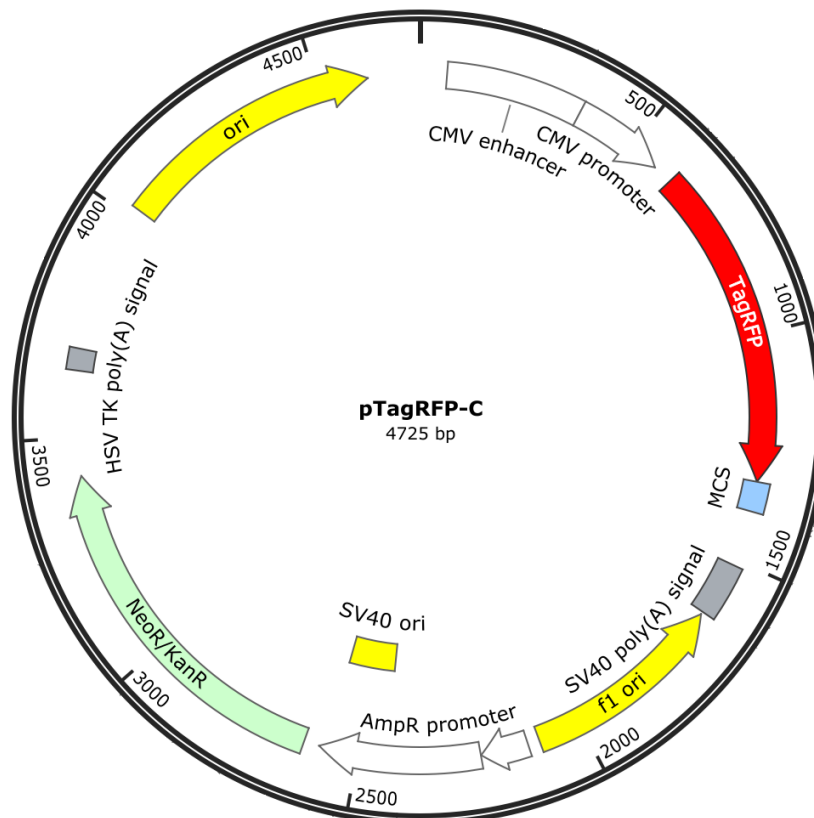
Figure 2.15. *The structre of the pTAGRFP-C vector used in this study. Picture generated by SnapGene ™*

The TagRFP protein structure contains four TagRFP protein chains arranged into two identical dimers, forming four beta-barrels (figure 2.16a). The chromophore structure includes Met63-Tyr64-Gly65 tripeptide(figure 2.16b), forming a 5-[(4-hydroxyphenyl)-methylene]-imidazolone chromophore. It exerts stable fluorescence when transfected into mammalian cell lines. The excitation and emission wavelengths for this protein is 555 and 584 nm, respectively [75].

(a)

(b)
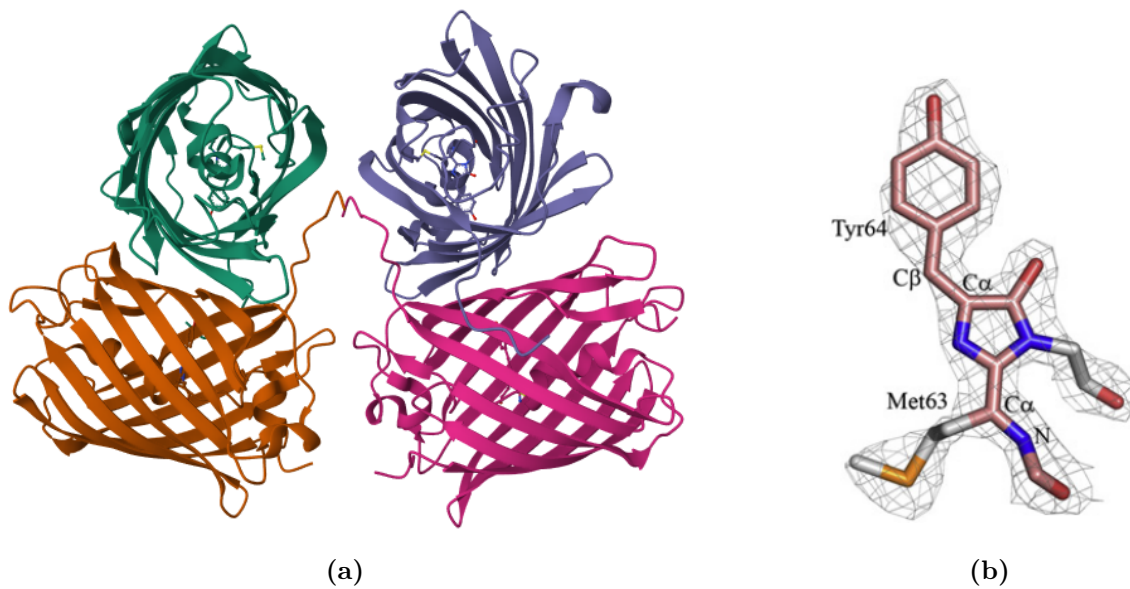
Figure 2.16. *a) the tetramer structure of TagRFP, b) The tripeptide Chromophore of TagRFP. Source: [75]*

Materials and Methods 3

3.1 Materials

A list of materials used in this study is provided in table 3.1

Table 3.1. *Chemicals and reagents*

Name	Other Name(s)	Lot number	Manufacturer	Use
10x Taq buffer+$(NH_4)_2SO_4$		1061028	Thermo Fisher	PCR reactions
AccuGENE Molecular biology water		8MB248	Lonza	Used in all tests regarding DNA
Acetonitrile		18C291590	VWR Chemicals	HPLC
Agar		BCCB1616	Sigma-Aldrich	culture media
Agarose		19H2056197	VWR Life Science	Agarose gel electrophoresis
BamH		10020678	NEB	DNA digestion
Calcein				Staining of live cells
Capric acid	Decanoic acid	1129483	Fluka	PEI modification
CutSmart \textregistered buffer	10x	1001506	NEB	DNA digestion
dATP	D-adenosine triphosphate	10105793	NEB	PCR reactions
DCM	Dichloromethane	V9L073289L	Iris Biotech	SPPS
DCM	Dichloromethane		Iris Biotech	SPSS solvent
dCTP	D-cytosine triphosphate	10105788	NEB	PCR reactions
dGTP	D-guanisine triphosphate	10105792	NEB	PCR reactions
DIEA	DIEPA, N,N-Diisopropylethylamine		Iris Biotech	SPPS coupling agent (-COOH activation)
Diethylether		V3B663013C	Iris Biotech	Peptide precipitation

Table 3.1. *Chemicals and reagents*

Name	Other Name(s)	Lot number	Manufacturer	Use
DMEM culture media			Gibco	HeLA cell culture
DMF	Dimethylformamide	P2F807112G	Iris Biotech	SPPS
DMF	Dimethylformamide		Iris Biotech	SPSS solvent
dTTP	D-thymidine triphosphate	10105791	NEB	PCR reactions
Duplex-Specific Nuclease		172170669	Evrogen	dsDNA digestion
EcoRI		151803	NEB	DNA digestion
EDC	1-Ethyl-3-(3-dimethylaminopropyl) carbodiimide	BCCC5909	Sigma	EDC/NHS chemistry
EDT	Ethane-1,2-dithiol	6018	Iris Biotech	Peptide cleavage
EDT	1,2 ethanedithiol			Peptide Cleavage
EDTA	Ethylenediamine tetraacetic acid	BCCF0095	Sigma	Chelating agent
Ethidium bromide	EtBr	SLBF7132V	Sigma	DNA intercalating agent, DNA visualization
HBTU	Hexafluorophosphate Benzotriazole Tetramethyl Uronium	110731	Iris Biotech	SPPS coupling agent (-COOH activation)
Hoechst	bis-Benzimide H 33258		Sigma	Nuclear staining of cells
Kanamycin monosulphate		104K01645	sigma	Antibiotic (Transformed \textit{E. coli} selection agent)
Lauric acid	Dodecanoic acid	1152452	Fluka	PEI modification
Lipofectamine 3000 Transfection Kit		2532085	Invitrogen	Transfection agent (positive control)
$MgCl_2.6H_2O$	Magnesium chloride hexahydrate	A0725033 730	Merck	Used in folding buffer and Origami AGE
$MgCl_2$ (PCR)		2622113	Thermo Fisher	PCR reactions
Muskuvite Mica V1 quality			Electron Microscopy Sciences	AFM substrate

Table 3.1. *Chemicals and reagents*

Name	Other Name(s)	Lot number	Manufacturer	Use
Mysristic acid	Tetradecanoic acid	080K1326	Sigma	PEI modification
NcoI		10012886	NEB	DNA digestion
NdeI		321802	NEB	DNA digestion
NHS	N-Hydroxysuccinimide	BCBF6027V	Aldrich	EDC/NHS chemistry
PAGE GelRed \textregistered	Nucleic acid gel stain	14P0731	Biotium	Staining ssDNA
PEG 8000	Polyethylene glycol 8000	85H0658	Sigma	Crowding agent
PEI	Poly-ethyleneimine	422595-	Sigma-Aldrich	Transfection agent
Piperidine				Deprotecting agent (N-fmoc removal)
PLL	Poly-L-lysine	75K2381	Sigma	Transfection agent
SOC Outgrowth Medium		10107463	NEB	\textit{E. coli} transformation
Sodium acetate				Buffering agent, ssDNA purification
Sodium chloride		22D144110	VWR Chemicals	LB medium ingredient
Taq Polymerase		981548	Thermo Scientific	PCR reactions
TFA	Tri-fluoroacetic acid	2115930	Iris Biotech	SPPS, HPLC
TIS	Triisopropylsilane	5433/0299552	Iris Biotech	Peptide cleavage
Tris base	Trizma \textregistered	SLCK7774	Sigma-Aldrich	DNA buffers, eg TAE, folding buffer, TE...
Tryptone	Peptone from casein	M0217W	VWR Chemicals	Culture media
Yeast extract		N0054W	VWR Chemicals	Culture media

3.2 *E. coli* Cell Culture

LB and LB-agar media was prepared according to the following recipe:

Ingredient	Amount
Tryptone	10 g
Yeast extract	5 g
NaCl	5 g
Agar (only for LB-agar)	15 g
MilliQ water	up to 1000 mL

The mixtures were autoclaved at 121 °C and 1 bar for 30 minutes. In order to make the media selective for transformed cells, the medium was supplemented with kanamycin to a final concentration of 30 mg/L, using a stock solution corresponding to 30 mg/mL kanamycin base in autoclaved Milli-Q water. The antibiotic was added when the medium was cooled to about 50°C,

LB-agar-kanamycin plates were made by pouring about 20 mL of the media to petri dishes and stored at 4°C.

3.3 *E. coli* Cell Transformation

Competent DH5α *E. coli* cells were retrieved from -80°C and thawed on ice. 40 µL of the cell suspension was added to a microtube and 10 µL was added to another microtube as control. 5 µL of the plasmid was added to the cells, mixed gently, and incubated on ice for 30 minutes. The microtubes were placed in a heat block (Eppendorf Thermomixer Comfort) at 42°C for 45 sec and put back on ice for 2 min. 0.5 mL of SOC medium, preheated to 37°C, was added to each tube, and incubated on the heat plate at 37°C and 400 rpm. 100 or 200 µL of each tube was added and spread on LB-agar-kanamycin plates and the plates were incubated overnight at 37°C. The plates were then observed for bacterial growth.

For production of pDNA, A single colony from LB-kanamycin plates was taken and incubated in 5 mL of LB-kanamycin medium in 15 mL culture tubes, and incubated overnight at 37°C and 270 rpm.

3.4 Plasmid DNA Isolation

Plasmid DNA was isolated from transformed *E. coli* cells using a GeneJet Plasmid Miniprep kit (Thermo Scientific) according to the manufacturer's instructions with minor modifications. The cells from each incubation tube were centrifuged at 6000 rcf for 5 minutes. 250 µL of Suspension solution was added to the pellets and vortexed. 250 µL Lysis buffer was then added and inverted 4-6 times, before addition of 350 µL Neutralization solution and 4-6 times inversion. The mixture was centrifuged at max rcf for 15-20 minutes. The supernatant was transferred to the spin column and centrifuged by a MiniSpin centrifuge (Eppendorf) at 12000 rpm for 1 min. Next, 500 µL Wash solution was added and spun for 1 min, which was repeated twice. The residual Wash solution was eliminated by centrifugation for 1 min. 50 µL of Elution buffer was then added and centrifuged for 2 min. The flow-through was collected and tested by AGE and Picodrop.

3.5   Agarose Gel Electrophoresis

Agarose gel electrophoresis (AGE) was carried out in several steps of this study, in order to identify, characterize, and extract various DNA fragments. Unless otherwise stated, the AGE protocol was done as follows: a stock solution of 1% agarose in 1x TAE buffer was prepared by adding agarose to TAE buffer and microwave pulses of 30 sec until the gel was molten and the solution was clear. The stock solution was made for up to 10 gels, and kept at 60°C. To cast the gel, 0.5 µL of ethidium bromide (10 mg/mL) was added to 30-35 mL of the agarose solution, gently mixed, and poured in a gel cassette with a suitable comb. The cassette containing the solidified gel was placed in a Mini-Sub Cell GT from BioRad filled with 1x TAE buffer.

The samples were prepared by mixing the DNA product with 6x loading dye at 5:1 ratio and mixed by pipetting up and down. 2 to 5 µL of 10 kb DNA ladder was used to determine the DNA length. The gel was run at 95 V until the visible dye reached the desired length in the gel. The bands were visualized under UV radiation.

3.5.1   Denaturing Agarose Gel Electrophoresis

Since ssDNA assumes multiple conformations in a native gel, denaturing gel electrophoresis was carried out. The running buffer was 1x TAE buffer containing 1 M urea. 2% agarose gel was also made using 1 M urea 1x TAE buffer. In order to better visualize ssDNA, 10000x GelRed was used instead of ethidium bromide;1 µL of GelRed was added for each 10 mL of the agarose solution. The loading buffer was also made in-house and contained 8 M urea, 1% v/v tritonX, 1 mM Tris, and minimal amount of bromophenol blue. The samples were mixed with the equal volume of the loading dye, incubated at 85°C for 10 min, and incubated on ice for 1 min before being loaded on the gel. The gel was run at 4°C (cold room) and 60-65 V, and then visualized under UV irradiation.

3.5.2   DNA Origami Agarose Gel Electrophoresis

For DNA origami AGE experiments, 0.5x TAE supplemented with 5 mM $MgCl_2$ was used to make the gel and run the electrophoresis. Due to heat generation, lower voltages were used and the running chamber was surrounded with packs of ice.

3.6   DNA Digestion

In order to confirm the presence of the pTAG plasmid, different nucleases were used and the expected fragments were investigated. The enzymes were selected based on availability and the presence of a restriction site on the plasmid. A list of the enzymes used and the expected fragments can be seen in table 3.2.

Table 3.2. *Restriction endonucleases and the expected fragments from digestion. source:[73]*

Enzyme (s)	Fragments size (bp)
NdeI, EcoRI	1119, 3606
NdeI, BamHI	1150, 3575
NCoI	251, 1867, 703, 1904

To digest the pDNA, the following mixture was prepared:

Plasmid	5 µL
10x CUTsmart buffer	2 µL
1st enzyme	1 µL
2nd enzyme	1 µL
DNA water	To 20 µL

First, DNA water was added to a microtube, followed by 10x CUTsmart buffer. The enzymes and plasmid were added afterward and mixed, and then incubated at 37°C for 30 minutes. Afterwards, 4 µL of 6x loading dye was added to the microtube, mixed, and loaded onto a 1% agarose gel to perform AGE.

3.7   Polymerase Chain Reactions (PCR)

Polymerase Chain Reaction (PCR) was performed in two steps. The goal of the first step was to generate a 1.9 kb dsDNA using pTag plasmid as template. The dsDNA would then be used in the next step to generate ssDNA scaffold using the asymmetric PCR method. The first step was initially attempted by the protocol from [7], but since no results were observed, different concentrations of the template, as well as different annealing temperatures were used to optimize the reaction.

Table 3.3. *PCR reaction components and their volumes.*

Reagent	Volume (µL)	Final Concentration
10x PCR buffer ($(NH_4)_2SO_4$)	5	
$MgCl_2$ (25 mM)	6	3 mM
dNTP (20 mM)	4x 0.5	0.8 mM
Primer forward (100 mM)	0.5	1 mM
Primer reverse (100 mM)	0.5	1 mM
Template DNA	1	120 ng / vial
Taq polymerase	0.5	0.5 U / vial
DNA water	Up to 50	

Table 3.4. *PCR program for amplification.*

Step	Temperature (°C)		Time
Initial denaturation (hot start)	94		5 min
Denaturation	94	x35 cycles	30 sec
Annealing	53 or 45		30 sec
Extension	72		2 min
Final extension	72		10 min

For asymmetric PCR, the following mixture and programs were used:

Table 3.5. *PCR reaction components and their volumes.*

Reagent	Volume (μL)	Final Concentration
10x PCR buffer ($(NH_4)_2SO_4$)	5	
$MgCl_2$ (25 mM)	6	3 mM
dNTP (20 mM)	4x 0.5	0.8 mM
Asymmetric primer (100 mM)	2	4 mM
Template DNA	1	160 ng / vial
Taq polymerase	0.5-1	1 U / vial
DNA water	Up to 50	

Table 3.6. *PCR program for amplification.*

Step	Temperature (°C)		Duration
Initial denaturation (hot start)	94		5 min
Denaturation	94	50 cycles	30 sec
Annealing	53		30 sec
Extension	72		1.5 or 2 min
Final extension	72		10 min

3.8 DNA Purification and Up-Concentration

3.8.1 Purification of dsDNA

DNA purification is required to eliminate salts, un-reacted dNTPs, etc. which may hinder the results of further enzymatic activities. PCR products of the first step were purified using a enElut™PCR clean-up kit (Sigma-Aldrich USA) according to the manufacturer's instructions. The cleanup process consists of column preparation, DNA binding and loading on the column, washing, and elution. In order to up-concentrate the PCR product, the binding step was repeated multiple times before the final wash and elution step, thus combining the PCR product from multiple PCR reactions in the final solution. The cleanup product was either used directly in the aPCR reaction, or ran on an agarose gel and extracted using a GeneJet Gel Extraction kit to remove pDNA, which may cause non-specific products in the aPCR reaction.

3.8.2 Purification of ssDNA

The products of aPCR reactions were cleaned up using a NEB PCR cleanup kit according to the manufacturer's instructions. The NEB cleanup kit uses isopropanol instead of ethanol in the binding step and is thus more suitable for ssDNA and smaller fragments. ssDNA product was separated from the dsDNA template by AGE. Different methods were tested for extraction of ssDNA from the gel. was extracted gel slice containing before formation of origami structures. The cleaned and up-concentrated product was thus run on an agarose gel and extracted from the gel.

Ethanol Precipitation

The gel slice containing ssDNA was frozen, then crushed between two leayers of parafilm and thawed. This is done to disrupt the gel matrix structure. The liquid and bits of the gel were added to an Ultrafree®-DA gel extraction spin column. The column consists of a conical

structure that turnes the gel into an slurry and a filter that retains the agarose and passes the liquid containing DNA. The column was spun at 10000 rpm for 10 min until all the liquid had flown through. To precipitate DNA, 1:10 volume of 3 M sodium acetate and 2x volume of 96% ethanol, cooled to 4°C. The mixture was centrifuged at 15000 rcf for 20 min at 4°C. The supernatant was carefully discarded and the pellet was washed again in 400 µL of 70% ethanol and centrifuged again at 15000 rcf for 15 min at 4°C.

Electroelution from Agarose Gel

For electroelution from agarose gel, a two-layer agarose gel was prepared as described by Bellot and co-workers [53] with modifications. first, 4% agarose solution in the running buffer was cast and allowed to solidify. A top layer of 1% agaorse gel cooled to about 40°C was poured on the solidified 4% layer. The gel was loaded in an empty electrophoresis chamber. The samples were then loaded in the wells. The running buffer was gradually added to the chamber to a level just below the gel to allow for passage of current without the gel being completely submerged. The AGE gel was monitored under UV light to observe the movement of bands. Once the desired band was sufficiently separated, a hole was punched just below the band with a depth equal to that of the top layer. The hole was then filled with the electrophoresis buffer. The electrophoresis was continued until the band had migrated into the well. The liquid inside the well was then removed by pipetting.

3.8.3 Electrodialysis of Agarose Gel

Gel slice containing ssDNA was placed in a dialysis tube with 100 kDa MWCO (Spectra-por), the empty spaces in the tube was filled with 1x TAE buffer and the tubewas sealed on both ends. The tube was immersed in AGE chamber containing 1xTAE buffer and ran at 90 V for 20 min. The buffer inside the dialysis tube was precipitated by isopropanol, resuspended with binding buffer from NEB PCR cleanup kit, which was subsequently up-concentrated and cleaned using the same kit.

3.9 Formation of DNA Nanostructures

All the staples (S1-S18) and fragments (1a-10b) were added to the folding mixture at a final concentration of 200 nM. The scaffold was added at 200 nM, providing a 1:10 scaffold: fragment ratio. 10x folding buffer was made as previously described (cite important) and contained (50 mM Tris, 10 mM EDTA, 50 mM NaCl) containing 200 mMvMgCl_2. Therefore, the final mixture contained Mg^2+ at 20 nM. The components were mixed by pipetting, and annealing was performed using a thermocycler with an initial incubation at 65 °C, followed by 41 cycles of incubation, cooling by 1 °C every 45 minutes (total incubation time was 30 h and 46 min).

3.10 Purification of DNA Nanostructures

Different methods were tested in order to find the most feasible method for purification of DNA nanostructures.

3.10.1 PEG Precipitation

PEG 8000 was used as a crowding agent to precipitate high Mw DNA while keeping oligonucleotides in solution [54]. The precipitation buffer contained 15% (w/v) PEG 8000, 5 mM Tris, 1 mM EDTA and 505 mM NaCl. Equal volume of the the precipitation buffer was added to $50\,\mu$L of the folding mixture, gently mixed by tube inversion, and spun at 18000 rcf for 25 min at room temperature. The supernatant was removed by pipetting, and the pellet was re-suspended in $20\,\mu$L of TB supplemented with 20 mM magnesium.

3.10.2 Ultrafilteration

Ultrafilteration was performed as previously described [40]. Amicon ULtra-2 centrifugal filter unit with a MWCO of 100K was used. The filter was conditioned by adding $500\,\mu$L of 1x folding buffer and centrifuging at 5000 rpm for 5 minutes. Then the sample was added to the fliter and spun at the same conditions until all the liquid flowed through the filter. $20\,\mu$L of 1x folding buffer was added to the filter and the filter was placed back to the tube in the reverse configuration. The tube was spun at 12500 rpm for 4 minutes, and the liquid was collected.

3.10.3 Electrodialysis

In order to avoid contamination from the gel, electrodyalisis was performed to remove excess staples and fragments. The folding product was loaded in a dialysis tube with 100 kDa MWCO (Spectra-por), which was sealed on both ends. The tube was immersed in AGE chamber containing 0.5x TAE supplemented with 11 or 5 mM $MgCl_2$, running at 85 V, while cooled by ice on the sides. The tube stayed for 15-20 minutes, reversed, and let for additional 2 min.

3.11 Solid Phase Peptide Synthesis

Peptide synthesis was carried out by Fmoc chemistry using an Activo-P11 Automated Peptide Synthesizer (Activotec, UK). The required reagents were calculated by the softwarename software based on the sequence. A list of reagents needed for the synthesis can be found in section A.2 Coupling agents and aminoacids were prepared according to the worksheet provided by the software.

Cleavage and deprotection of synthesized peptide was done by a P-14 cleavage device (Activotec, UK). 4 mL of freshly prepared cleavage cocktail (TFA, TIS, H_2O, 95:2.5:2.5 v/v) was added to the reaction vial and loaded on the cleavage device. After running for 45 minutes, the solvent was collected in a 50 mL Granier tube. Next, 6 mL of TFA was added to the reaction vial and inverted for another 5 minutes and gathered in the tube. To precipitate the product, 20 mL of diethylether (cooled down to -20°C) was added to the Granier tube. The tube was centrifuged at 6500 rcf for 5 minutes, and the supernatant was discarded. The remainder of the diethylether was left to evaporate under a fume hood. To remove the TFA salts, the precipitate was re-suspended in glacial acetic acid, frozen, and freeze-dried [76]. The crude product was analyzed by HPLC.

3.12 Liquid Chromatography (HPLC)

HPLC analysis was carried out using an Ultimate 3000 HPLC machine.

For analytical HPLC, a Jupiter 5U C16 analytik 300 A column was used. The solvent system was 0.1% TFA (solvent A) vs. acetonitrile (solvent B). About 10 mg of the product was dissolved in 400 µL 0.1% TFA, and injected to the HPLC machine. The gradient started at 100% solvent A, decreasing linearly to 20% over 40 min, then increasing again to 100% solvent A over 20 minutes. The flow rate was set at 1 mL/min.

For preparative HPLC, a Jupiter 5u C18 300A semi-prep column was used. 50 mg of the product was dissolved in 2 mL 0.1% TFA and injected into the device. The solvents used were 0.1% TFA in water (solvent A) and acetonitrile (solvent B) and the flow rate was 4 mL/min. The gradient was initiated with 100% solvent A, changing linearly to 80% solvent B over 40 minutes. then returning to 100% solvent A over 20 minutes.

The fractions were collected using an automated ACF-3000 fraction collector (Thermo Scientific). In all HPLC experiments, the column was equilibriated at 100% solvent A for 30 min before injection of the samples. After the final experiment, the column was washed at 65% acetonitrile and and 35% MiliQ water for 30 min.

3.13 Mass Spectrometry

Liquid Chromatography-Electrospray Ionization Mass Spectrometry (LC-ESI MS) was performed to identify the content of each HPLC fraction obtained from semi-preparative HPLC (section 3.12). The fractions were dissolved in 1 mL 0.1% (v/v) formic acid in water inside. The tubes were vortexed and centrifuged for 2 minutes at max rpm for two minutes to exclude any undissolved particles. The supernatant was transferred to special sample vials and inserted in the LC-MS spectrometer automated sample tray. The analysis was carried out by HPLC-DAD-HRMS using a Hitachi LaChrome Elite (Hitachi Ltd., Tokyo, Japan) HPLC system equipped with a pump (L-2130), autosampler (L-2200), column oven at 40°C (L-2300) with a Hexyl-Phenyl column (150 × 4.6 mm Ascentis Xpress 2.7 µm, Sigma-Aldrich, St. Louis, MO, USA) and a DAD detector (L-2450) recording from 190 to 900 nm. The setup was coupled to a high-resolution mass spectrometer (Bruker compact MS ESI-qTOF, Bruker Daltonics, Bremen, Germany) (operated in positive mode with capillary: 4500 V, end plate offset 500 V, 4 L/min dry gas at 200°C) through a 5:95 flow splitter.

The solvents used were 0.1% formic acid in water (solvent A) and 0.1% formic acid in acetonitrile (solvent B) and the flow rate was 1.2 mL/min. The gradient was initiated with 98% solvent A and 2% solvent B, changing linearly to 30% solvent A and 70% solvent B over 17 minutes, then raised to 100% solvent B and held for five minutes.

The LC-MS was controlled by HyStar v. 3.2 (Bruker Daltonics) and the data analysis was done in Compass DataAnalysis v. 4.2 (Bruker Daltonics).

3.14   Modification of PEI

EDC/NHS chemistery was applied to attach fatty acids with varying side chains to the primary amines of PEI. The carboxylic acid groups were activated by addition of EDC and NHS at the same molar amount as the substituents and incubated at room temperature and stirring for 2 h. PEI solution (50 mg in 2 mL water) was then added drop-wise to the stirred mixture, and incubated overnight. The solution was then dialysed in a Spectra Por dialysis tube with molecular weight cut-off (MWCO) of 12-14 kDa against water for 24 h. After dialysis, the solutions were freeze-dried and stored at -20°C.

3.15   Gel Retardation Assay

In order to determine whether the peptide or polymers interact with and complex DNA, pDNA was complexed with PEI, TAT, PLL, or modified PEI at varying carrier to plasmid (c/p) weight ratios. Each of the polymers were prepared as 50 ng/µL in molecular biology water and added in different amounts to 100 ng DNA. The final volume of all samples were adjusted to 5 µL using DNA water. 1 µL of 6x loading dye was then added to each sample, mixed and run on a 1% agarose gel at 90 V.

3.16   Ninhydrin Assay

The ninhydrin assay was used to determine the level of substitution of primary amines on PEI, in order to evaluate the outcome of the reaction and estimate the extent of substitution. 2,2-dihydroxyindane-1,3-dione, also known as Ninhydrin is a compound that reacts mainly with primary amines to form a colored dimer known as the Ruhemann's purple [77]. A brief schematic of the the reaction of ninhydrin is summarized in figure 3.1 :
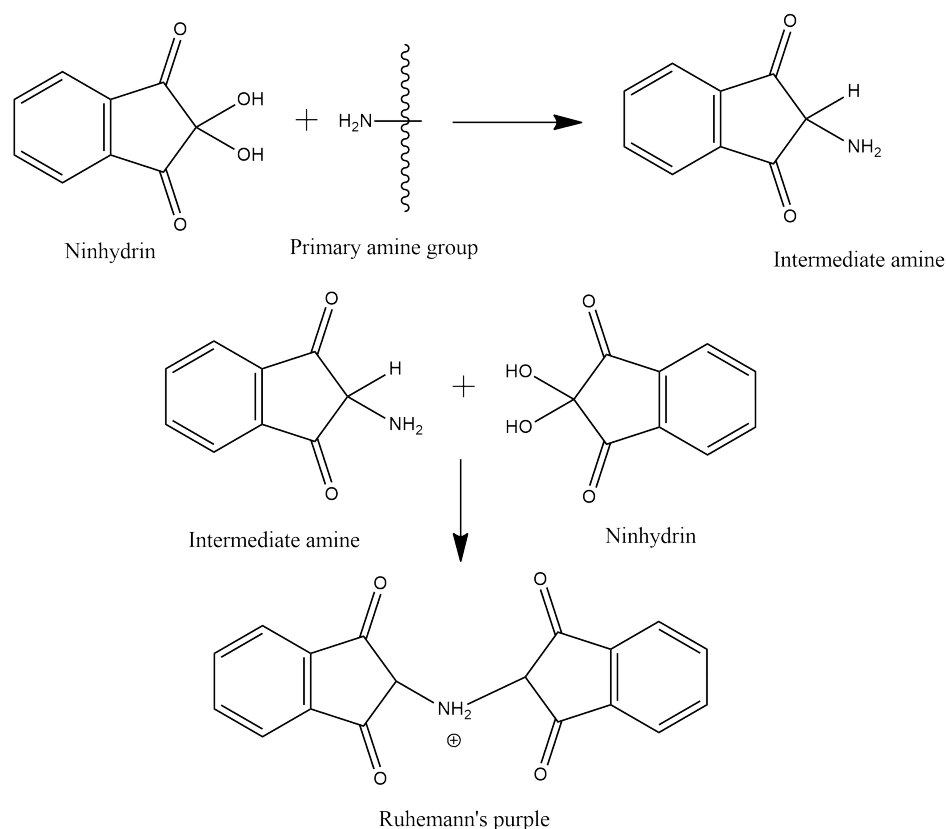
Figure 3.1. *Mechanism of reaction of nindydrin with primary amines (Image generated using ChemDraw Ultra 12.0 software)*

In order to perform the assay, a ninhydrin stock solution of 100 mg/mL in absolute ethnol was prepared. In order to make a standard curve, PEI solution in PBS (pH=7.4) was prepared at concentrations ranging from 0 to 10 mg/mL, with 1 increments. Three concentrations of the modified PEIs were also prepared in PBS. The ninhydrin solution was added to each of the samples to a final concentration of 5 mg/mL. The samples were vortexed, and incubated at 70°C and 250 rpm for 39 min on a heat plate. The tubes were then centrifuged at max rpm for 3 minutes and the supernatant was collected in another tube. The liquid was split in three in 96-well plates. Absorbance at 570 nm was then read using a plate reader. The blank sample (PBS+ninhydrin) underwent the same treatment and was used to subtract background. The equivalent PEI concentration for each of the modified samples were determined using linear regression. The amount of reacted pimary amines were calculated using the equivalent PEI concentrations. For calculation details, see section A.1.

3.17 HeLa Cell culture

HeLa cells were used throught the transfection studies. Dulbecco's Modified Eagle Medium (DMEM) suplemented with 10% fetal bovinve serum (FBS) 1% Penicillin-Streptomyin was used in cell culture. Serum-free DMEM was used in some cases for transfection studies.

Passaging cells

HeLa cells were maintained in culture flasks at 80-100 % confluency. For cell's continuous growth while avoiding overpopulation of cells, the cells were passaged to new flasks. The

media from the old flask was removed and the cells were washed by sterile PBS once. Then an appropriate amount of trypsin/EDTA tock solution was added to the cells, gently swirled to cover all of the cells and incubated at 37°C for 5 to 10 min. The flasks were gently tapped on a surface to fascilitate detachment of the cells. The trypsin was then deactivated by addition of 3 times the volume of growth medium. The detached cells were then mixed by pipetting and 10 µL of the cell suspension was used for cell counting. The cell suspenson was then spun at 300 rcf for 5 min at room temperature. The supernatant was discarded and the cells were re-suspended in suitable amount of medium for cell culture.

Cell Counting

10 µL of the cell suspension was added to a hemocytometer. An optical microscope was used to count the number of cells in 4 quadrants. The total number of cells in the suspension can be calculated as:

$$\text{Total number of cells} = \left(\frac{\text{Sum of all counted cells}}{\text{Number of quadrants}}\right) \times \text{Total volume of cell suspension} \times 10^4$$

(3.1)

3.18 Alamar Blue Viability Assay

HeLa cells were seeded in 96-well plate at a concentration of 5000 cells per 200 µL medium per well. The plate was incubated for at 37°C for 24 hours. Based on the results from gel retardation assay, (section 3.15) polyplexes containing 200 ng of DNA and different ratios of polymers were added to each well (in triplicate) and incubated overnight. Then, 20 µL 10x alamar blue stock solution was added to each well and incubated at 37°C for 2 additional hours. The culture media was then moved to another 96-well plate and fresh media was added to the wells. The medium from each well was split into 2 wells 100 µL each. The alamar blue fluorescence was measured by a ..... plate reader at the excitation and emission wavelengths of 530 and 555, respectively. Three wells containing culture media were used to measure background fluorescence. Optical microscope images were taken before and after incubation with the polyplexes.

3.19 Transfection Assays

All transfection-related studies were performed on HeLa cell line. The amount of reagents based on the size of the wells are shown in table...Hela cells were seeded in 96-well plates, 24 well plates, or 8-well chambered coverslips and incubated oyvernight. The samples were then added. In case of short term transfection, the medium was removed and serum-free DMEM was added before addition of polyplexes. After 6 h of exposeure, the serum free medium was replaced with serum-supplemented medium and left overnight. The samples were then observed using a fluorescent microscope for detection of cells expressing TagRFP. Lipofectamine™3000, a commercially available transfection agent was used as positive control. In the case of lipofectamine™, 100 ng DNA was diluted in 5 µL serum-free DMEM, and P3000™Reagent (2 µL µg^{-1} DNA) was added. in another tube, 0.15 or 0.3 µL Lipofectamine™3000 reagent was added to 5 µL of serum-free media. The diluted DNA

was then added to the diluted Lipofectamine solution and incubated for 15 min at room temperature. The mixture was then added to each well and incubated for 24 or 48 hours. The cells were then stained and visualized by fluorescent microscopy. The tested polyplexes were made in the same way but without the P3000™Reagent. Once the assays were set up, the transfection study was done using DNA origami-like structures.

3.20   Cell Fixation

Cell fixation was done using 4% formaldehyde solution in PBS and tritonX-100 0.1% in PBS as permeabilization agent. The cell culture medium was removed and cells were washed with PBS. Then, formaldehyde solution was added and incubated at room temperature for 15 min. The formaldehyde solution was removed and the cells washed with PBS. Triton-X was added to the wells and incubated for 5 min. The solution was then removed and cells were rinsed with PBS twice before staining.

3.21   Cell Staining

In order to compare the number of cells expressing the reporter TagRFP to the number present in the well, nuclear staining was carried out by Heochst. The cells were incubated with .... Hoechst solution for 30 min at room temperature while protected from light. The staining solution was then removed and the cells were washed with PBS before microscopy.

Calcein.. was also used in the staining to determine the amount of live cells. In case of calcein and Hoechst staining, the dyes were added to culture medium at ratios of 1:5000 for Hoechst and 1:1000 for calcein. The cell media was then replaced with dye-containing media and the cells were incubated for 45 min at 37°C.

3.22   Fluorescent Microscopy

The cells were observed using a Zeiss inverted fluorescence microscope. The images were processed using the Zeiss Zen 3.7 software. Alternatively, some samples were observed using an Olympus fluorescent microscope. Images obtained from this microscope were processed by the Opencv Python package.

Results and Discussion 4

4.1   Production and Characterization of Plasmid DNA

4.1.1   Plasmid DNA Production

E.coli cells were transformed by the pTagRFP-C plasmid. The transformed cells were grown on LB-agar plates supplemented with kanamycin as a selection marker, while no growth was observed on control plates (non transformed cells). Plasmid DNA (pDNA) was extracted using a Termo Fisher™GeneJet Miniprep DNA extraction kit. The plasmid DNA was identified by AGE. As seen in figure 4.1, the DNA from transformed cells shows the same pattern as the pDNA used to transform the *E. coli* cells. The pDNA samples were stored at 4 °C for short-term and −20 °C for long-term use.

It is noteworthy that the multiple bands observed correspond to different coiling states of the pDNA [78]. The strongest band slightly above 3 Kb corresponds to the super-coiled form of pDNA, which migrates faster than expected. The band between 4 and 5 Kb, which matches the expected 4.7 kb length of the plasmid, to an open circle monomer, and the bands at 10 Kb and above correspond to knots, catenanes, or other structures containing more than one plasmid.
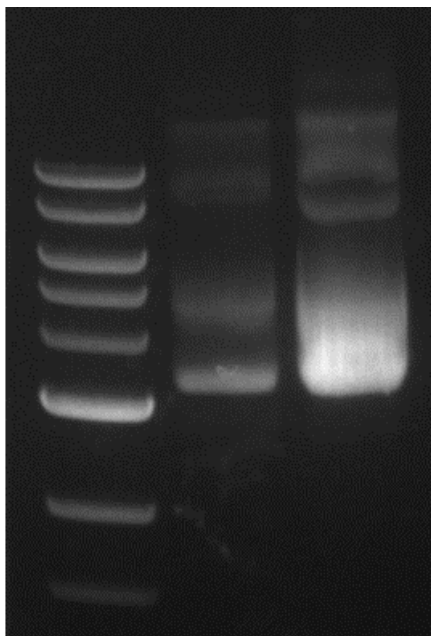
Figure 4.1.   *Comparison of the plasmid DNA used to transform E. coli cells(lane2), and the plasmid harvested from transformed cells (lane 3).*

4.1.2   Plasmid DNA Digestion

In order to further confirm that the extracted DNA contains the desired plasmid, DNA digestion performed by the endonucleases with restriction sites on the plasmid according to the plasmid restriction map [73]. Initially, only a combination of EcoRI and NdeI was used (figure 4.2a), but due to lack of product in the PCR reactions (section 4.2), the digestion experiment was repeated to rule-out possible malfunction of the plasmid due to mutations. BamHI+NdeI, and NcoI were used as enzymes for digestion. As seen in figure 4.2, the products of digestion are consistent with the expected fragment sizes, shown in table 3.2. However, a 251 band after digestion with NcoI is not observed (figure 4.2b), probably due to lower signal intensity of the signal from the small fragment compared to larger fragments. Moreover, in the second digestion experiment (figure 4.2b), for the BamHI+NdeI and ECoRI+NdeI enzyme combinations, a band between 4 and 5 kb was also observed which correspond to the linearized form of the plasmid.This observation can be attributed to incomplete digestion by one of the restriction enzymes, as the incubation time for these enzymes were 20 min instead of the initial 30 min for the first digestion attempt, where the band was not observed figure 4.2a.

(a)   (b)
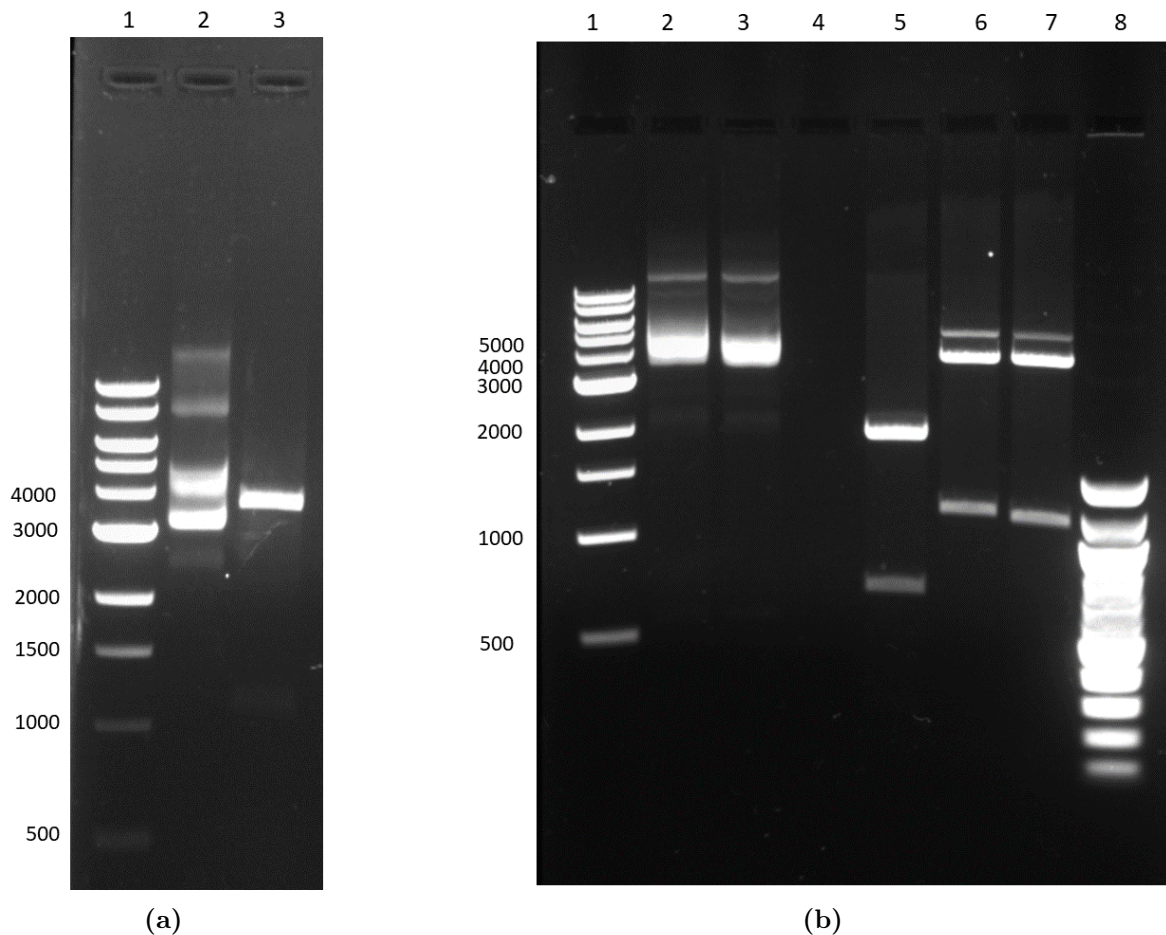
Figure 4.2.   *Restriction enzyme digestion of pTag plasmid: (a) 2: undigested plasmid, 3: treated with ECoRI+ NdeI. (b) 2 and 3: pTag plasmid, 5: treated with NcoI,6: treated with BamHI + NdeI, 7: treated with ECoRI+ NdeI*

4.2 PCR Reactions

In order to produce the single-stranded DNA scaffold, first a double-stranded DNA template was generated by amplification of the corresponding region on the plasmid. The dsDNA template was subsequently used in an asymmetric PCR (aPCR) reaction to produce the ssDNA scaffold.

4.2.1 Production of dsDNA Template

The first step of PCR was initially attempted using parameters reported by a previous project [7]. However, the PCR reactions did not produce any visible product. A variety of parameters were changed to troubleshoot the PCR reaction, including optimization of the amount of template pDNA, and annealing temperature. New primers, Taq polymerase, and dNTPs were also used in place of year-old primers and Taq polymerase used initially.

Increasing the concentration of Taq polymerase, as well as adjusting the annealing temperature improved the yield of the dsDNA product. The optimal parameters for the first PCR reaction were 120-150 ng of plasmid DNA (as measured by the Picodrop) , 1 U of Taq polymerase per 50 µL of PCR mixture, and annealing temperature of 46°C figure A.1. Other parameters such as primer concentration were also explored but did not seem to provide any benefit. The PCR product was confirmed as a 1.9 Kb band on using AGE. The salts and oligos were subsequently removed by a GeneElute™cleanup kit (figure 4.3.
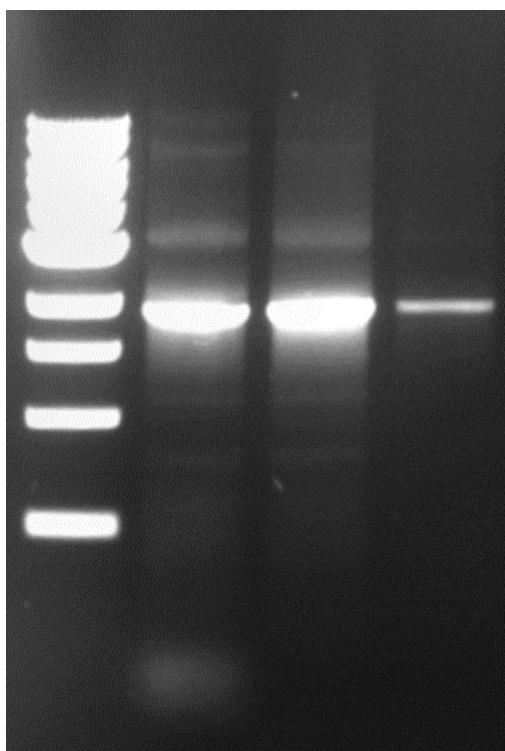
Figure 4.3. *dsDNA template before (lane 2) and after (lane 3) cleanup using the GeneElute™PCR cleanup kit. Lane three represents a second round of elution from the spin column*

In standard PCR protocols, the annealing temperature is set a few degrees below the melting temperature (T_m) of the primers. However, The T_m can be calculated by different equations taking into consideration different parameters. The simplest method to predict the T_m of the

primers only takes into account the GC content of the primers. More advanced models also take into account the concentration of the oligos, as well as concentration of monovalent and divalent salts [79]. The GC-content T_m of the forward and reverse primers for the reaction were 44.7 and 47.0 °C, respectively. The salt-adjusted T_ms were 50.2, and 60.3 °C, as calculated by Oligoanalyzer tool. In further optimization of the first step PCR reactions, both annealing temperatures of 46 and 53 °C seemed to produce results, with 46 having a higher yield. However, more non-specific products were also observed with the lower annealing temperature. The lower annealing temperature was preferred in this study, as the non-specific products could be efficiently removed by gel extraction

### 4.2.2 Production of ssDNA Scaffold by Asymmetric PCR

The dsDNA product from subsection 4.2.1 was used as a template in an asymmetric PCR reaction containing only one primer, which leads to amplification of only one of the strands. A variety of parameters were also adjusted for this reaction, including annealing temperature, number of cycles, and amount of template DNA. A comparison was also made by using Template DNA directly from the cleanup step, or dsDNA extracted from the gel using a GeneJet gel extraction kit. Since the gel extraction removes residues of the plasmid DNA which was used as template in the first PCR reaction, less non-specific products were observed, especially at higher number of cycles. It appears that salt and oligo concentration adjustment of the the annealing temperature for the aPCR reaction plays a more important role than in the normal PCR reaction figure A.3. This could possibly be due to the higher initial concentration and slower decrease in the concentration of oligos in aPCR due to linear progression of the reaction.

In order to separate the ssDNA scaffold from the dsDNA template and non-specific products, a preparative gel was used. The In case of larger-scale production, the aPCR products were first up-concentrated using the NEB PCR cleanup kit so that the sample volume would fit inside the agarose gel wells. an example of a preparatory gel can be seen in figure 4.4. Since ssDNA assumes multiple conformations and thus produces multiple bands, it is preferable to run it in a denaturing gel. However, the urea-containing agarose gel that was used in this study did not show a difference in the pattern of the ssDNA band. Therefore, further experiments were done using native agarose gel.

4.2.3 ssDNA Extraction

Different methods were tested for extraction of ssDNA from the gel as described in subsection 3.8.2. The ethanol precipitation method had an extremely low yield, which can be attributed to the small size and single-stranded nature of the scaffold. ssDNA is more polar than dsDNA and therefore more soluble in ethanol. Substitution of ethanol with isopropyl alcohol resulted in a higher yield. The use of isopropyl alcohol is especially useful in case of large-scale production, as ssDNA can be up-concentrated before cleanup. Another advantage of using isopropanol is cooling of the alcohol is not required [80].

Electro-elution from gel was first tested using pDNA (in order to preserve the highly precious ssDNA). pDNA was successfully eluted using this method with a yield of approximately 60% as measured by PicoDrop figure 4.5. Separation of ssDNA template, however, was not successful due to low concentration of the ssDNA, as well as the multiple-band pattern on the
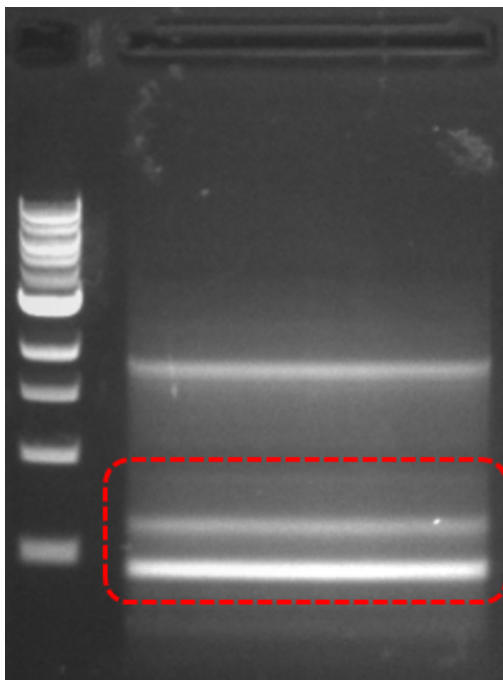
Figure 4.4. *preparatory gel for separation of ssDNA. The dotted area shows the excision site.*

gel. However, at larger-scale production, electrodialysis of a slice of gel containing the desired band was effective in separation of ssDNA with acceptable yield, but this method necessitates an extra round of up-concentration.
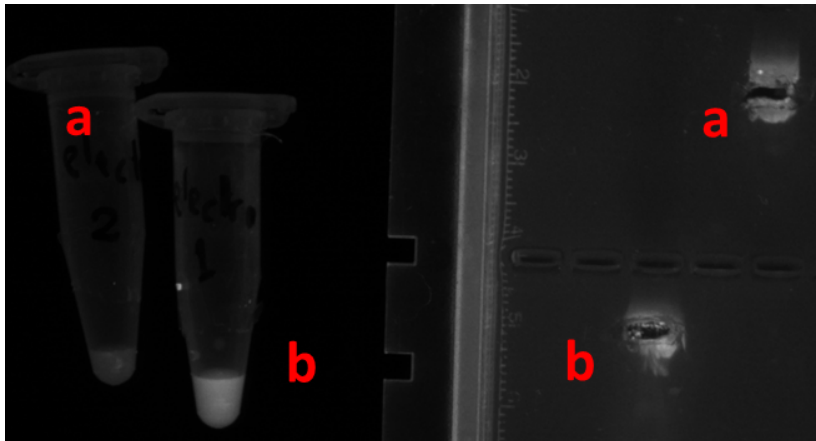
Figure 4.5. *Electroelution of pDNA from agarose gel. a) first attempt, b)second attempt.*

The most sequence for ssDNA purification that has the highest yield is summarized in the figure 4.6.

4.3 DNA Origami-Like Nanostructure Formation

The DNA origami-like nanostructure (DON) was formed using gradual overnight annealing procedure. The product of the annealing was run on an agarose gel supplemented with $MgCl_2$. Initially, 0.5x TAE buffer containing 11 mM $MgCl_2$ was used [8]. However, due to

Figure 4.6. *Suggested ssDNA purification process.*

heat generation, the concentration of Mg^{2+} was lowered to 5 mM. Ice packs were also used to cool down the electrophoresis chamber.

Various scaffold:staple ratios and Mg^{2+} concentration were tested for optimal folding of the DON, and the results can be seen in figure 4.7. Three different scaffold:staple ratios were tested, by including 20, 50, and 70 nM concentration of scaffold with 200 nM staple concentration. Mg^{2+} concentrations of 5 and 10 mM were also tested. The same amount of ssDNA as in the folding product was used for comparison. It can be seen in lanes 3, 5, and 7, the band between 1500 and 1000 bp is evidence for the formation of the DON, when compared to the lanes containing only ssDNA scaffold.

Increasing the scaffold:staple molar ratio form 1:10 (20 mM) to 1:4 (50 nM) and 1:3.5 (70 nM) resulted in higher intensity in the band attributed to the DON, while also increasing a smearing view on the gel, which implies higher amount of non-specific products. On the one hand, higher yield is preferred as the product can be more easily isolated at higher concentrations, on the other hand, the waste of expensive and difficult-to-produce ingredients should be kept in a minimum. Therefore, the 20 nM ssDNA concentration were used to make other batches of the DON.


ssDNA (nM)	20	20	50	50	70	70	20	20	20	20	50	50	50
Mg²⁺(mM)	-	20	-	20	-	20	-	5	-	10	-	5	10
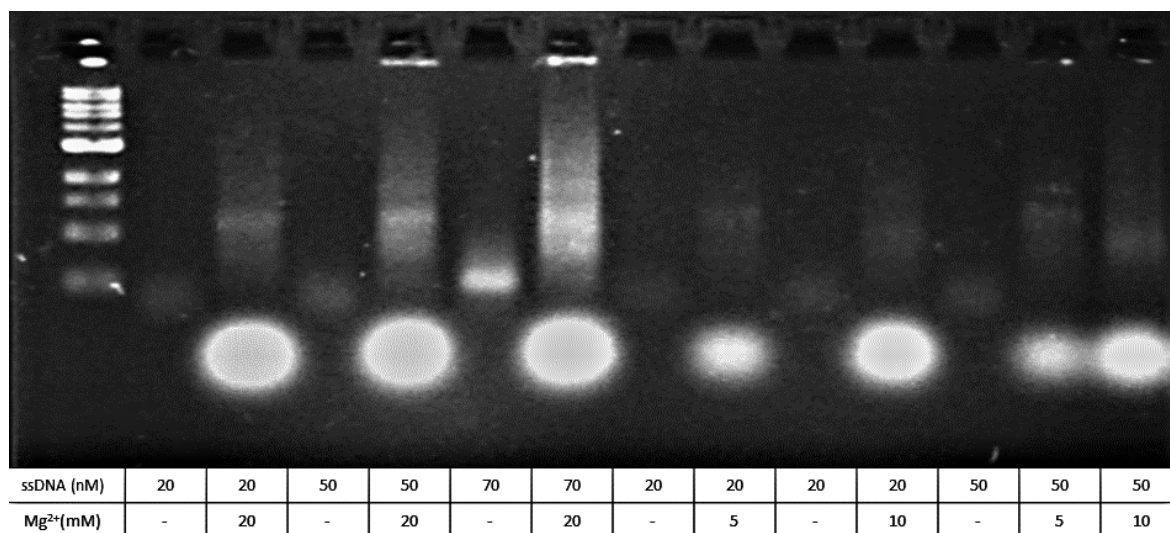
Figure 4.7. *Optimization of DON folding. The concentration of Mg^{2+} and ssDNA scaffold is specified under each lane.*

Different annealing temperature gradients were also used (figure 4.8). However, no difference could be observed from AGE data. An interesting observation in further folding experiments was that the band observed for the DON did traveled the same distance as the corresponding amount of ssDNA scaffold. This observation may imply that the subsequent folding

experiments were did not result in proper folding. However, the same observation were also made in the previous study [7], and the reason was attributed to the packaging of DNA, which result in the the DON move faster and thus travel the same amount as the smaller ssDNA scaffold.

Lane	Condition
2	65(10 min) 60-40 (20x 1h)
4	80 (5min) 79-66 (15x 1 min) 65-30 (35 x 10 min)
5	94 (3 min) 87-77 (10x 10 min) 78-58 (20x 40 min) 58-25 (33x 10 min)
6	ssDNA
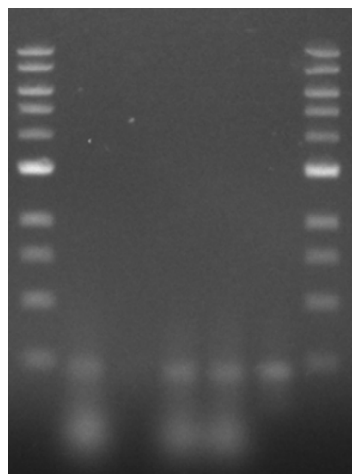
Figure 4.8. *Otimization of DON folding temperature gradients*

4.4 DNA Origami Isolation

Several methods were tested to separate the DON from excess oligos and other impurities.

The PEG precipitation method did not seem to yield any observable DON on the AGE gel. Since the method had been optimized for larger DNA origami, the optimization data from the original paper were re-visited to find the best conditions for smaller-sized origami([54], supplementary data). Higher concentration of PEG, which had been shown to precipitate smaller DNA structure was tested, which did not make a difference. Similarly, ultra-filtration using did not yield any observable results.

The reason that these otherwise standard and widely used methods did not seem to work can be attributed to the small size of the DON, as well as its incomplete folding by design. Although the structure seemed to be stable in the computational studies performed in the previous report [7], the structure does not have physical properties of a DNA origami because not all parts of it are compacted using staple. For instance, in the case of filtration, centrifugal forces may deform the structure, such that it passes through smaller membrane pores, or get adsorbed to the membrane structure.

Electrodialysis seemed the only method that was successful in separation of The DON from staple sequences. The method was first set up using pDNA as a dummy (in order to preserve the scarce inventory of the DON). As seen in figure 4.9a, the method successfully separated pDNA from added oligos. When performed on the folded DON mixture, however, residual amounts of the oligos could be detected by AGE (figure 4.9b, note that only staple and fragments were run on the gel). The reason for this observation could be the presence of Mg^{2+} ions in DON dialysis, which hinder the movement of negatively charged DNA sequences. It should be noted, however, that increasing the running time did not result in complete removal of the oligos.

(a)   (b)
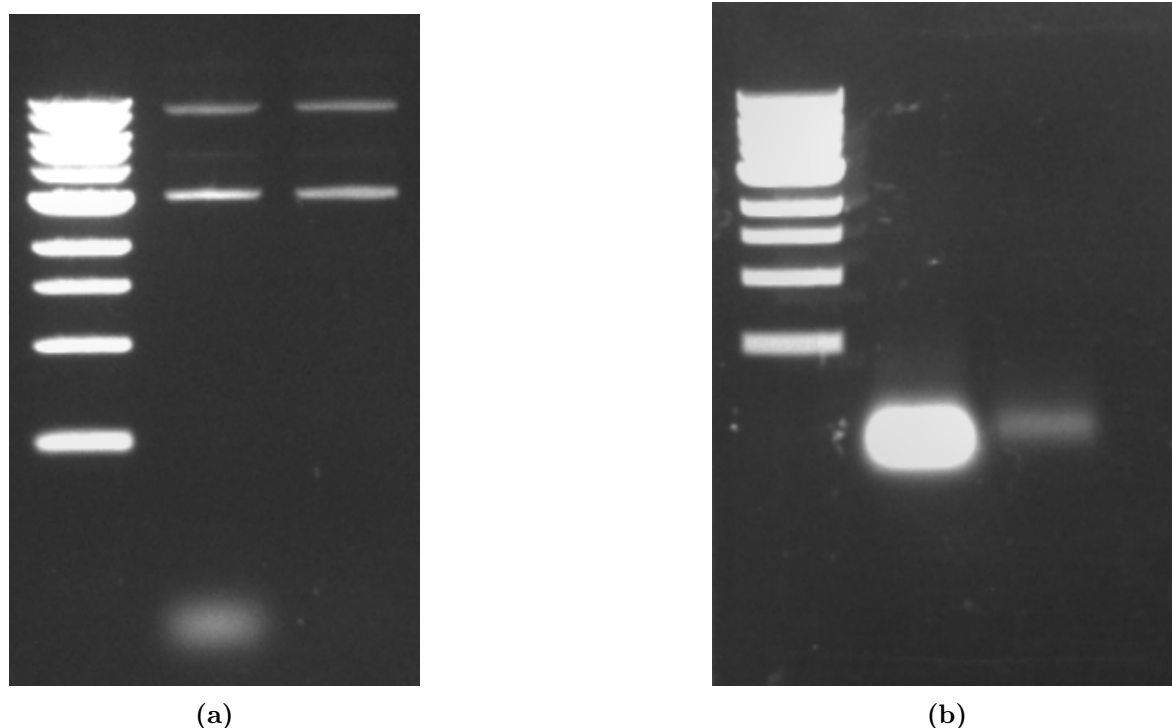
Figure 4.9. *Electrodialysis for separation of staples and fragments a) pDNA +*
staples b) Staples in Mg^{2+}-containing buffer

4.5 TAT Peptide Synthesis and Characterization

TAT peptide was synthesized by automated solid supported Fmoc chemistry. The peptide
was cleaved and deprotected using a TFA/TIS/water cocktail. The yield of the crude product
was 304 mg, which is 0.84% of the theoretical yield.

4.5.1 HPLC Analysis and Fractionation

High Performance Liquid Chromatography (HPLC) was used to determine the purity of the
synthesized peptide. Ideally, only one peak for the designed peptide should be observed.
However, ss shown in figure figure 4.10, multiple peaks were observed, which implies
the product has impurities. Therefore, semi-preparatory HPLC coupled with automated
fractionation was perfomed.
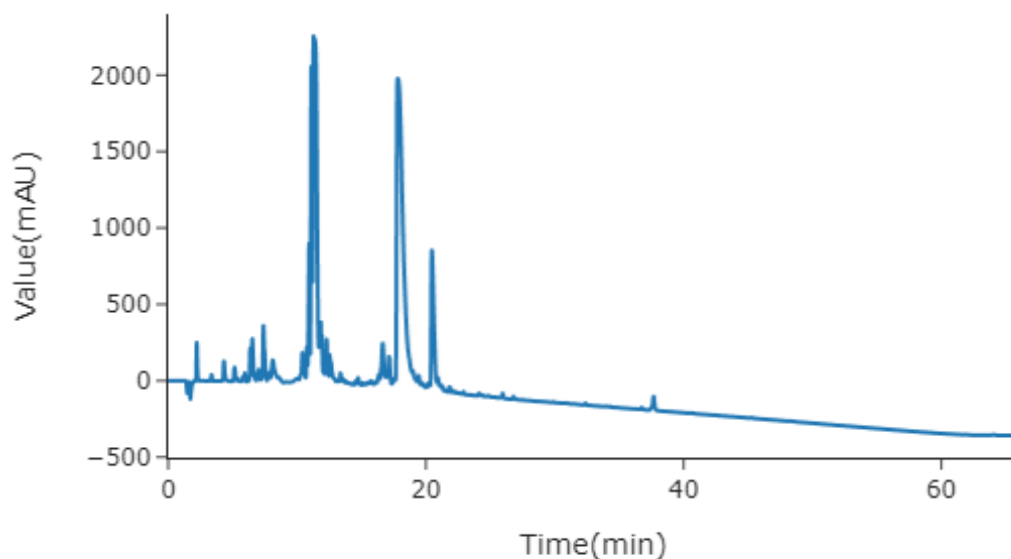
Figure 4.10.   *Analytical HPLC chromatogram of crude product of peptide synthesis*

The fractionation device is equipped with an inverter valve that derives the effluent either to fractionation tubes or waste. A malfunction in the valve resulted in loss of samples due to several unsuccessful fractionation attempts. However, a semi-automatic protocol was improvised by manually moving the nozzle when it was idle, thus preventing overflow. Using this method, the fractions corresponding to the three main peaks were successfully collected and freeze-dried.
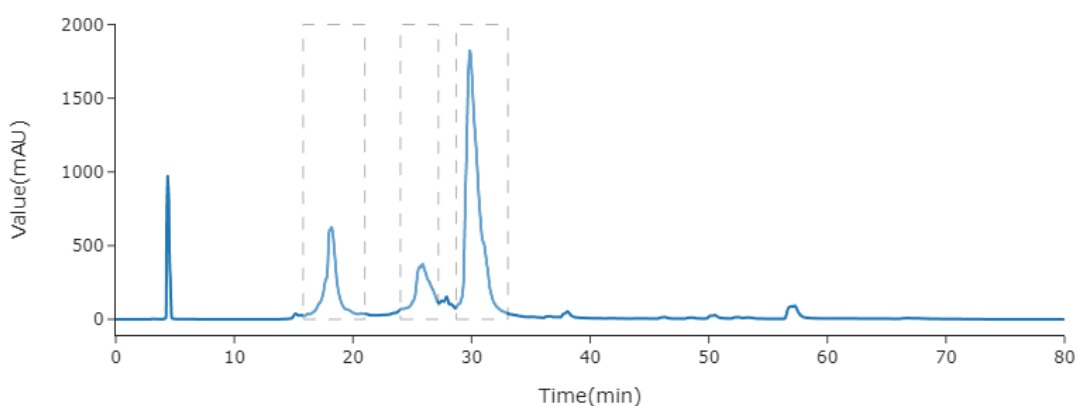

Figure 4.11. *Semi-preparatory HPLC chromatogram of synthesized TAT peptide. Dashed rectangles indicate collected fractions.*

4.5.2   Mass Spectrometry

In order to identify the contents of each peak, the fractions corresponding to each peak was analyzed by LC-ESI mass spectrometry.The results showed that the fraction with the lowest retention time contains a molecule with Mw of 1558.9488, in accordance with the calculated monoisotopic mass, which is 1558.951 Da (figure 4.12). The mass accuracy, which is 1.41 ppm is well within the acceptable deviation range of the instrument.

The other two fractions contained compounds with a monoisotopic mass of 1811.0328 Da, but at two different retention times, suggesting the may contain isomeric compounds. The calculated difference in mass is 252.0818 Da, which is equal to the Mw of 2,2,4,6,7-pentamethyldihydrobenzofuran-5-sulfonyl group (Pbf), which is the protecting group for Arginine[76]. A mechanistic depiction of deprotection of Pbf can be seen in figure 2.12.
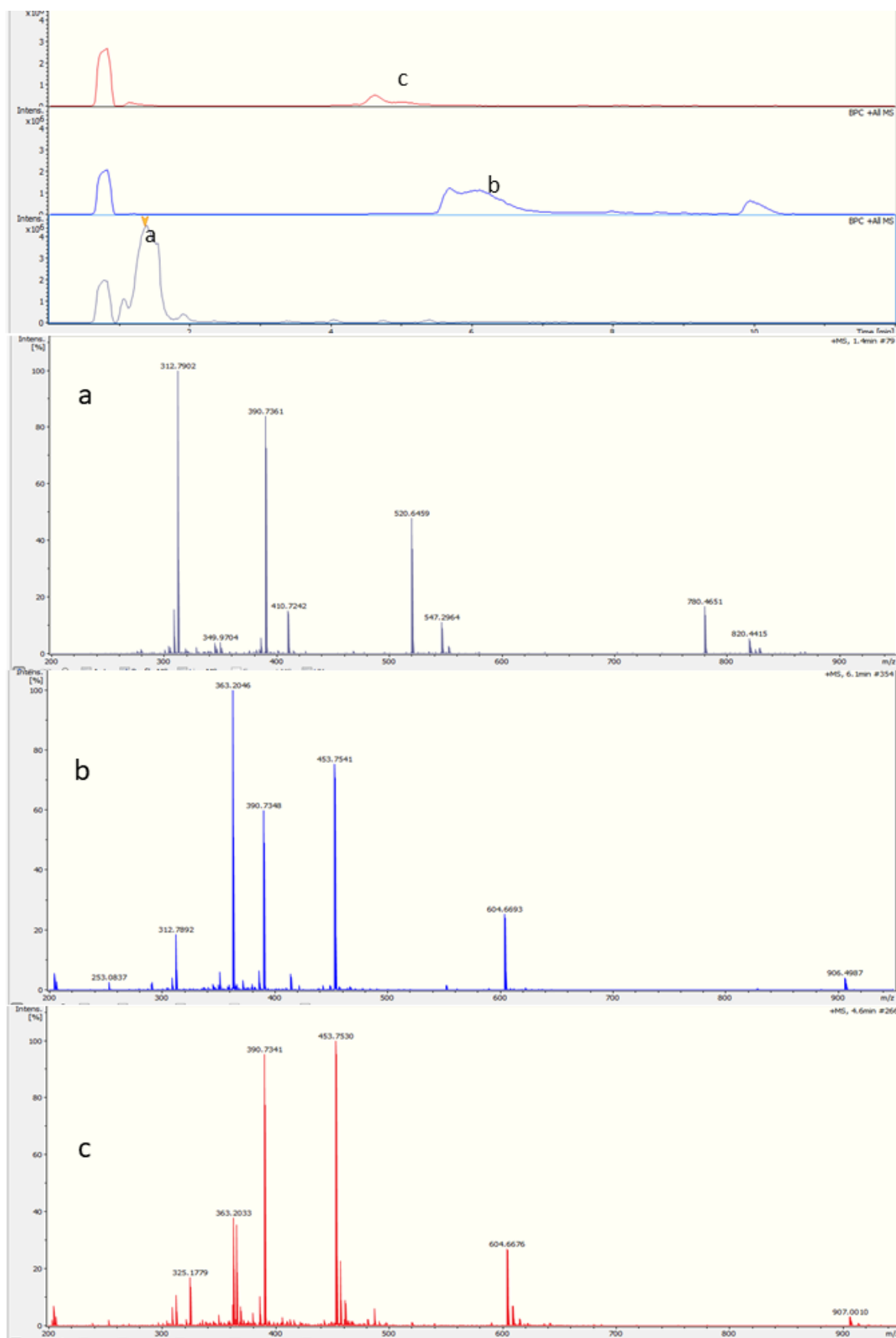
Figure 4.12. *LC-MS analysis of peptide fractions. The top diagram is the HPCL chromatogram fro each fraction. each letter (a,b, and c) on the chromatogram indicates the peaks corresponding to the mass spectrum with the same label*

One possible explanation for this mass difference can be attributed to Pbf- protection group that is still attached to arginine residues on the peptide. In other words, the other two peaks correspond to the TAT sequence that has not been completely deprotected. This is also supported by the fact that two separate HPLC peaks with distinct retention times were found to have the same molecular weight, probably due to the Pbf residue being attached to different Arginine residues.

With the introduction of pbf as a protecting group in 1993, the cleavage time required for arginine reduced significantly [81]. However, it still requires up to 2 hours of cleavage time, especially if multiple arginines are present, and more so if there are consecutive arginine residues in the sequence, as is the case with our TAT sequence [76].

TFA cleavage results in the formation of carbocation byproducts, which are highly reactive, especially in the case of Cys(Trt), Met, or Arg(Pbf). They may react with side chains of tyrosine, tryptophan, methionine and cysteine (which are rich in electrons) generating undesirable products [82]. To prevent this, strong scavengers such as thioanisole (methylsulfanylbenzene) and 1,2-ethanedithiol (EDT) should be used [66]. Other sources also point at cocktails such as TFA/TES/EDT/water (92.5/2.5/2.5/2.5) can be useful [63].

The cleavage cocktail proposed by the Activotec P-12 peptide synthesizer supplier contains EDT, thioanisol, and phenol as scavanging reagents for cleavage and deprotection of arginine-containing peptides. Nevertheless, due to unavailability of thioanisol, which is specifically helpful in deprotection of Arg, a normal cleavage cocktail (TFA:TIS:water, 95:2.5:2.5) was used. This leads to another possible explanation for the observed peaks: insufficient scavenging of reactive cleaved Pbf groups, that has resulted in irreversible reaction with other functional groups.

To test which of these two explanations is more likely, a second round of deprotection was performed using TFA/TES/EDT/water (92.5/2.5/2.5/2.5) as deprotection cocktail and reaction time of 4 h. However, no significant change was observed in the HPLC pattern after this treatment, which implies an irreversible reaction of the Pbf group with the peptide. For further experiments only the fraction containing the peptide was used.

## 4.6   PEI Modification

4.6.1   Ninhydrin Assay

PEI was modified with three fatty acids with different chain lengths and an aromatic amino acid, using EDC/NHS chemistry. In order to confirm the substitution of primary amines with the substituents, ninhydrin assay was carried out. This assay provides an estimate of the available primary amine groups, as previously described in section 3.16.

Initially, standard solutions of PEI with concentrations ranging from 0 to 10 mg/mL in 1 mg/mL increments were prepared. However, a brownish color was developed instead of the expected blue color at concentrations higher than 2 mg/mL. The color is a result of the reaction of ninhydrin with secondary amines, that yields an iminium salt [77]. The concentrations were therefore lowered 10 fold i.e. from 0-1 mg/mL in 0.1 mg/mL increments. The concentrations for test samples were also decreased by a factor of 5 (0.5, 1.5, and 2 mg/mL). Ninhydrine

concentration was also decreased to 1 mg/mL, and the incubation time was decreased to 20 min at 60°C. The rationale for these modifications were to increase the specificity of the assay for primary amines by allowing for more favorable reactions (primary amines) to dominate, and exclude the reactions with secondary amines as much as possible.

The standard curve and corresponding points for modified samples is visualized in figure 4.13
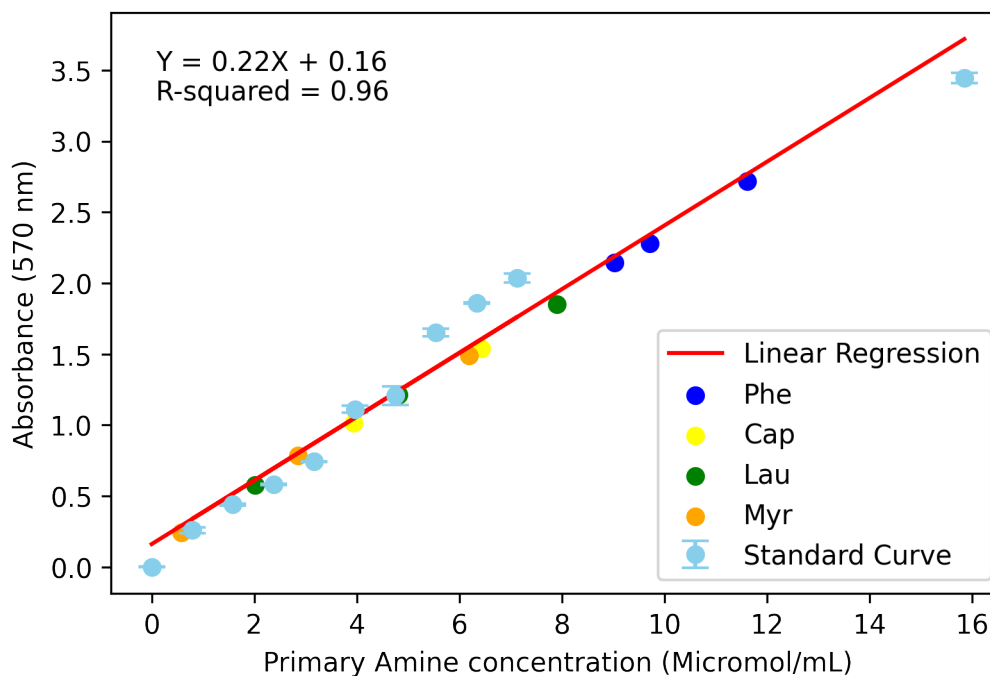
Figure 4.13. *Ninhydrin test. Absorbance is plotted against PEI concentration. The dots represent the PEI concentrations with the same amount of primary amines as the modified samples.*

Based on the corresponding PEI concentrations, the extent of substitution of primary amines on modified PEIs can be calculated (For calculation details, see section A.4). The results were summarized in figure 4.14 In the case of PEI-Lau and PEI-Myr, the three tested concentrations tested (0.5, 1, 1.5 mg/mL) showed comparable results in terms of degree of modification. However, in the case of PEI-Cap, only one of the concentrations tested showed an acceptable result. In the case of PEI-Phe, the results were not consistent. The reason for that is probably the fact that phenylalanine provides an additional reaction site for ninhydrin (the α amino group), compared to the fatty acids. Also, based on the method for PEI modification, the preferred way to modify PEI with an aminoacid is by using Carboxy- protected aminoacids. Although reports of successfully attaching aminoacids such as histidine using EDC chemistry and unprotected aminoacids has been reported before[15], the problem with this method is the reaction of the amine- activated aminoacid with the carboxy- group of other aminoacids, resulting in bi- or oligo-peptides of the same aminoacid, instead of reaction with the amine group on the polycation. Therefore, the efficiency of modification, as well as the uniformity of the product are compromised with this method.
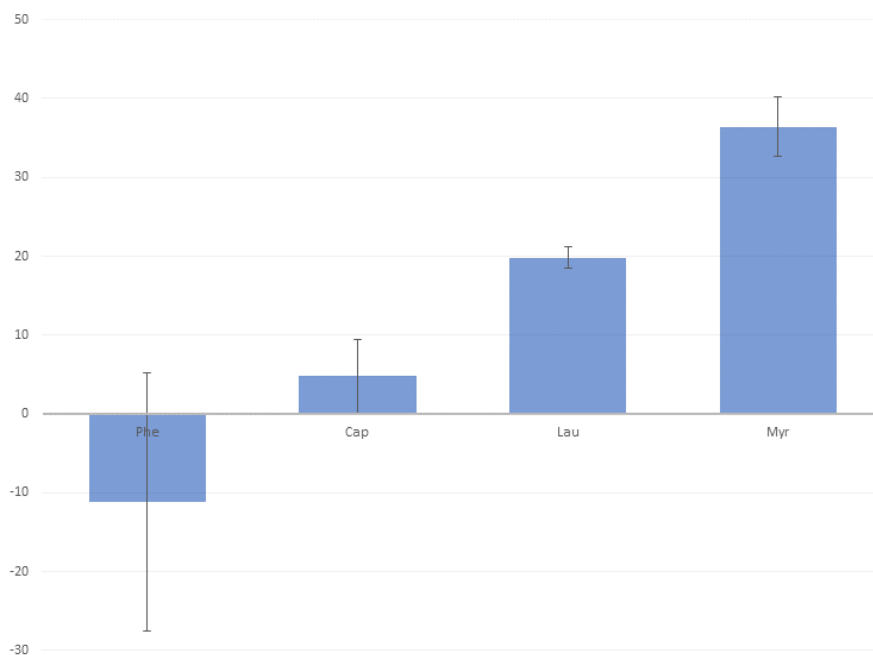
Figure 4.14. *The degree of substitution of modified PEIs expressed in % of primary amines.*

The reproducibility of the results with PEI-Myr an PEI-Cap may be due to the fact that longer-chain fatty acids may cause more steric hindrance, thus decreasing the availability of secondary amines, which do not yield the blue color. Ultimately, the assay is suitable to give a general idea about the primary amine content of the modified PEI, but due to side reactions with secondary amines, the results are not definitive. Other characterization methods such as FT-IR and NMR are more likely to provide more reliable and reproducible results. However, these tests were not conducted due to time constraints.

4.6.2 Gel Retardation Assay

The gel retardation assay was done to determine the ability of the polymer to bind to DNA, thereby inhibiting its movement in agarose gel electrophoresis.

Initially, carrier to plasmid (c/p) ratios of 1, 2, 3, and 4 were used, (results not shown). However, since the the movement of DNA inside agarose gel was completely inhibited by complexing with PEI at c/p ratio of 1 and higher, lower c/p ratios were tested.

The lowest ratio of PEI to fully inhibit DNA movement through the gel was found to be 0.5 (figure 4.15a). Gel retardation was also tested using modified PEI. As seen in figs. 4.15b to 4.15d, The lowest carrier to DNA ratio for PEI-Phe, PEI-Cap, and PEI-Lau, were 0.5, 0.75, and 1, respectively. Myristic acid which did not show satisfactory condensation in the first round (figure 4.15e), and was therefore tested at higher ratios, which showed full inhibition of DNA migration at C:P ratio of 1.75. As for PLL and TAT, the lowest ratios were 1. The results of the assay is summarized in figure 4.17

(a) *PEI*

(b) *PEI-Phe*

(c) *PEI-Cap*

(d) *PEI-Lau*
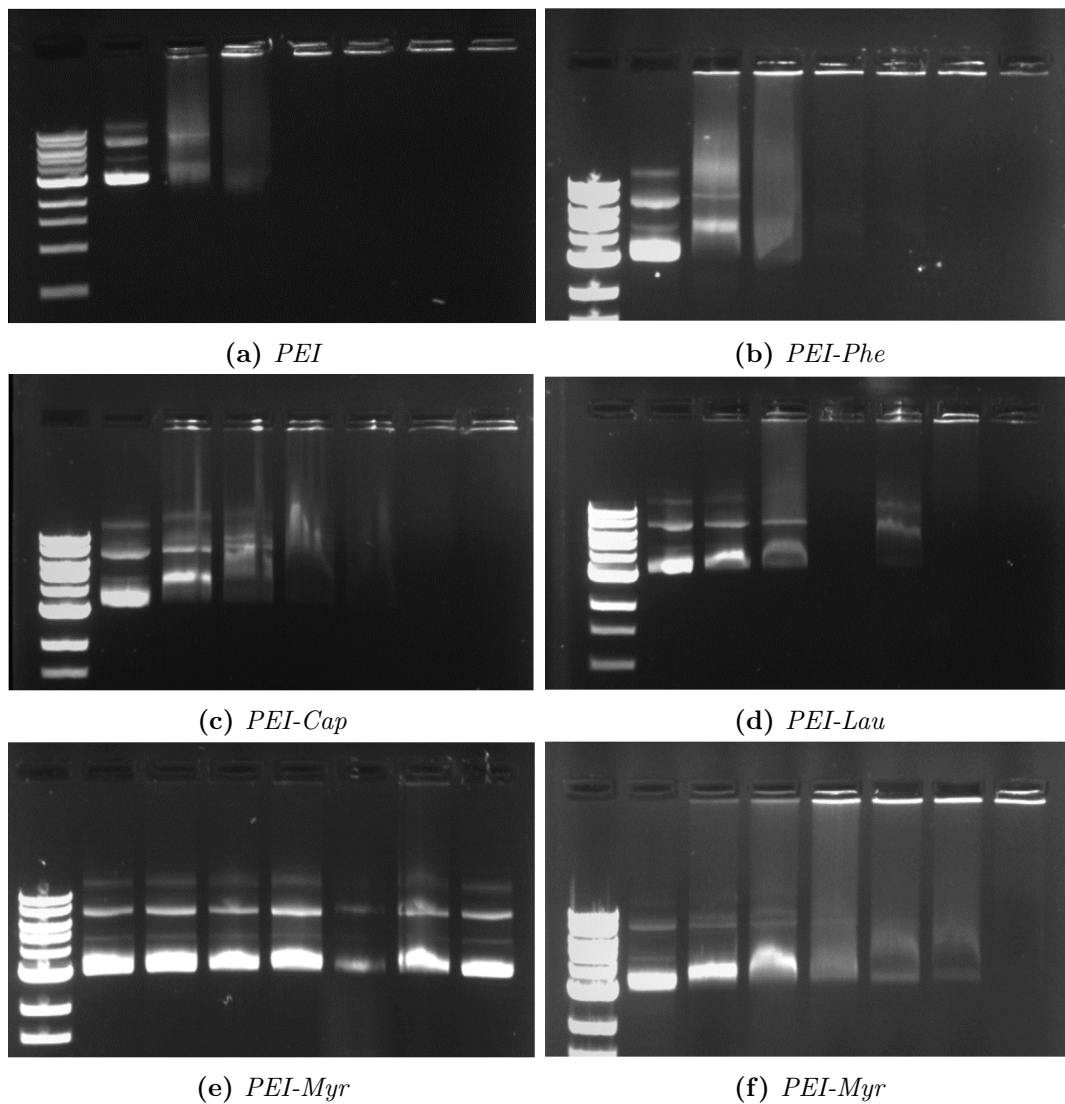
(e) *PEI-Myr*

(f) *PEI-Myr*

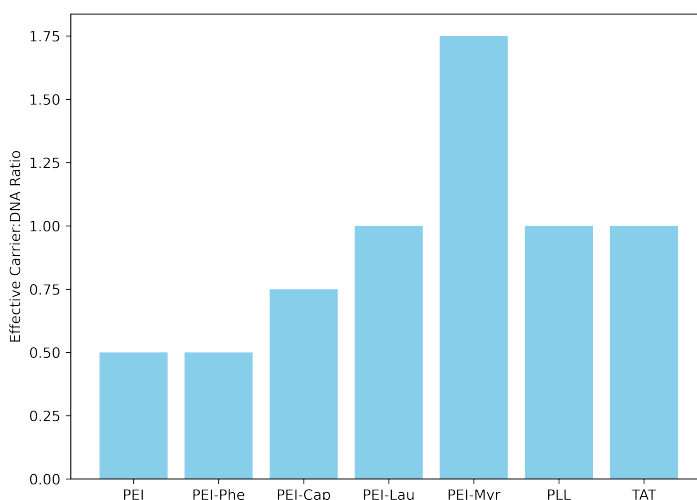**Figure 4.15.** *Gel retardation assay. a-e) Carrier:DNA ratios: 0, 0.25, 0.375, 0.5, 0.625, 0.75, 1. f)PEI-Myr:DNA ratio: 0, 0.5, 0.75, 1, 1.25, 1.5, 1.75.*

As for PLL and TAT, the lowest ratios were 1 (figure 4.16).

(a)

(b)
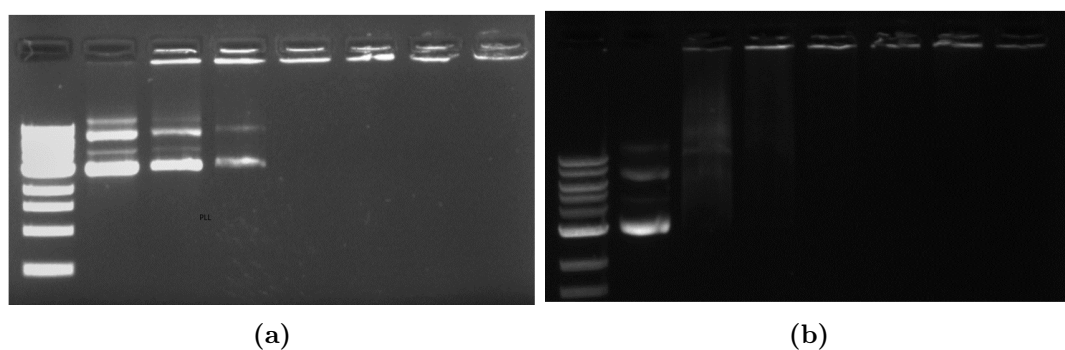
Figure 4.16. *Gel retardation assay. a) PLL:DNA ratio: 0, 0.5, 0.75, 1, 1.25, 1.5, and 2, respectively. b) TAT:DNA ratio 0, 0.5, 0.75, 1, 1.25, 1.5, and 2, respectively).*

Figure 4.17. *Gel retardation assay: the lowest carrier:DNA ratio for complete DNA condensation for each carrier*

The results of this assay can provide an insight into the interaction of the PEI with DNA, which will be useful in determining initial ratios to be used in the coating of the origami-like structure with PEI. It also sheds light on the PEI:DNA ratios to be used as a positive control in transfection studies. These results show that the both un-modified and modified PEIs, as well as PLL and TAT were able to form complexes with plasmid DNA. A comparison between modified and unmodified PEI shows that higher ratios of the modified polymers were required to condense DNA. This effect was more evident in the case of myristic acid, which did not show sufficient condensation in the first round, and needed to be tested with higher ratios. However, the DNA binding properties of the carriers were retained after these modifications, which is favorable in designing a gene carrier. A trend for higher c/p ratio with increasing length of the fatty-acid side-chains was also observed, which can be attributed to masking of primary amine moieties by the longer acyl- chains. These observations are also consistent with the results from the nindydrin assaay (subsection 4.6.1. The results of this assay was then considered in the setup for transfection and cell viability assays.

4.7 The Alamar Blue Cell Viability Assay

The alamar blue assay was used to determine the viability of HeLa cells after treatment with transfection agents at different c/p ratios. The results are illustrated in figure 4.18
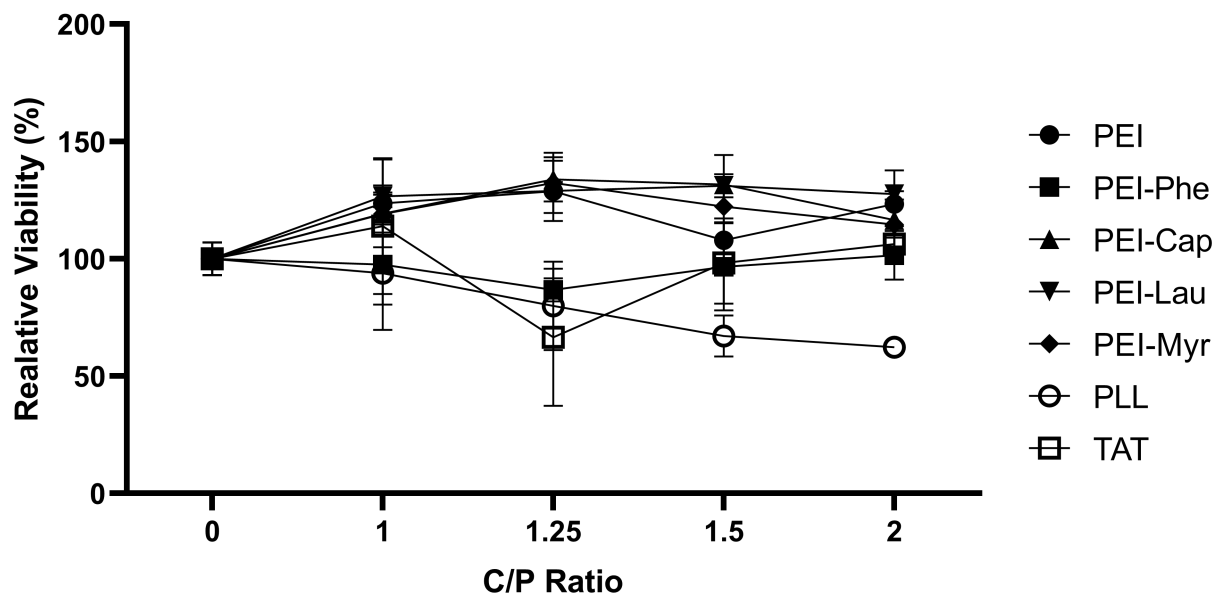
Figure 4.18. *The alamar blue test: viability of HeLa cells after treatment with polyplexes*

Statistical analysis of the results showed that The at $c/p = 1$, there is no significant difference in viability between different carriers. At $c/p = 1.25$, PEI-Phe ($p < 0.01$), PLL($p < 0.001$), and TAT ($p < 0.0001$) resulted in significantly lower viability compared to unmodified PEI. In the case of TAT, the result for this c/p ratio could be interpreted as an outlier, as higher ratios showed higher viability. At $c/p = 1.5$ and 2, PLL was the only carrier with significantly lower viability compared to unmodified PEI. PLL was the only carrier that showed a dose-dependent toxicity, with significant reduction of viability when comparing c/p ratios 1.25, 1.5, and 2.

Collectively, these results show that at the c/p ratios tested, the carriers can be used for transfection assay without major concerns of cytotoxicity.

4.8 DNA Transfection

The first set of transfection studies were performed to evaluate the transfection activity of the PEI, PLL, and TAT peptide at different c/p ratios. pTAG plasmid was used as the model DNA. The fluorescent was measured at and 555 and 584 nm excitation and emission, respectively. Although there's a general trend of increased fluorescence intensity with increasing c/p ratios, only PEI at c/p ratios of 1.75 ($p < 0.01$) and 2 ($p < 0.0001$) showed statistically significant increase in fluorescence compared to control ($C/P = 0$). Visual examination by fluorescent microscopy showed little transfection activity in PEI- and PLL-transfected cells, with few cells sporadically fluorescing.

(a)

(b)

(c)
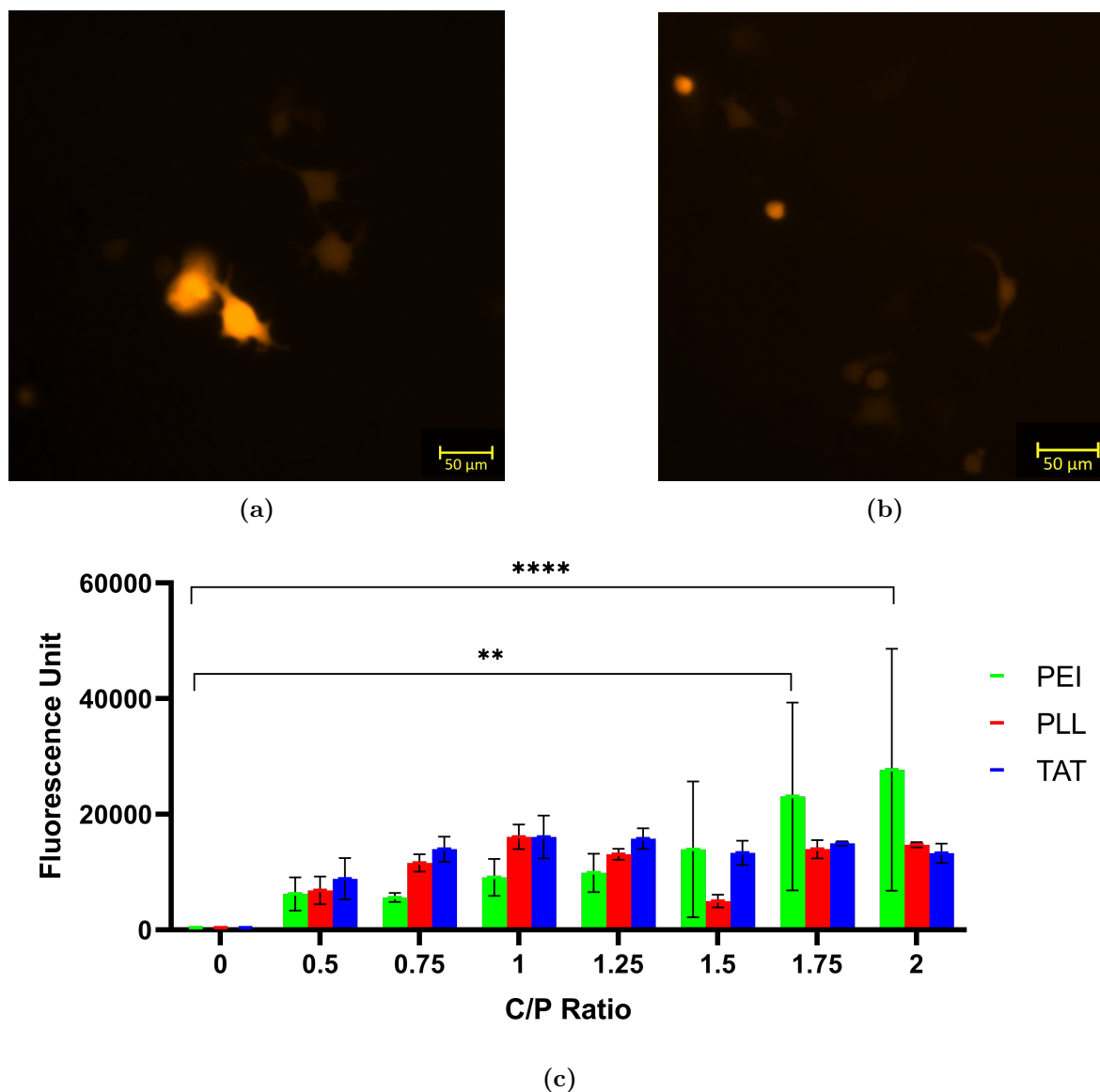
Figure 4.19.   *a) HeLa cells transfected using PEI (c/p=2) b) HeLa cells transfected with PLL (c/p=2) c)Transfection activity of PEI,PLL, and TAT as measured by fluorescence at 555 nm excitation and 583 nm emission.*

Although initial analysis based on fluorescence showed significantly higher activity, the results were not consistent with microscopy. two examples are shown in figure 4.19c, a) and b), where PLL shows the comparable activity to PEI, while the measured fluorescence is markedly lower.

In the next step, modified PEIs were tested for transfection activity. However, neither showed enhanced transfection compared to unmodified PEI. These carriers also resulted in very low number of fluorescent cells which could not be reliably quantified. A sample field of view for each of the modified carriers can be seen in figure 4.20.
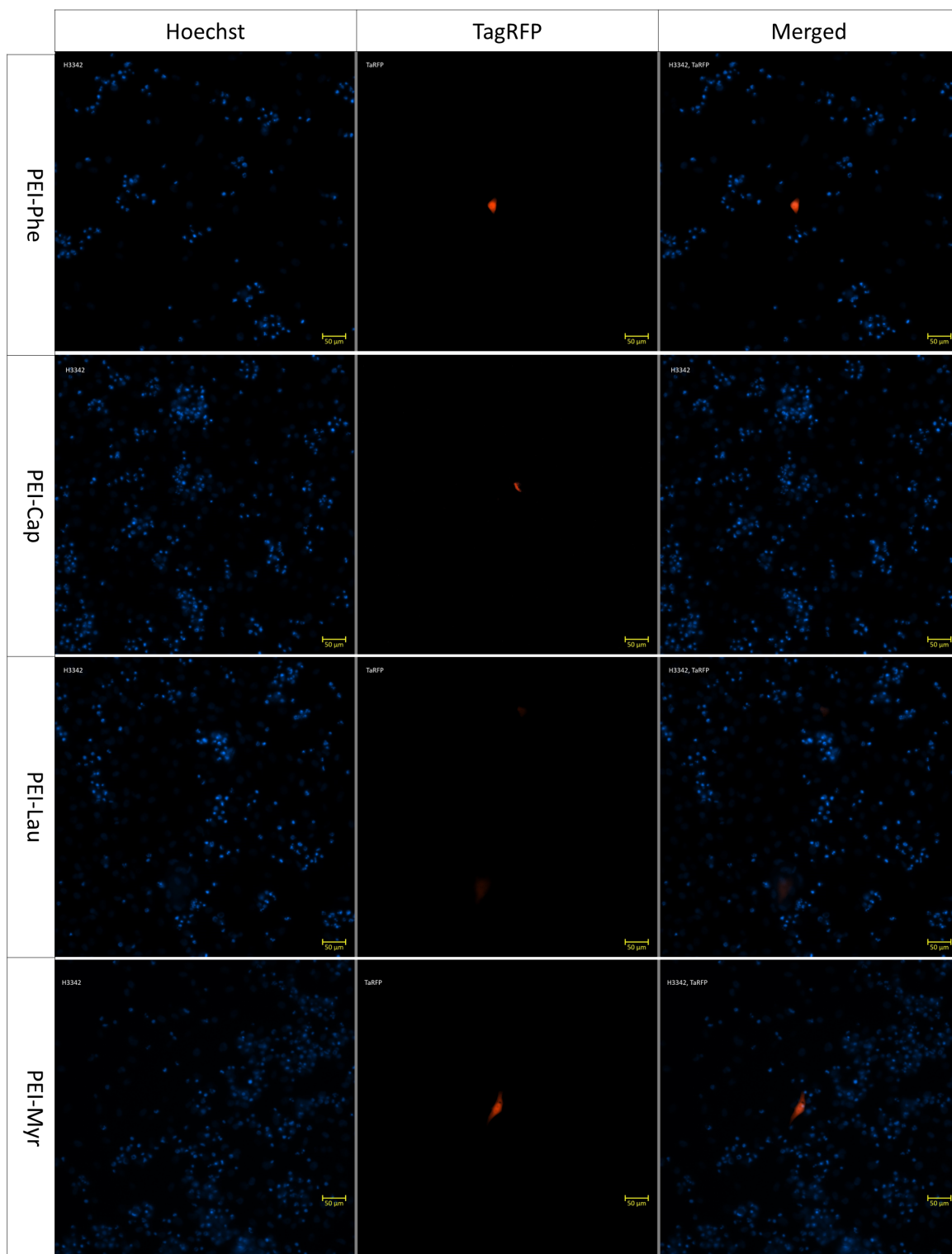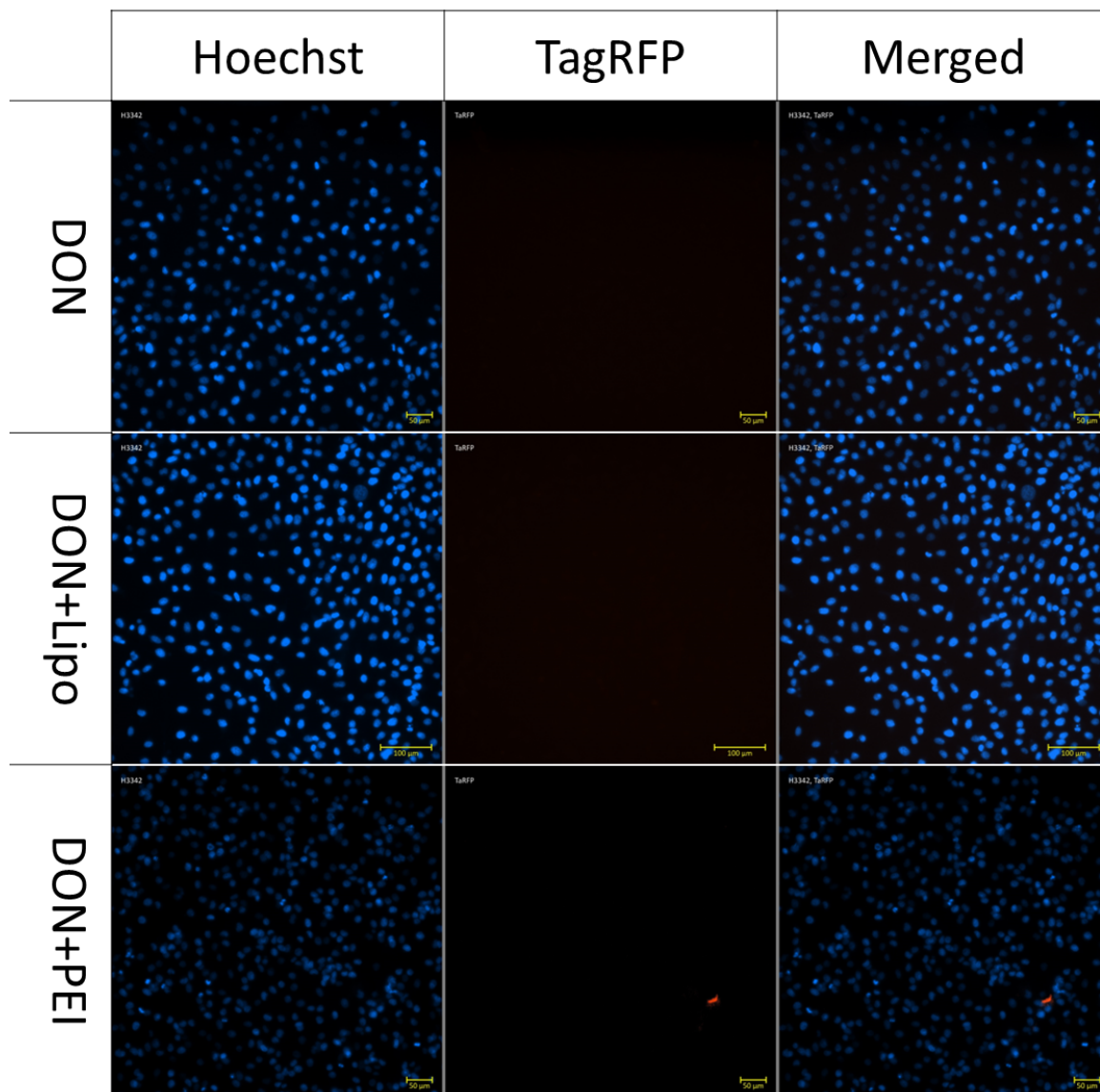
Figure 4.20. *Transfection activity of the modified PEIs complexed with pDNA*

Due to very low transfection activity, these results cannot reliably prove that the modifications done on PEI result in higher transfection activity.

4.9   Transfection of DNA Origami

Initial attempts to express the reporter gene encoding for TagRFP using the DON did not result in any observable transfection. Therefore, a step-by step approach was adopted. First, the cells were treated by the DON alone, or complexed with PEI (c/p =2), or in combination with Lipofectamine 3000. The results did not show any considerable activity, as shown in figure 4.21

Figure 4.21.   *Transfection activity of the DON alone, complexed with Lipofectamine 3000, or PEI (c/p=2).*

In the next step, the three DNA structures that contain the coding gene were tested, including the pDNA, the dsDNA template used in the aPCR reactions, and the ssDNA scaffold. As seen in figure 4.22, both pDNA and dsDNA template show observable and considerable transfection activity when delivered using Lipofectamine. On the other hand, the ssDNA scaffold shows no transfection activity (multiple fields of view were scanned for fluorescent cells).
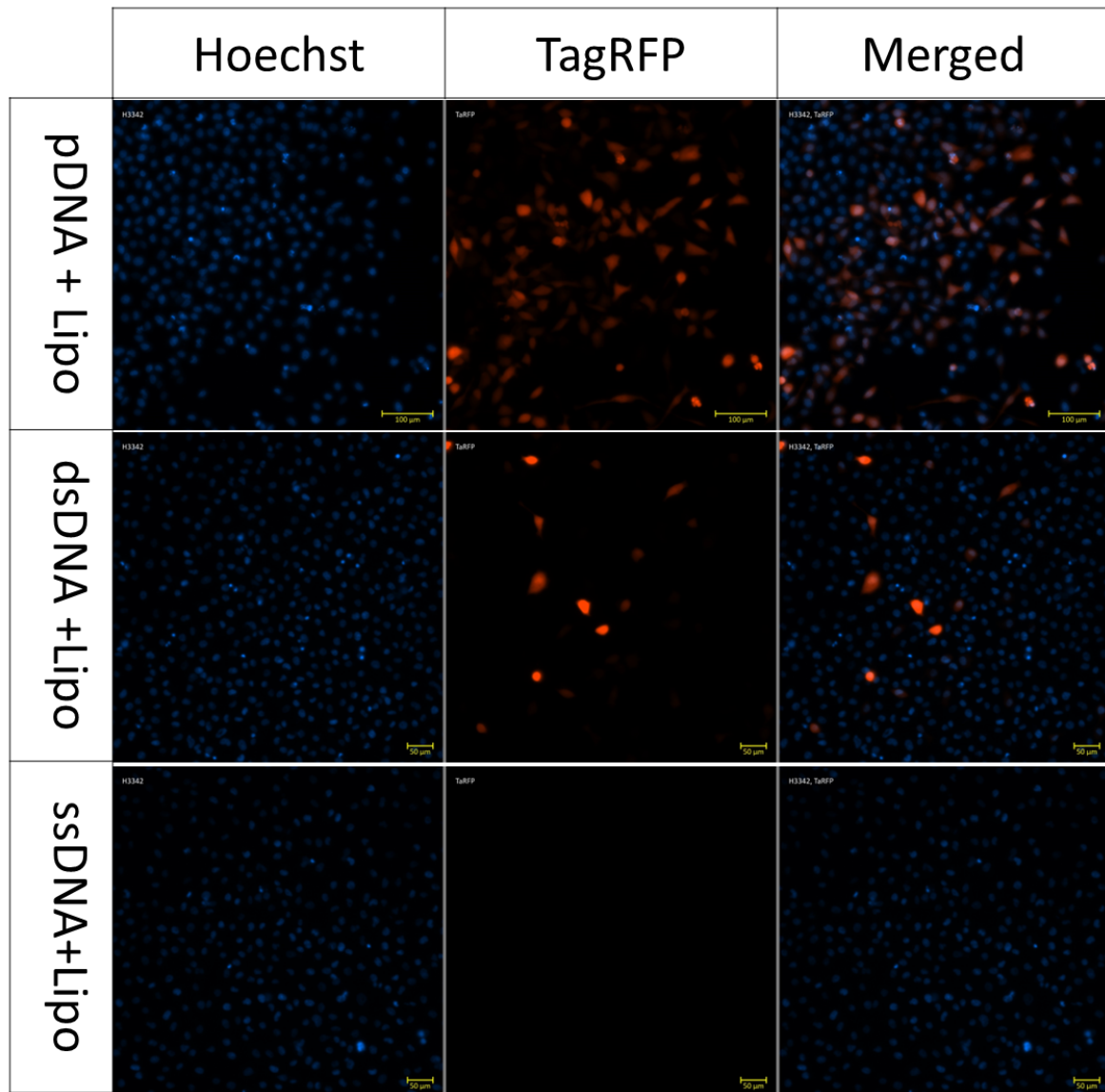
Figure 4.22. *Transfection activity of the pDNA, dsDNA template, and ssDNA scaffold complexed with Lipofectamine 3000*

Taken together, these results point to a defect in the ssDNA scaffold as the main underlying reason for lack of transfection activity of the DON. As discussed in section 2.7, The CMV promoter used in this sequence is optimized for dsDNA transcription. Therefore, in order for the sequence to be effective, it needs to undergo an extra round of replication so that the second strand would also be present. This acts a bottle-neck for the transcription of the RNA sequence and therefore decreases the expression miserably. A similar observation was made in a very recent study: it was observed that a long continuous staple segment with no crossovers resulted in up to 50% higher transfection. Also, incorporation of AAV-2-inspired ITRs in staple sequences at the 5' region of the promoter sequence resulted in up to two-fold increase in transfection activity [5]. Therefore, a promising solution to lack of transfection activity may be to redesign the promoter sequence such that it is optimized for transcroption without a need for complementary DNA strand within the cell.

Conclusion 5

5.1 Conclusion

This study attempted to use non-viral chemical methods to enhance transfection activity of a DNA origami-like nanostructure mediated by cationic polymers and TAT, a cell-penetrating peptide. Another goal of this study was to improve the process of of production and isolation of the ssDNA scaffold.

To achieve these goals, numerous conditions for aPCR reactions, DNA purification, up-concentration, and DNA folding was attempted. Some of these methods such as PEG precipitation ([54]) were not effective, probably due to the fact that these methods are optimized for conventional DNA origamis made using 7 kb scaffold and full integration of the scaffold into a DNA origami structure, wehreas the design in our study is much smaller and is only partially folded into an origami-like structure. These methods should therefore be optimized for such a structure. Alternatively, the staple sequences could be designed such that a fully integrated origami structure is formed.

The reagents designed for enhanced transfection showed minimal activity when delivering pDNA. PEI is one of the most widely studied transfection reagent. However, PEIs used in transfection studies ususally have higher molecular weights, for example 25 kDa, which is the gold standard transfection agent.

Also, the DON did not show detectable transfection activity, which can be attributed to lack of transcription activity due to lack of promoter optimization for ssDNA transcription.

5.2 Future Perspectives

Many lessons were learned from this study, which can be used in future projects. First and foremost, the pTagRFP-C vector used in this study should be revisited for possible optimization of the promoter sequences. For example, self-complementary promoter regions could be explored [71]. These regions could be designed as ITRs. However, some challenges should be considered when designing such a scaffold, as self-complementary regions may complicate the folding process. Additionally, optimizing the shape and design of the structure into a practical origami can be helpful.

Another important issue was the time-consuming process of scaffold production and isolation. The design of a microfluidic device to separate different products based on dielectrophoretic forces could be an extremely useful tool for this and other studies involving DNA.

Application of more potent cationic transfection agents, as well as exploring physical

transfection such as electroporation could be of advantage.

Finally, alternative ways of attachment of transfection enhancers to the origami structures could be explored[83].

Bibliography

[1]   Andersen, E. S. et al. "Self-assembly of a nanoscale DNA box with a controllable lid".
      In: *Nature* 459.7243 (2009), pp. 73–76.

[2]   Banerjee, A. et al. "Role of nanoparticle size, shape and surface chemistry in oral drug
      delivery". In: *Journal of Controlled Release* 238 (2016), pp. 176–185.

[3]   Sun, R. et al. "The tumor EPR effect for cancer drug delivery: Current status,
      limitations, and alternatives". In: *Advanced Drug Delivery Reviews* (2022), p. 114614.

[4]   Davis, M. E. "Non-viral gene delivery systems". In: *Current opinion in biotechnology*
      13.2 (2002), pp. 128–131.

[5]   Kretzmann, J. A. et al. "Gene-encoding DNA origami for mammalian cell expression".
      In: *Nature Communications* 14.1 (2023), p. 1017.

[6]   Fan, D. et al. "Engineering DNA logic systems with non-canonical DNA-nanostructures:
      Basic principles, recent developments and bio-applications". In: *Science China Chemistry*
      65.2 (2022), pp. 284–297.

[7]   Giarentis, K. "Compaction of DNA into an Origami-like Structure for Efficient Gene
      Delivery". MA thesis. Denmark: Aalborg University, 2022.

[8]   Ahmadi, Y., De Llano, E. and Barišić, I. "(Poly) cation-induced protection of
      conventional and wireframe DNA origami nanostructures". In: *Nanoscale* 10.16 (2018),
      pp. 7494–7504.

[9]   Mirón-Barroso, S., Domènech, E. B. and Trigueros, S. "Nanotechnology-based strategies
      to overcome current barriers in gene delivery". In: *International journal of molecular
      sciences* 22.16 (2021), p. 8537.

[10] Rols, M.-P. "Mechanism by which electroporation mediates DNA migration and entry
      into cells and targeted tissues". In: *Electroporation Protocols: Preclinical and Clinical
      Gene Medicine* (2008), pp. 19–33.

[11] Wells, D. "Gene therapy progress and prospects: electroporation and other physical
      methods". In: *Gene therapy* 11.18 (2004), pp. 1363–1369.

[12] Merten, O.-W. and Al-Rubeai, M. *Viral vectors for gene therapy.* Vol. 737. Humana
      Press Totowa, NJ, 2011.

[13] Lundstrom, K. "Viral vectors in gene therapy". In: *Diseases* 6.2 (2018), p. 42.

[14]   Zu, H. and Gao, D. "Non-viral vectors in gene therapy: Recent development, challenges, and prospects". In: *The AAPS journal* 23.4 (2021), p. 78.

[15]   Hashemi, M. et al. "Gene delivery efficiency and cytotoxicity of heterocyclic amine-modified PAMAM and PPI dendrimers". In: *Materials Science and Engineering: C* 61 (2016), pp. 791–800.

[16]   Hashemi, M. et al. "Preparation of effective and safe gene carriers by grafting alkyl chains to generation 5 polypropyleneimine". In: *Aaps Pharmscitech* 16 (2015), pp. 1002–1012.

[17]   Taranejoo, S. et al. "A review of the developments of characteristics of PEI derivatives for gene delivery applications". In: *Journal of Applied Polymer Science* 132.25 (2015).

[18]   Forrest, M. L., Gabrielson, N. and Pack, D. W. "Cyclodextrin–polyethylenimine conjugates for targeted in vitro gene delivery". In: *Biotechnology and bioengineering* 89.4 (2005), pp. 416–423.

[19]   Peng, Q., Zhong, Z. and Zhuo, R. "Disulfide cross-linked polyethylenimines (PEI) prepared via thiolation of low molecular weight PEI as highly efficient gene vectors". In: *Bioconjugate chemistry* 19.2 (2008), pp. 499–506.

[20]   Proulx, J. et al. "Arginine-modified polymers facilitate poly (lactide-co-glycolide)-based nanoparticle gene delivery to primary human astrocytes". In: *International journal of nanomedicine* (2020), pp. 3639–3647.

[21]   Ogris, M. et al. "PEGylated DNA/transferrin–PEI complexes: reduced interaction with blood components, extended circulation in blood and potential for systemic gene delivery". In: *Gene therapy* 6.4 (1999), pp. 595–605.

[22]   Hiraki, J. et al. "Use of ADME studies to confirm the safety of ε-polylysine as a preservative in food". In: *Regulatory Toxicology and Pharmacology* 37.2 (2003), pp. 328–340.

[23]   Kadlecova, Z. et al. "DNA delivery with hyperbranched polylysine: A comparative study with linear and dendritic polylysine". In: *Journal of controlled release* 169.3 (2013), pp. 276–288.

[24]   Li, L., Wei, Y. and Gong, C. "Polymeric nanocarriers for non-viral gene delivery". In: *Journal of Biomedical Nanotechnology* 11.5 (2015), pp. 739–770.

[25]   Manzanares, D. and Ceña, V. "Endocytosis: the nanoparticle and submicron nanocompounds gateway into the cell". In: *Pharmaceutics* 12.4 (2020), p. 371.

[26]   Sriraman, S. K., Aryasomayajula, B. and Torchilin, V. P. "Barriers to drug delivery in solid tumors". In: *Tissue barriers* 2.3 (2014), e29528.

[27]   Kang, Z. et al. "The rational design of cell-penetrating peptides for application in delivery systems". In: *Peptides* 121 (2019), p. 170149.

[28] Guidotti, G., Brambilla, L. and Rossi, D. "Cell-penetrating peptides: from basic research to clinics". In: *Trends in pharmacological sciences* 38.4 (2017), pp. 406–424.

[29] Derakhshankhah, H. and Jafari, S. "Cell penetrating peptides: A concise review with emphasis on biomedical applications". In: *Biomedicine & Pharmacotherapy* 108 (2018), pp. 1090–1096.

[30] Ramsey, J. D. and Flynn, N. H. "Cell-penetrating peptides transport therapeutics into cells". In: *Pharmacology & therapeutics* 154 (2015), pp. 78–86.

[31] Rizzuti, M. et al. "Therapeutic applications of the cell-penetrating HIV-1 Tat peptide". In: *Drug discovery today* 20.1 (2015), pp. 76–85.

[32] Rothbard, J. B. et al. "Arginine-rich molecular transporters for drug delivery: role of backbone spacing in cellular uptake". In: *Journal of medicinal chemistry* 45.17 (2002), pp. 3612–3618.

[33] Leontiadou, H., Mark, A. E. and Marrink, S. J. "Antimicrobial peptides in action". In: *Journal of the American Chemical Society* 128.37 (2006), pp. 12156–12161.

[34] Yesylevskyy, S., Marrink, S.-J. and Mark, A. E. "Alternative mechanisms for the interaction of the cell-penetrating peptides penetratin and the TAT peptide with lipid bilayers". In: *Biophysical journal* 97.1 (2009), pp. 40–49.

[35] Eguchi, A. et al. "Protein transduction domain of HIV-1 Tat protein promotes efficient delivery of DNA into mammalian cells". In: *Journal of Biological Chemistry* 276.28 (2001), pp. 26204–26210.

[36] Yamano, S. et al. "Long-term efficient gene delivery using polyethylenimine with modified Tat peptide". In: *Biomaterials* 35.5 (2014), pp. 1705–1715.

[37] Seeman, N. C. and Kallenbach, N. R. "DNA Branched Junctions". In: *Annual Review of Biophysics and Biomolecular Structure* 23.1 (1994). PMID: 7919792, pp. 53–86. DOI: `10.1146/annurev.bb.23.060194.000413`.

[38] Rothemund, P. W. "Folding DNA to create nanoscale shapes and patterns". In: *Nature* 440.7082 (2006), pp. 297–302.

[39] Lin, C. et al. "DNA tile based self-assembly: building complex nanoarchitectures". In: *ChemPhysChem* 7.8 (2006), pp. 1641–1647.

[40] Wagenbauer, K. F. et al. "How we make DNA origami". In: *ChemBioChem* 18.19 (2017), pp. 1873–1885.

[41] Jiang, W. et al. "Recent Advances of DNA Origami Technology and Its Application in Nanomaterial Preparation". In: *Small Structures* (2023), p. 2200376.

[42] Dey, S. et al. "DNA origami". In: *Nature Reviews Methods Primers* 1.1 (2021), p. 13.

[43]   LaBoda, C., Duschl, H. and Dwyer, C. L. "DNA-enabled integrated molecular systems for computation and sensing". In: *Accounts of chemical research* 47.6 (2014), pp. 1816–1824.

[44]   Zhang, Y. et al. "Dynamic DNA structures". In: *Small* 15.26 (2019), p. 1900228.

[45]   Weiden, J. and Bastings, M. M. "DNA origami nanostructures for controlled therapeutic drug delivery". In: *Current Opinion in Colloid & Interface Science* 52 (2021), p. 101411.

[46]   Douglas, S. M. et al. "Rapid prototyping of 3D DNA-origami shapes with caDNAno". In: *Nucleic acids research* 37.15 (2009), pp. 5001–5006.

[47]   Williams, S. et al. "Tiamat: a three-dimensional editing tool for complex DNA structures". In: *DNA Computing: 14th International Meeting on DNA Computing, DNA 14, Prague, Czech Republic, June 2-9, 2008. Revised Selected Papers 14*. Springer. 2009, pp. 90–101.

[48]   Benson, E. et al. "DNA rendering of polyhedral meshes at the nanoscale". In: *Nature* 523.7561 (2015), pp. 441–444.

[49]   Llano, E. de et al. "Adenita: interactive 3D modelling and visualization of DNA nanostructures". In: *Nucleic acids research* 48.15 (2020), pp. 8269–8275.

[50]   Doye, J. P. et al. "Coarse-graining DNA for simulations of DNA nanotechnology". In: *Physical Chemistry Chemical Physics* 15.47 (2013), pp. 20395–20414.

[51]   Snodin, B. E. et al. "Introducing improved structural properties and salt dependence into a coarse-grained model of DNA". In: *The Journal of chemical physics* 142.23 (2015), pp. 11–12.

[52]   Praetorius, F. et al. "Biotechnological mass production of DNA origami". In: *Nature* 552.7683 (2017), pp. 84–87.

[53]   Bellot, G. et al. "Recovery of intact DNA nanostructures after agarose gel–based separation". In: *Nature methods* 8.3 (2011), pp. 192–194.

[54]   Stahl, E. et al. "Facile and scalable preparation of pure and dense DNA origami solutions". In: *Angewandte Chemie* 126.47 (2014), pp. 12949–12954.

[55]   Henning-Knechtel, A. et al. "Dielectrophoresis of gold nanoparticles conjugated to DNA origami structures". In: *Beilstein Journal of Nanotechnology* 7.1 (2016), pp. 948–956.

[56]   Dimaki, M. et al. "Sub–100 Nm Nanoparticle Upconcentration in Flow by Dielectrophoretic Forces". In: *Micromachines* 13.6 (2022), p. 866.

[57]   Effenhauser, C. S. et al. "High-speed separation of antisense oligonucleotides on a micromachined capillary electrophoresis device". In: *Analytical Chemistry* 66.18 (1994), pp. 2949–2953.

[58] *Role of KCl and MgCl2 in PCR*. Accessed: July 19, 2023. URL: https : / / biotecharticles . com / Biotech - Research - Article / Role - of - KCl - and - MgCl2 - in-PCR-3271.html.

[59] Poddar, S. "Symmetric vs asymmetric PCR and molecular beacon probe in the detection of a target gene of adenovirus". In: *Molecular and Cellular probes* 14.1 (2000), pp. 25–32.

[60] Sanchez, J. A. et al. "Linear-After-The-Exponential (LATE)–PCR: An advanced method of asymmetric PCR and its uses in quantitative real-time analysis". In: *Proceedings of the National Academy of Sciences* 101.7 (2004), pp. 1933–1938.

[61] Tolnai, Z. et al. "A simple modification increases specificity and efficiency of asymmetric PCR". In: *Analytica Chimica Acta* 1047 (2019), pp. 225–230.

[62] Behrendt, R., White, P. and Offer, J. "Advances in Fmoc solid-phase peptide synthesis". In: *Journal of Peptide Science* 22.1 (2016), pp. 4–27.

[63] Jensen, K. J., Shelton, P. T. and Pedersen, S. L. *Peptide synthesis and applications*. Springer, 2013.

[64] Carpino, L. A. and Han, G. Y. "9-Fluorenylmethoxycarbonyl amino-protecting group". In: *The Journal of Organic Chemistry* 37.22 (1972), pp. 3404–3409.

[65] Dourtoglou, V. et al. "O-Benzotriazolyl-N, N, N, N-tetramethyluronium hexafluorophosphate as coupling reagent for the synthesis of peptides of biological interest". In: *Synthesis* 1984.07 (1984), pp. 572–574.

[66] Pires, D. A. T., Bemquerer, M. P. and Nascimento, C. J. do. "Some mechanistic aspects on Fmoc solid phase peptide synthesis". In: *International Journal of Peptide Research and Therapeutics* 20.1 (2014), pp. 53–69.

[67] Li, J. and Liu, C. "Coding or noncoding, the converging concepts of RNAs". In: *Frontiers in genetics* 10 (2019), p. 496.

[68] Landolfo, S. et al. "The human cytomegalovirus". In: *Pharmacology & therapeutics* 98.3 (2003), pp. 269–297.

[69] Boshart, M. et al. "A very strong enhancer is located upstream of an immediate early gene of human cytomegalovirus". In: *cell* 41.2 (1985), pp. 521–530.

[70] Samulski, R. J. and Muzyczka, N. "AAV-mediated gene therapy for research and therapeutic purposes". In: *Annual review of virology* 1 (2014), pp. 427–451.

[71] McCarty, D. M. "Self-complementary AAV vectors; advances and applications". In: *Molecular therapy* 16.10 (2008), pp. 1648–1656.

[72] Le Bec, C. and Douar, A. "Gene therapy progress and prospects–vectorology: design and production of expression cassettes in AAV vectors". In: *Gene therapy* 13.10 (2006), pp. 805–813.

[73]   Evrogen. *pTagRFP-C vector restriction map*. 2022. URL: `https : / / tools .`
        `thermofisher . com / content / sfs / brochures / cms _ 040654 . pdf` (visited on
        11/01/2022).

[74]   *pTagRFP-C vector Data Sheet*. Accessed: July 19, 2023. URL: `https://evrogen.com/`
        `vector-descriptions/pTagRFP-C/pTagRFP-C.pdf`.

[75]   Subach, O. M. et al. "Structural characterization of acylimine-containing blue and red
        chromophores in mTagBFP and TagRFP fluorescent proteins". In: *Chemistry & biology*
        17.4 (2010), pp. 333–341.

[76]   Fisher, T. *Cleavage, Deprotection, and Isolation of Peptides after Fmoc Synthesis*. 2022.
        URL: `https://tools.thermofisher.com/content/sfs/brochures/cms_040654.pdf`
        (visited on 11/01/2022).

[77]   Jeong, S. et al. "Ninhydrin Loaded Microcapsules for Detection of Natural Free Amino
        Acid". In: *Chemosensors* 11.1 (2023), p. 49.

[78]   Martın-Parras, L. et al. "Topological complexity of different populations of pBR322 as
        visualized by two-dimensional agarose gel electrophoresis". In: *Nucleic acids research*
        26.14 (1998), pp. 3424–3432.

[79]   Owczarzy, R. "Melting temperatures of nucleic acids: discrepancies in analysis". In:
        Biophysical chemistry 117.3 (2005), pp. 207–215.

[80]   Green, M. R. and Sambrook, J. "Precipitation of DNA with Isopropanol." In: *Cold
        Spring Harbor Protocols* 2017.8 (2017), pdb–prot093385.

[81]   Carpino, L. A. et al. "The 2, 2, 4, 6, 7-pentamethyldihydrobenzofuran-5-sulfonyl group
        (Pbf) as arginine side chain protectant". In: *Tetrahedron letters* 34.49 (1993), pp. 7829–
        7832.

[82]   Chan, W. and White, P. *Fmoc solid phase peptide synthesis: a practical approach*.
        Vol. 222. OUP Oxford, 1999.

[83]   Wilner, O. I. and Willner, I. "Functionalized DNA nanostructures". In: *Chemical reviews*
        112.4 (2012), pp. 2528–2556.

Appendices

Appendices A

A.1   CAlculations

$$N/Pratio = \frac{\text{nmoles of polycation x number of amine groups per polycation}}{\text{nmols of DNA x number of phosphate groups per DNA}} \tag{A.1}$$

$$\text{nmol polycation} = \frac{\text{concentration of polycation(mg/ml) x μL of Polycation x } 10^3}{\text{Mw of polycation(g/mol)}} \tag{A.2}$$

$$\text{Mw of DNA} = \text{number of basepairs x average Mw of one basepair (660 g/mol)}$$
$$\text{or} \tag{A.3}$$
$$\text{Mw of DNA} = \text{number of nucleotides x average Mw of one nucleotide (330 g/mol)}$$

$$\text{Number of phosphate in one DNA origami } = \text{number of nucleotides per origami} \tag{A.4}$$

For plasmid DNA

Plasmid size = 4725 bp

4725 bp x 660 g/mol = 3.12 x 10^6 g/mol

1 mol plasmid : 2 x 4725 = 9450 mol phosphate

For origami

Origami size = 3544 nt

3544 nt x 330 g/mol = 1.17 x 10^6 g/mol

1 mol origami = 3544 mol phosphate

For PEI

Mw of PEI = 1300

number of N per monomer = 12

number of C per monomer = 22

number of H per monomer = 57

Mw of monomer = 489

number of repeats = 1300 / 489 = 2.66

12 x 2.66 = 31.92   32

1 mol PEI : 32 mol N

A.2 Worklist for synthesis of TAT sequence

Thursday, November 17, 2022 15:20:33 Version 1.4.4.32

Sequence: Tyr Gly Arg Lys Lys Arg Arg Gln Arg Arg Arg

N-terminal de-protected, C-terminal acid

Monoisotopic molecular weight: 1558.951

Theoretical yield: 0.230 millimole

Time for synthesis: 28 Hours 29 Minutes

Maximum reactor contents: 6.0 ml, use 40 ml reactor

PV not used

Maximum amino acid vial contents: 5.0 ml, use 15 ml vials

Multitask mode: Just in time

Simple wizard used: Single coupling, Swell, Final deprotection, Final DCM wash

UV monitoring used

Resin data:

Substitution: 0.500 mmoles/gram, Quantity: 0.460 grams, Preloaded with Arg, Deprotect before first coupling

Fluid Allocation

Bottle	Fluid	Molarity	millilitres
External 1	DMF	na	3506.0
External 2		na	0.0
External 3		na	0.0
Internal 4		na	0.0
Internal 5		na	0.0
Internal 6	DCM	na	21.0
Internal 7	DIEA 1.0 M	1.00	45.0
Internal 8	HBTU 0.48 M	0.48	45.0
Internal 9	Piperidine 25%	na	275.0

Sequence Data

Vial	Seq	Protected amino acid		Quantity	Protocol
	0	C terminal			initial
1	1	Arg attached to resin	No vial	0 mg	-
2	2	Fmoc-Arg(Pbf)-OH	powder	811 mg	standard cycle
3	3	Fmoc-Arg(Pbf)-OH	powder	811 mg	standard cycle
4	4	Fmoc-Gln(Trt)-OH	powder	763 mg	standard cycle
5	5	Fmoc-Arg(Pbf)-OH	powder	811 mg	standard cycle
6	6	Fmoc-Arg(Pbf)-OH	powder	811 mg	standard cycle
7	7	Fmoc-Lys(Boc)-OH	powder	586 mg	standard cycle
8	8	Fmoc-Lys(Boc)-OH	powder	586 mg	standard cycle
9	9	Fmoc-Arg(Pbf)-OH	powder	811 mg	standard cycle
10	10	Fmoc-Gly-OH	powder	372 mg	standard cycle
11	11	Fmoc-Tyr(tBu)-OH	powder	574 mg	standard cycle
	12	N terminal			final

A.3 Optimization of PCR Reactions

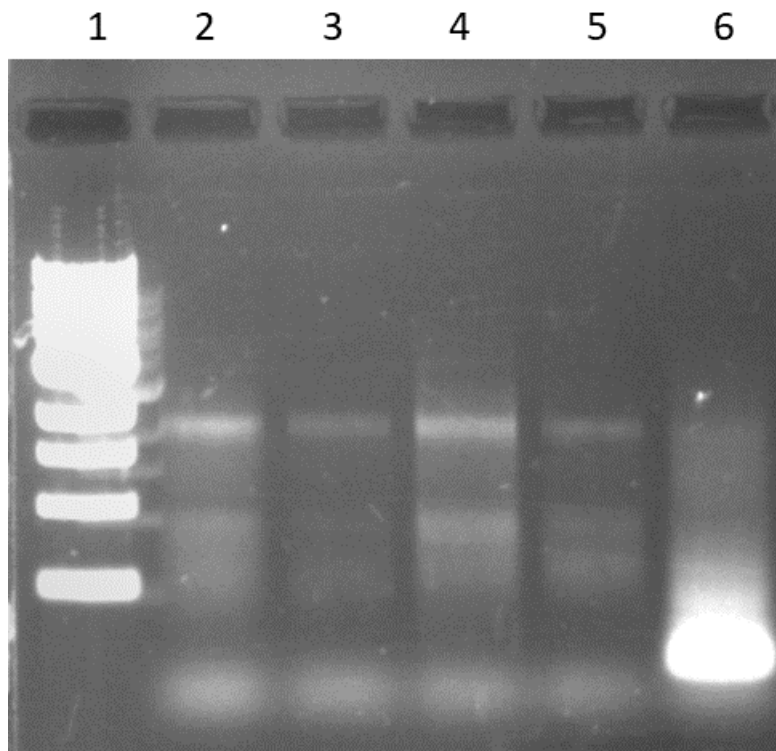### A.3.1 First PCR Reaction Optimization
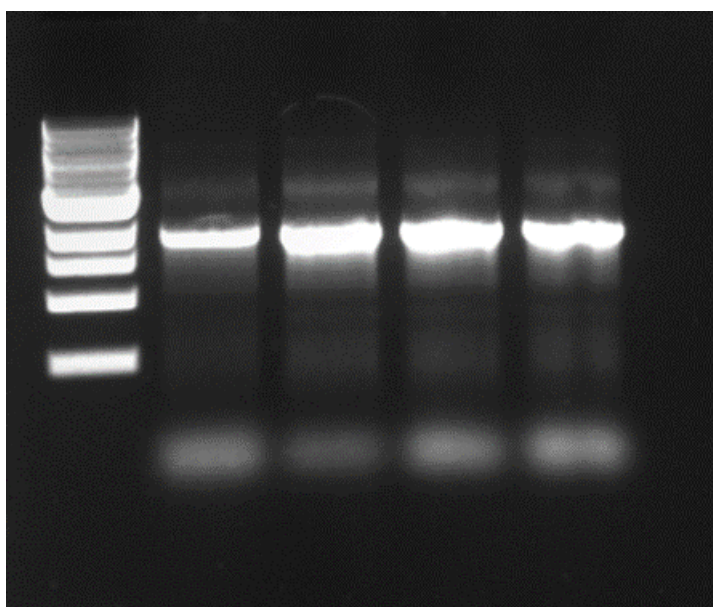
Figure A.1. *Optimization of annealing temperature: 53, 44.6, 46.3, 49.7°C, respectively*
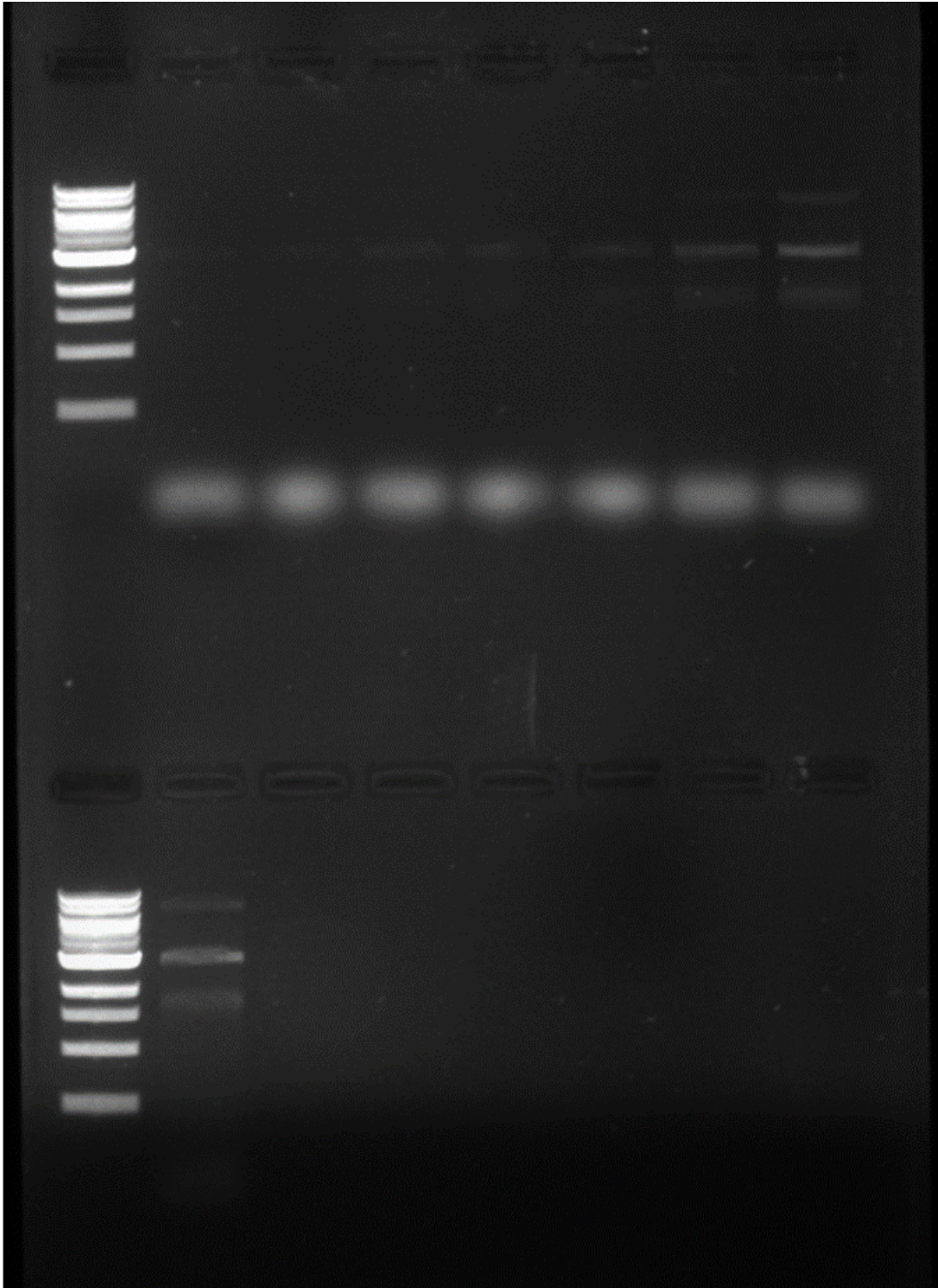
Figure A.2. *Optimization of aPCR by Template concentration: 7, 14, 28, 35, 56, 70, 140, 240 ng*

A.3.2 Asymmetric PCR Otimization

Lane	T_{anneal} (°C)	Cycles	Template
2	45	25	PCR
3	45	25	Gel
4	53	25	PCR
5	53	25	Gel
6	53	75	PCR
7	53	75	Gel

Figure A.3. *Optimization of aPCR by annealing temperature, template source, and number of cycles. 2,4,6: ds template from cleanedup PCR. 3,5,7: ds template extracted from gel. 2,3: $T_anneal = 45$ ℃, 4to7: $T_anneal = 53$ ℃, 2to5: x25 cycles, 6,7: x75 cycles*

A.4 Ninhydrin Calculations

$$N = N' \tag{A.5}$$

N is the total mol -NH2 in corresponding PEI.

N' is the total mol -NH2 in modified PEI.

$$M \cdot 10.3 = M' \cdot (10.3 - n) \tag{A.6}$$

M is the total mol corresponding PEI. M' is the total mol of modified PEI.

n is the number of substituted amines per modified PEI molecule.

10.3 is the number of primary amines per PEI molecule.

$$M = \frac{m}{Mw_{PEI}} \tag{A.7}$$

$$M' = \frac{m'}{Mw'} \tag{A.8}$$

m is the mass of corresponding PEI.

m' is the mass of modified PEI.

$$\frac{m}{Mw_{PEI}} \cdot 10.3 = \frac{m'}{Mw'} \cdot (10.3 - n) \tag{A.9}$$

$$Mw' = Mw_{PEI} + n \cdot Mw_{Subs} \tag{A.10}$$

Mw_{Subs} is the Mw of substituent molecule.

$$\frac{m}{Mw_{PEI}} \cdot 10.3 = \frac{m'}{Mw_{PEI} + n.Mw_{subs}} \cdot (10.3 - n) \tag{A.11}$$

$$n = \frac{13390 \cdot (m' - m)}{(10.3 \cdot m \cdot Mw_{subs}) + 1300} \tag{A.12}$$

$$\% \text{ modification} = \frac{n}{10.3} \cdot 100 \tag{A.13}$$